

Title: Simulation of Binary Black Hole Mergers

Date: Apr 26, 2006 02:00 PM

URL: <http://pirsa.org/06040024>

Abstract: I will describe some recent advances in the simulation of binary black hole spacetimes using a numerical scheme based on generalized harmonic coordinates. After a brief overview of the formalism and method, I will present results from the evolution of a couple of classes of initial data, including Cook-Pfiefer quasi-circular inspiral data sets, and binaries constructed via scalar field collapse. In the latter case, preliminary studies suggest that in certain regions of parameter space there is extreme sensitivity of the resulting orbit to the initial conditions. In this regime the equal mass black holes exhibit behavior reminiscent of "zoom-whirl" particle trajectories in the test-mass limit.

Simulation of Binary Black Hole Mergers

Frans Pretorius
University of Alberta

Perimeter Institute
April 26, 2006

Simulation of Binary Black Hole Mergers

Frans Pretorius
University of Alberta

Perimeter Institute
April 26, 2006

Outline

- Why study binary black hole systems?
 - expected to be among the strongest and most promising sources of gravitational waves that could be observed by **gravitational wave detectors**
 - understand the strong-field regime of general relativity
- Why do we need to *simulate* them?
 - understanding the nature of the gravitational waves emitted during a merger event may be *essential* for successful detection
 - the two-body problem in GR is **unsolved**, and no analytic solution techniques (perturbative or other) known that could be applied during the final stages of an inspiral and merger
- Methodology
 - brief overview of numerical relativity, the difficulties in discretizing the field equations
- Simulation results
 - evolution of quasi-circular initial data sets
 - binaries constructed via scalar field collapse

The network of gravitational wave detectors

LIGO/VIRGO/GEO/TAMA
ground based laser interferometers

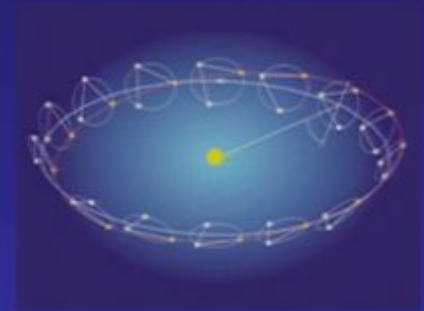


LIGO Livingston



LIGO Hanford

LISA
space-based laser interferometer (hopefully
with get funded for a 201? Lauch)



ALLEGRO/NAUTILUS/AURIGA/...
resonant bar detectors



ALLEGRO

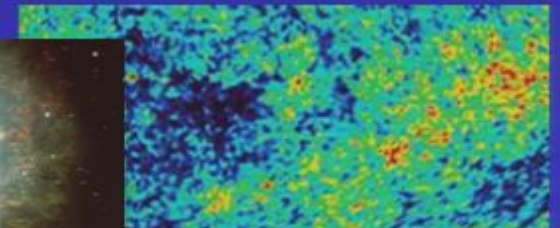


AURIGA

Pulsar timing network, CMB anisotropy

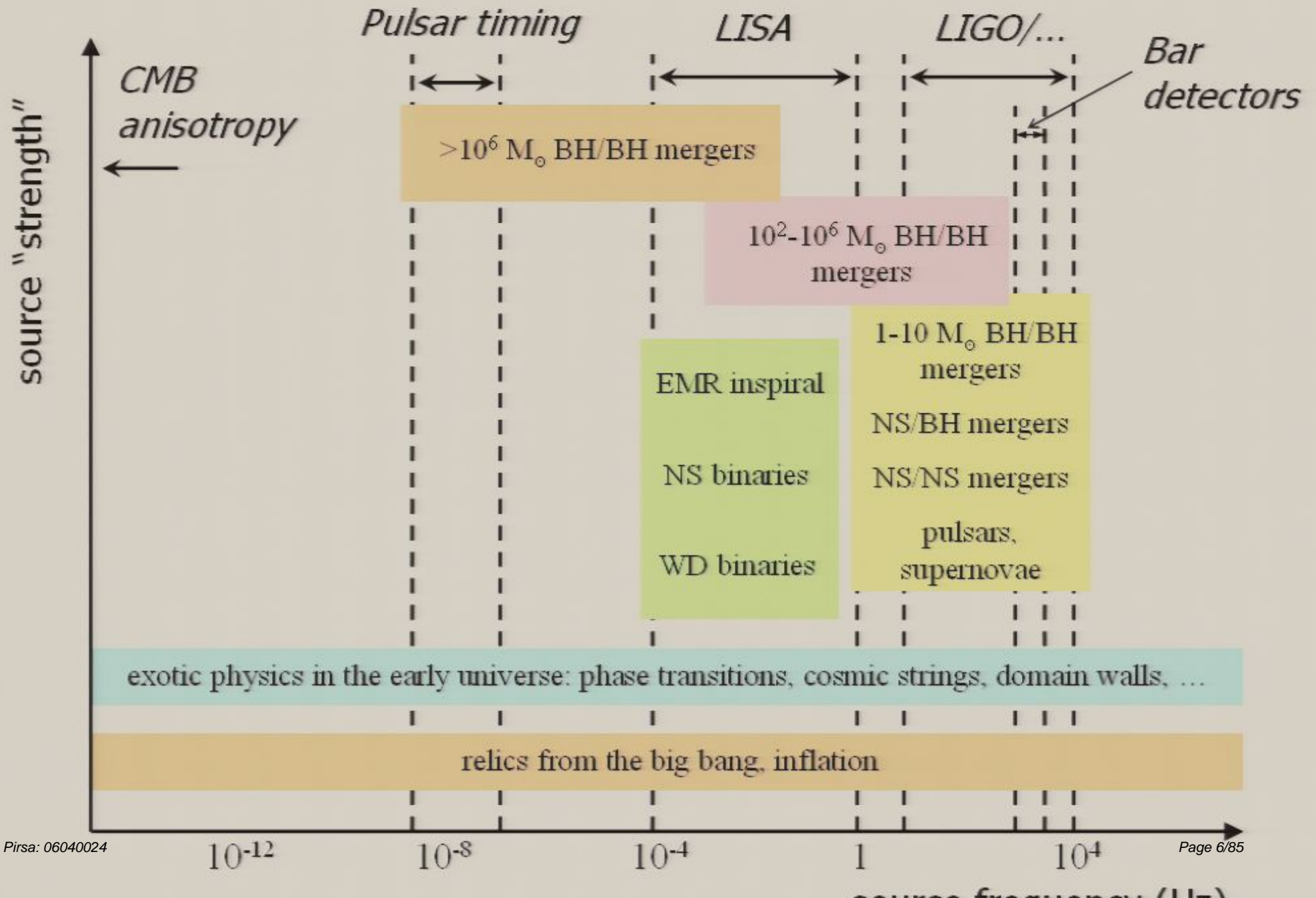


*The Crab nebula ... a supernovae
remnant harboring a pulsar*



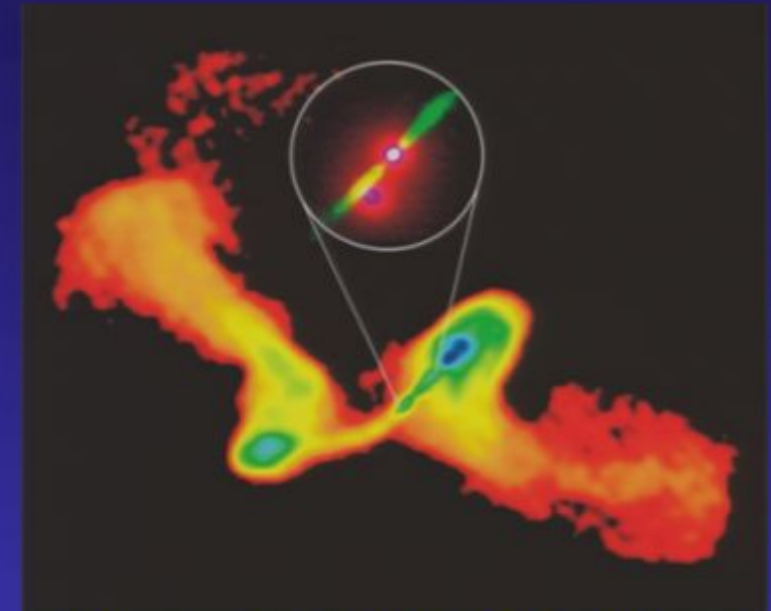
*Segment of the CMB
from WMAP*

Overview of expected gravitational wave sources



Binary black holes in the Universe

- strong, though *circumstantial* evidence that black holes are ubiquitous objects in the universe
 - supermassive black holes ($10^6 M_{\odot}$ - $10^9 M_{\odot}$) thought to exist at the centers of most galaxies
 - high stellar velocities near the centers of galaxies, jets in active galactic nuclei, x-ray emission, ...
 - more massive stars are expected to form BH's at the end of their lives
 - a few dozen candidate stellar mass black holes in x-ray binary systems ... companion too massive to be a neutron star



VLA image of the galaxy NGC 326, with HST image of jets inset. CREDIT: NRAO/AUI, STScI (inset)



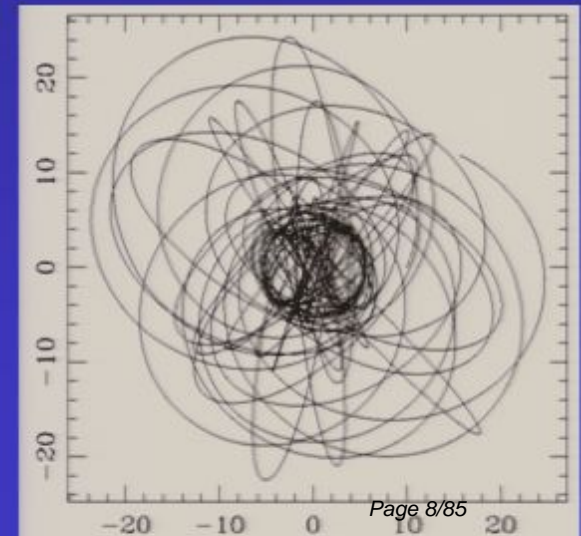
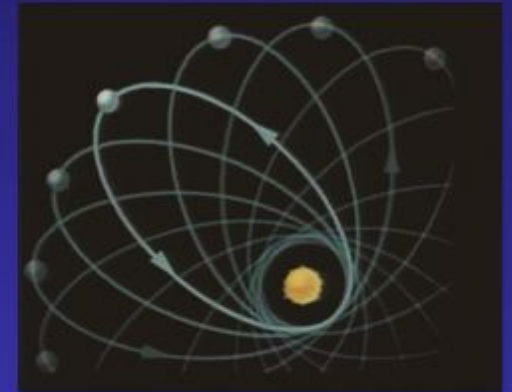
Pirsa: 06040024

Two merging galaxies in Abell 400. Credits: X-ray, NASA/CXCI

- detection of gravitational waves from BH mergers would provide **direct evidence for black holes**, as well as give valuable information on stellar evolution theory and large scale structure formation and evolution in the universe
- this will also be an **unprecedented test of general relativity**, as the last stages of a merger takes place in the highly dynamical and non-linear strong-field regime

The two body problem

- Newtonian gravity solution for the dynamics of two point-like masses in a bound orbit: motion along an ellipse
- in general relativity there is no (analytic) solution ... several approximations with different realms of validity
 - test particle limit
 - geodesic motion of a particle about a black hole (i.e. self-gravity of particle is ignored)
 - already get some very interesting behavior
 - perihelion precession
 - unstable and chaotic orbits
 - “zoom-whirl” behavior
 - Post-Newtonian (PN) expansions
 - self-gravity accounted for, though slow motion (relative to c) and weak gravitational fields assumed
 - begins to incorporate “radiation-reaction”; i.e. how the orbit decays via the emission of gravitational waves
 - black hole (BH) perturbation theory
 - can be used to model the “ring-down” of the final BH that is formed in a collision
 - can also describe the radiation caused by a test particle in orbit about the BH
- binary black hole mergers
 - all the above assumptions break down close to the merger of comparable mass BHs: self gravity can't be ignored, the gravitational fields are not weak, and the BHs are moving at sizeable fractions of the speed of light



Numerical Relativity

- Numerical relativity is concerned with solving the field equations of general relativity

$$G_{\alpha\beta} = 8\pi T_{\alpha\beta}$$

using computers.

- When written in terms of the spacetime metric, defined by the usual line element

$$ds^2 = g_{\alpha\beta} dx^\alpha dx^\beta$$

the field equations form a *system of 10 coupled, non-linear, second order partial differential equations, each depending on the 4 spacetime coordinates*

- it is this system of equations that we need to solve for the 10 metric elements (plus whatever matter we want to couple to gravity)
 - for many problems this has turned out to be quite an undertaking, due in part to the mathematical complexity of the equations, and also the heavy computational resources required to solve them
- The field equations may be complicated, but they are the equations that we believe govern the structure of space and time (barring quantum effects and ignoring matter). That they can, in principle, be solved in them in many “real-universe” scenarios is a remarkable and unique situation in physics.

Minimal requirements for a formulation of the field equations that *might* form the basis for a successful numerical integration scheme

- Choose coordinates/system-of-variables that fix the character of the equations
 - three common choices
 - free evolution — system of hyperbolic equations
 - constrained evolution — system of hyperbolic and elliptic equations
 - characteristic or null evolution — integration along the lightcones of the spacetime
- For free evolution, need a system of equations that is well behaved off the “*constraint manifold*”
 - analytically, if satisfied at the initial time the constraint equations of GR will be satisfied for all time
 - numerically the constraints can only be satisfied to within the truncation error of the numerical scheme, hence we do not want a formulation that is “unstable” when the evolution proceeds slightly off the constraint manifold
- Need well behaved coordinates (or gauges) that do not develop pathologies when the spacetime is evolved
 - typically need dynamical coordinate conditions that can adapt to unfolding features of the spacetime
- Boundary conditions also historically a source of headaches
 - naive BC’s don’t preserve the constraint nor are representative of the physics
 - fancy BC’s can preserve the constraints, but again miss the physics
 - solution ... compactify to infinity
- Geometric singularities in black hole spacetimes need to be dealt with

Numerical Relativity

- Numerical relativity is concerned with solving the field equations of general relativity

$$G_{\alpha\beta} = 8\pi T_{\alpha\beta}$$

using computers.

- When written in terms of the spacetime metric, defined by the usual line element

$$ds^2 = g_{\alpha\beta} dx^\alpha dx^\beta$$

the field equations form a *system of 10 coupled, non-linear, second order partial differential equations, each depending on the 4 spacetime coordinates*

- it is this system of equations that we need to solve for the 10 metric elements (plus whatever matter we want to couple to gravity)
 - for many problems this has turned out to be quite an undertaking, due in part to the mathematical complexity of the equations, and also the heavy computational resources required to solve them
- The field equations may be complicated, but they are the equations that we believe govern the structure of space and time (barring quantum effects and ignoring matter). That they can, in principle, be solved in them in many “real-universe” scenarios is a remarkable and unique situation in physics.

Minimal requirements for a formulation of the field equations that *might* form the basis for a successful numerical integration scheme

- Choose coordinates/system-of-variables that fix the character of the equations
 - three common choices
 - free evolution — system of hyperbolic equations
 - constrained evolution — system of hyperbolic and elliptic equations
 - characteristic or null evolution — integration along the lightcones of the spacetime
- For free evolution, need a system of equations that is well behaved off the “*constraint manifold*”
 - analytically, if satisfied at the initial time the constraint equations of GR will be satisfied for all time
 - numerically the constraints can only be satisfied to within the truncation error of the numerical scheme, hence we do not want a formulation that is “unstable” when the evolution proceeds slightly off the constraint manifold
- Need well behaved coordinates (or gauges) that do not develop pathologies when the spacetime is evolved
 - typically need dynamical coordinate conditions that can adapt to unfolding features of the spacetime
- Boundary conditions also historically a source of headaches
 - naive BC’s don’t preserve the constraint nor are representative of the physics
 - fancy BC’s can preserve the constraints, but again miss the physics
 - solution ... compactify to infinity
- Geometric singularities in black hole spacetimes need to be dealt with

Numerical relativity using generalized harmonic coordinates – a brief overview

- *Harmonic coordinates*

$$\nabla^\alpha \nabla_\alpha x^\mu \equiv \frac{1}{\sqrt{-g}} \partial_\alpha (\sqrt{-g} g^{\alpha\mu}) = 0$$

does to the Einstein equations what the Lorenz gauge does to Maxwell's equations ... the *principle part* of each component of the Einstein tensor becomes a wave equation for the corresponding metric element

$$\nabla^\delta \nabla_\delta g_{\alpha\beta} + \dots = 0$$

- the character of each field equation is now hyperbolic
- the ellipsis denote all the lower order terms, which contain the non-linearity and messy couplings between the metric elements
- Harmonic coordinates are in a sense older than the field equations themselves, as they were used by Einstein as early as 1912 while searching for a relativistic theory of gravity
- over the years they have played an instrumental role in the formal analysis of the field equations, and the study of gravitational radiation
 - “avoided” in numerical relativity because of the *somewhat* misguided belief that they were prone to developing coordinate pathologies in generic scenarios
 - Garfinkle [PRD 65, 044029 (2002)] recently noted a possible resolution to this problem

Summary of Equations solved

- Einstein equations in generalized harmonic form with constraint damping:

$$g^{\gamma\delta}g_{\alpha\beta,\gamma\delta} + 2g^{\gamma\delta}_{,(\alpha}g_{\beta)\delta,\gamma} + 2H_{(\alpha,\beta)} - 2H_\delta\Gamma_{\alpha\beta}^\delta + 2\Gamma_{\delta\beta}^\gamma\Gamma_{\gamma\alpha}^\delta + 8\pi(2T_{\alpha\beta} - g_{\alpha\beta}T) + \kappa(n_\mu C_\nu + n_\nu C_\mu - g_{\mu\nu}n^\alpha C_\alpha) = 0$$

- Gauge evolution equations

$$\nabla^\mu \nabla_\mu H_t = -\xi_1 \frac{\alpha - 1}{\alpha^n} + \xi_2 \partial_\mu H_t \cdot n^\mu$$

$$H_x = H_y = H_z = 0$$

- time source function prevents the lapse from “collapsing” in black hole spacetimes

- Matter stress energy supplied by a massless scalar field Φ :

$$T_{\alpha\beta} = 2\Phi_{,\alpha}\Phi_{,\beta} - g_{\alpha\beta}\Phi_{,\mu}\Phi^{,\mu}$$

$$\nabla^\mu \nabla_\mu \Phi = 0$$

Brief (and incomplete) history of the binary black hole problem in numerical relativity

- L. Smarr, *PhD Thesis* (1977) : First head-on collision simulation
- P. Anninos, D. Hobill, E. Seidel, L. Smarr, W. Suen *PRL* 71, 2851 (1993) : Improved simulation of head-on collision
- B. Bruegmann *Int. J. Mod. Phys. D* 8, 85 (1999) : First grazing collision of two black holes
- B. Bruegmann, W. Tichy, N. Jansen *PRL* 92, 211101 (2004) : First full orbit of a quasi-circular binary
- FP, *PRL* 95, 121101 (2005) : First “complete” simulation of a non head-on merger event: orbit, coalescence, ringdown and gravitational wave extraction
- M. Campanelli, C. O. Lousto, P. Marronetti, Y. Zlochower (*gr-qc/0511048*); J. G. Baker, J. Centrella, D. Choi, M. Koppitz, J. van Meter (*gr-qc/0511103*) : similar complete merger event as FP(2005), though using very different numerical techniques. Their methods reproduced by F. Herrmann, D. Shoemaker, P. Laguna (*gr-qc/0601026*).

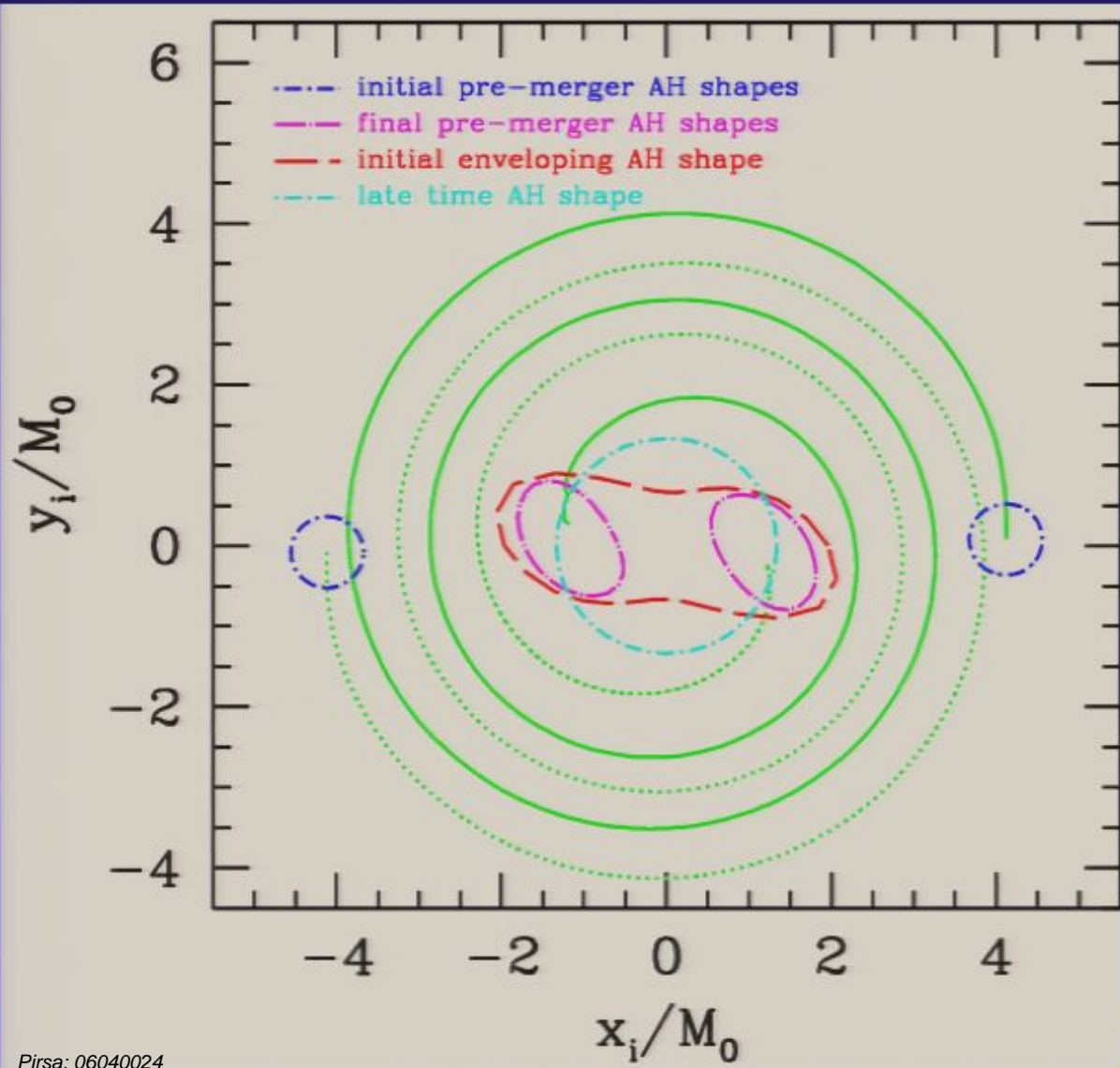
The initial data problem ...

- It is *not* easy specifying astrophysically realistic binary black hole (BBH) initial data for evolution
 - the initial geometry must satisfy the constraint equations, and so cannot be freely specified
 - state of the art methods available today for solving the constraints for BBH initial data do *not* include the radiation that would have been generated by the prior inspiral history of the BHs
 - PN (and other approximate solutions) do *not* satisfy the constraints, and might not even have black holes
 - several suggestions for melding PN methods with constraint equation solving methods, though none have yet been tested

Evolution of Cook-Pfeiffer Quasi-Circular Initial Data Sets

- Initial data provided by H. Pfeiffer, based on solutions to the constraint equations with free data and black hole boundary conditions as described in *Cook and Pfeiffer, PRD 70, 104016 (2004)*
 - approximation to the structure of spacetime describing a BBH system composed of equal mass, corotating black holes, initially on circular orbits
 - “good” assumptions used, except
 - no gravitational radiation content
 - no tidal deformation of the BHs
 - no radial component to BH velocities
 - data sets are parameterized by the initial separation of the binaries
 - the closer the BHs are the more pronounced the above errors will be

A Cook-Pfeiffer Inspiral Orbit



Initial coordinate (proper) separation:

$$7.4M \text{ (} 9.8M \text{)}$$

Final BH angular momentum:

$$J = 0.70 \pm 0.02 M^2$$

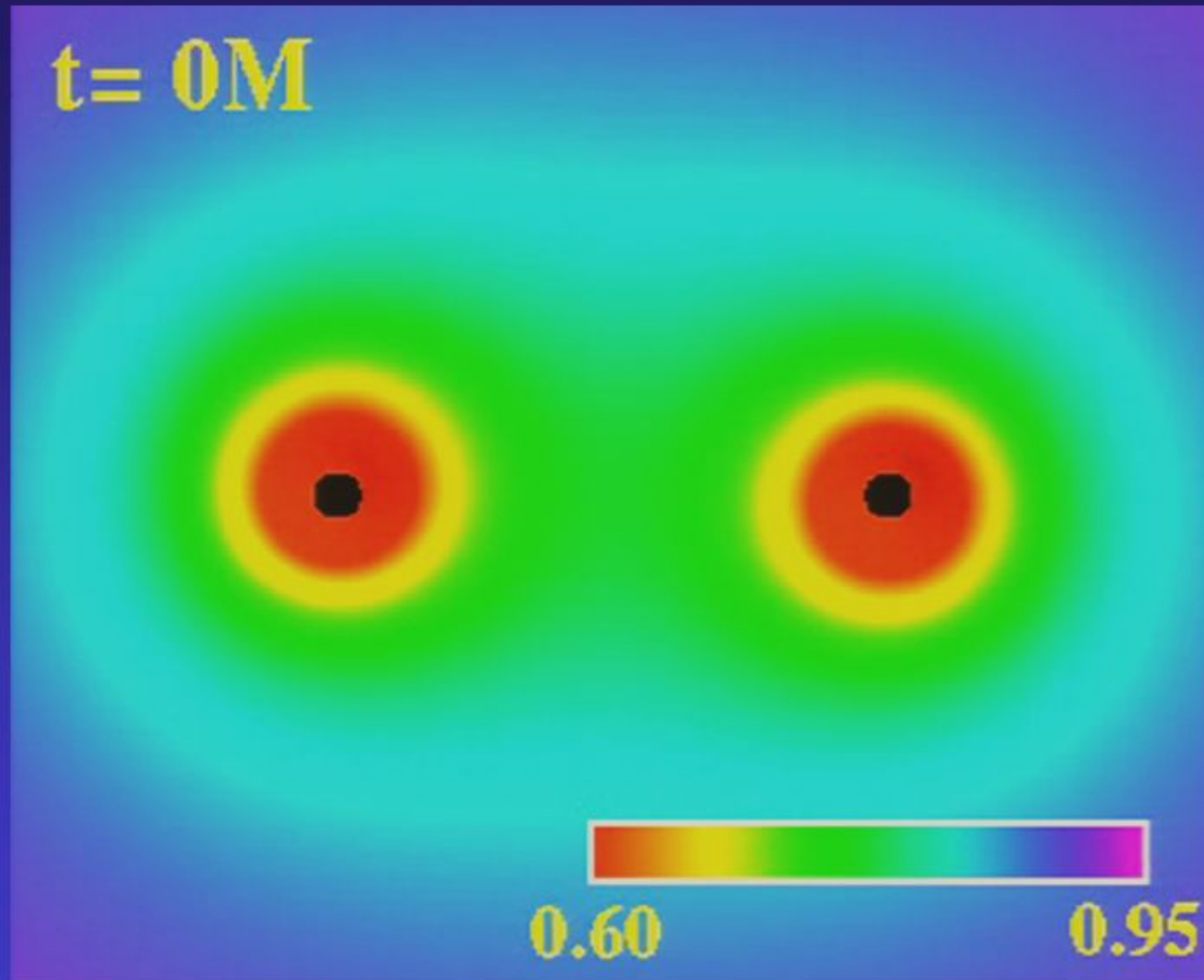
Energy radiated:

$$0.043M \pm 0.004M$$

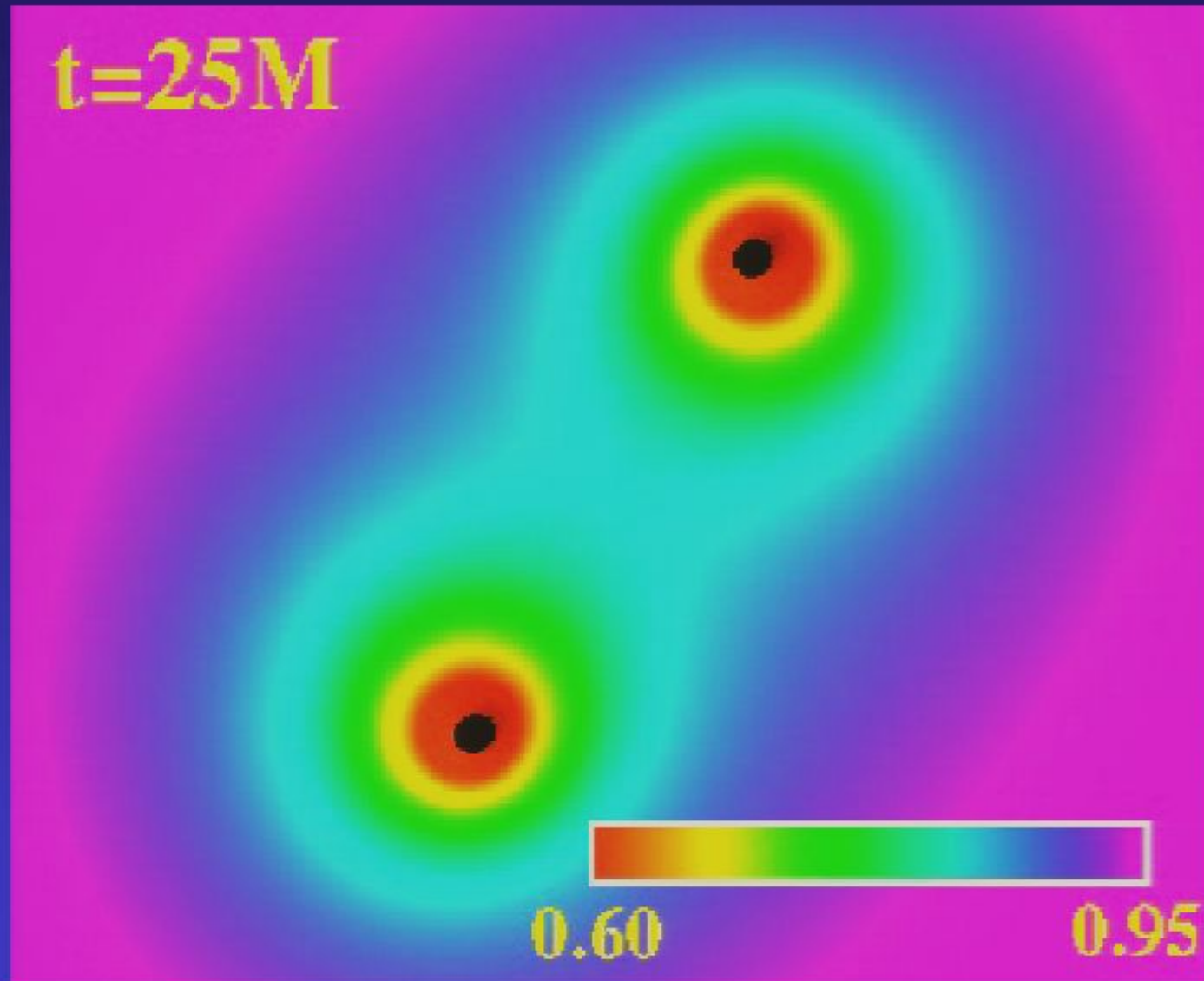
Errors estimated from simulations with three characteristic resolutions.

Highest-res simulation details: ~ 60,000 CPU hours on UT *lonestar* cluster (3 weeks total on 128 nodes), ~ 2TB disk usage (infrequent output), ~ 25GB total RAM usage. (other machines used include Westgrid's *glacier* and *matrix*, and UBC's *vrp4*)

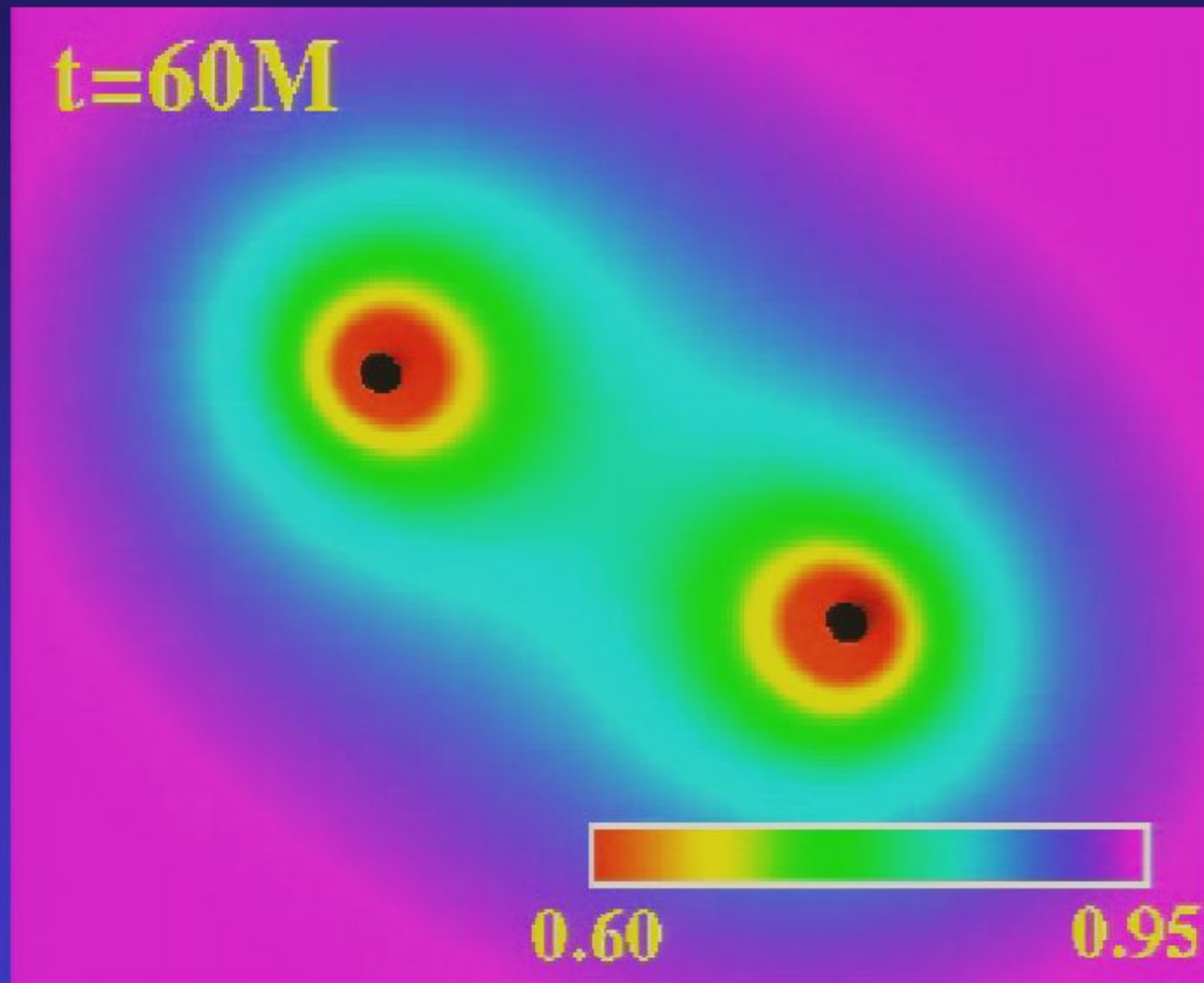
Lapse function α , orbital plane



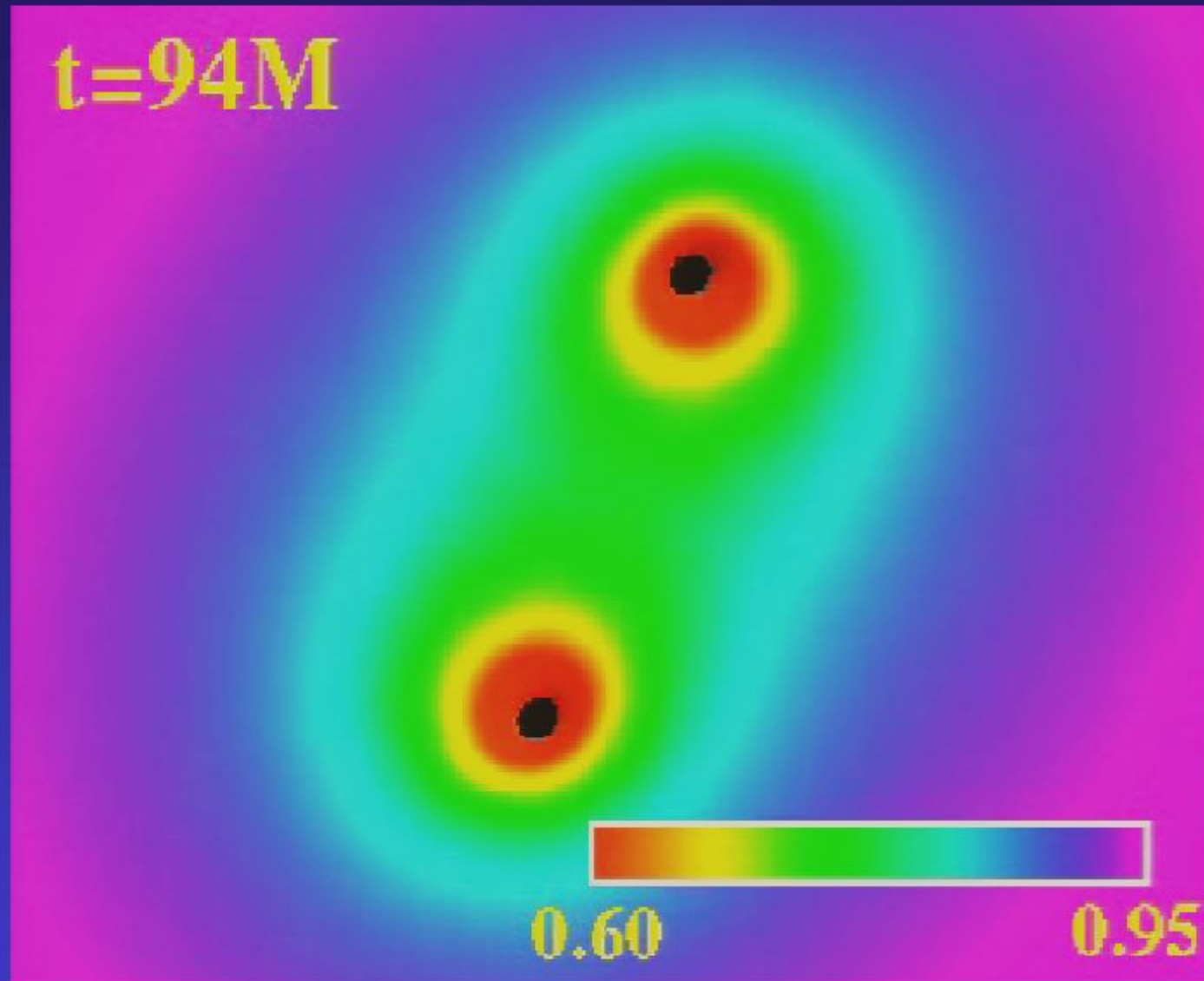
Lapse function α , orbital plane



Lapse function α , orbital plane

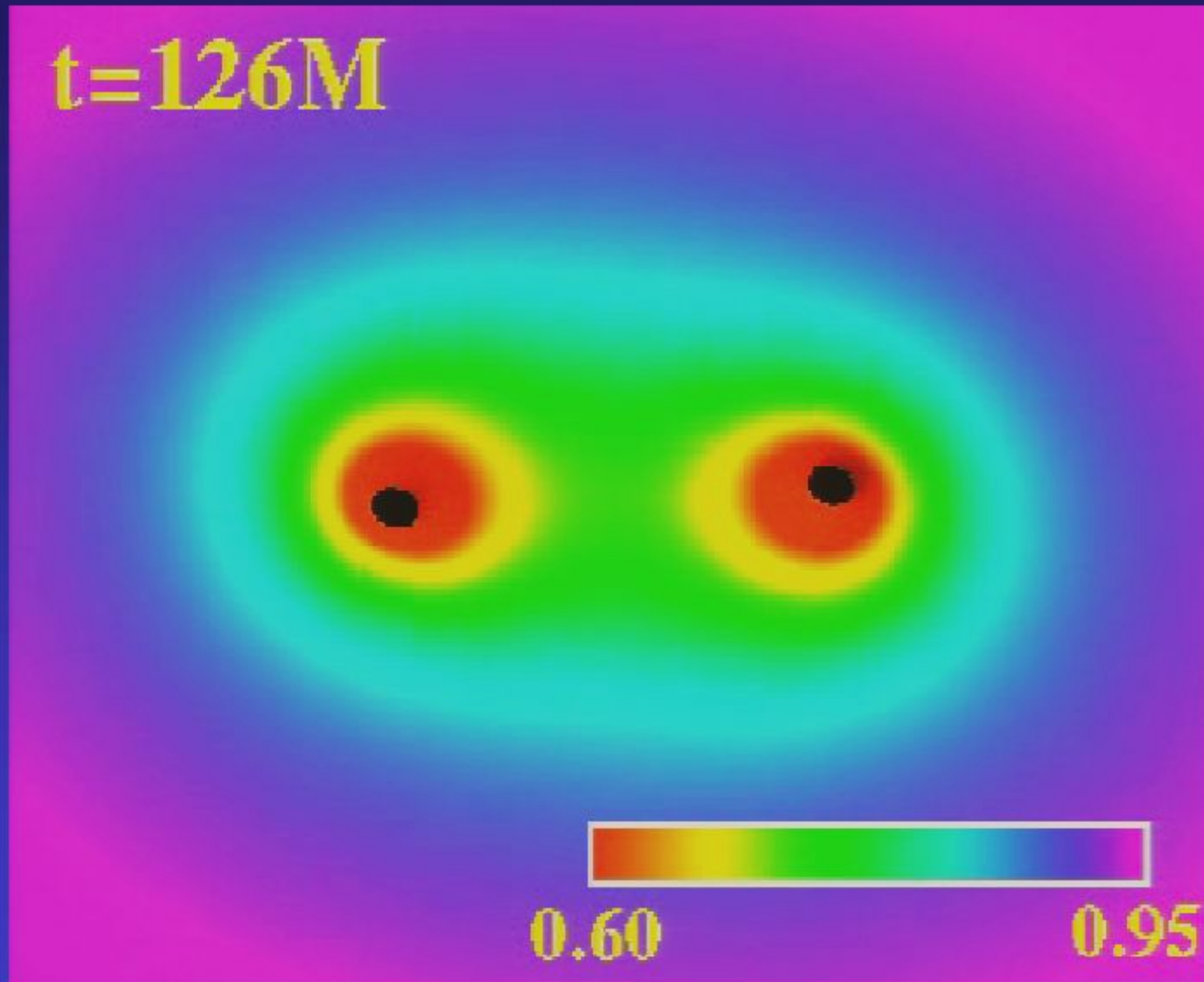


Lapse function α , orbital plane



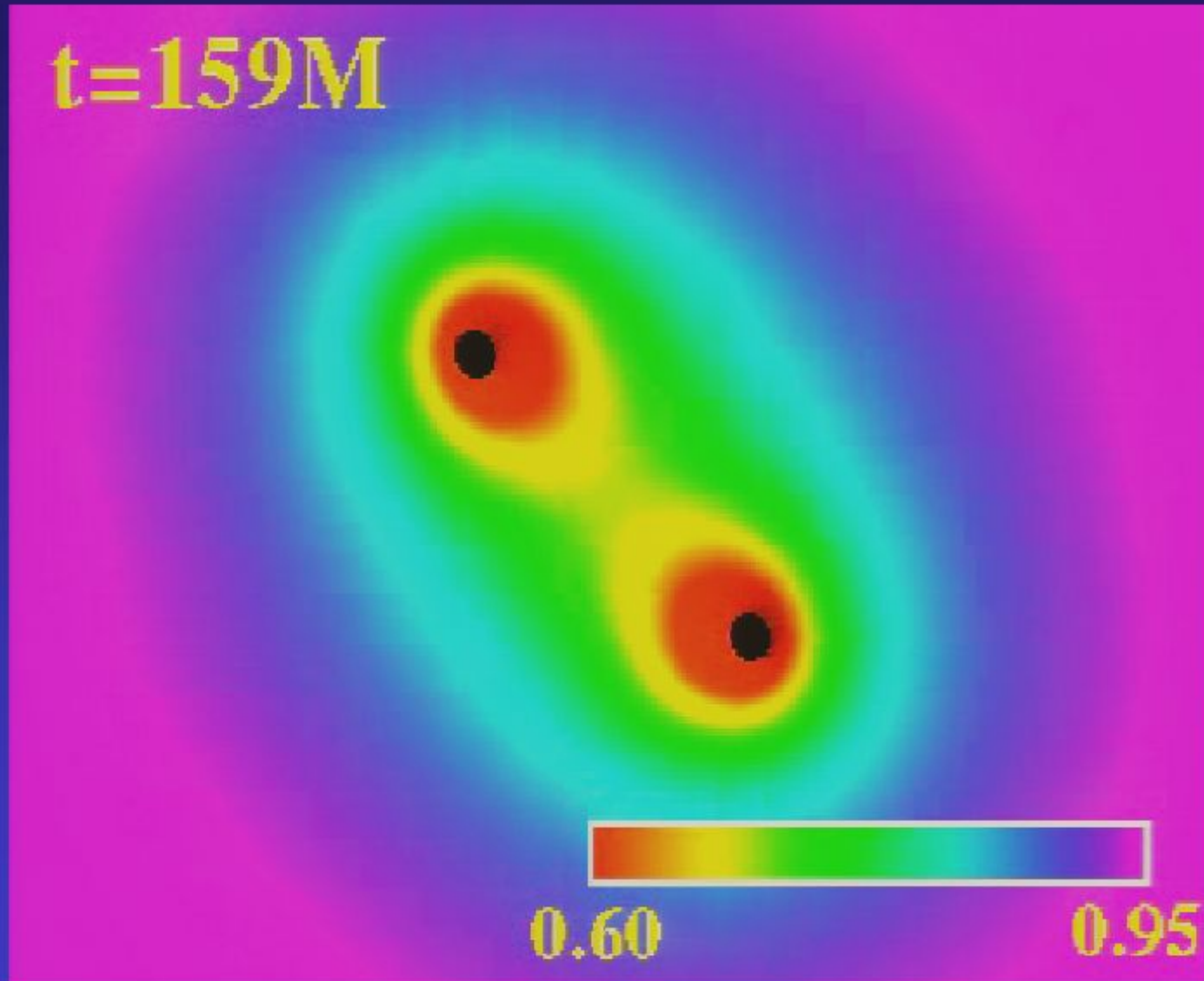
Lapse function α , orbital plane

$t=126M$

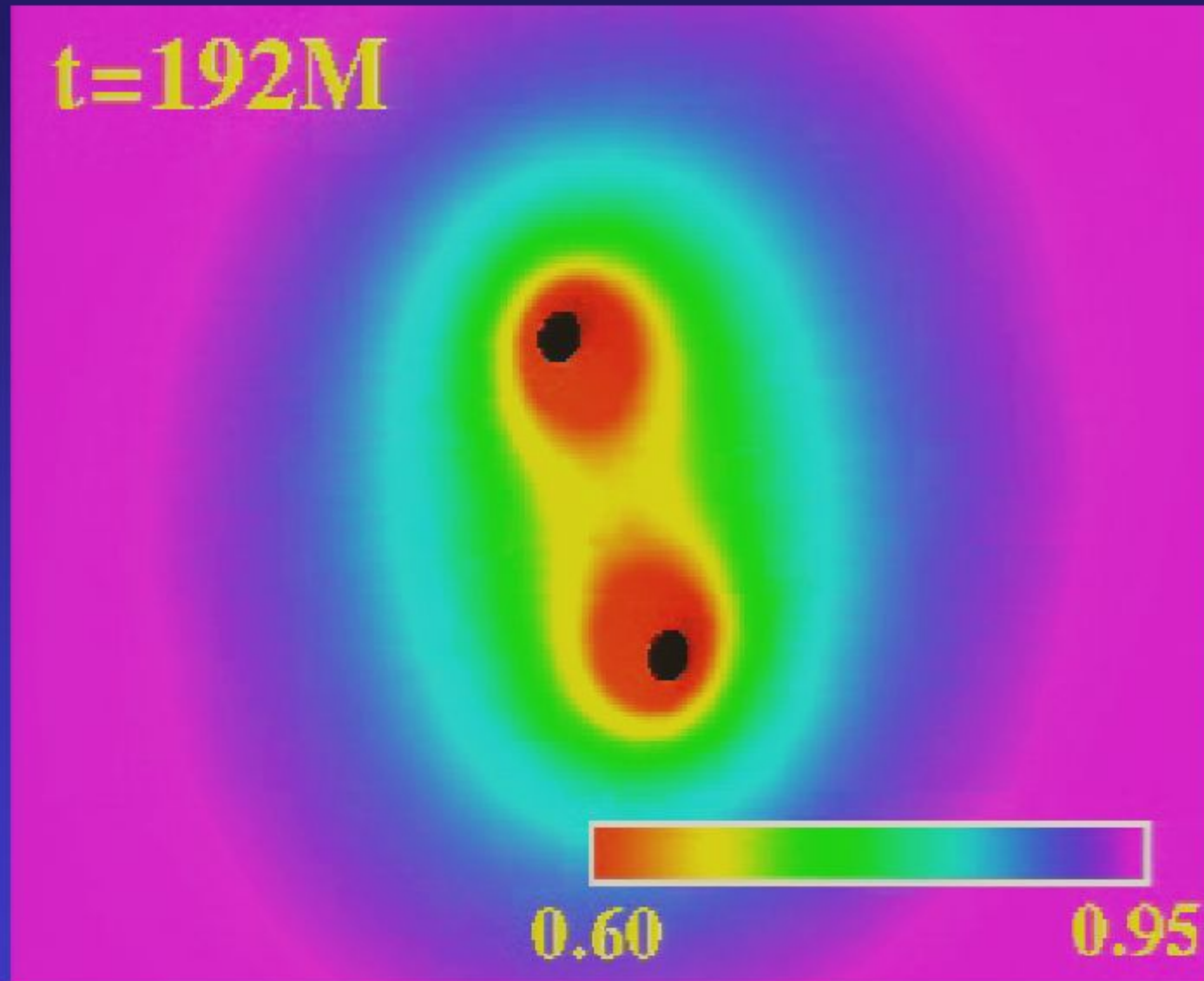


Lapse function α , orbital plane

$t=159M$

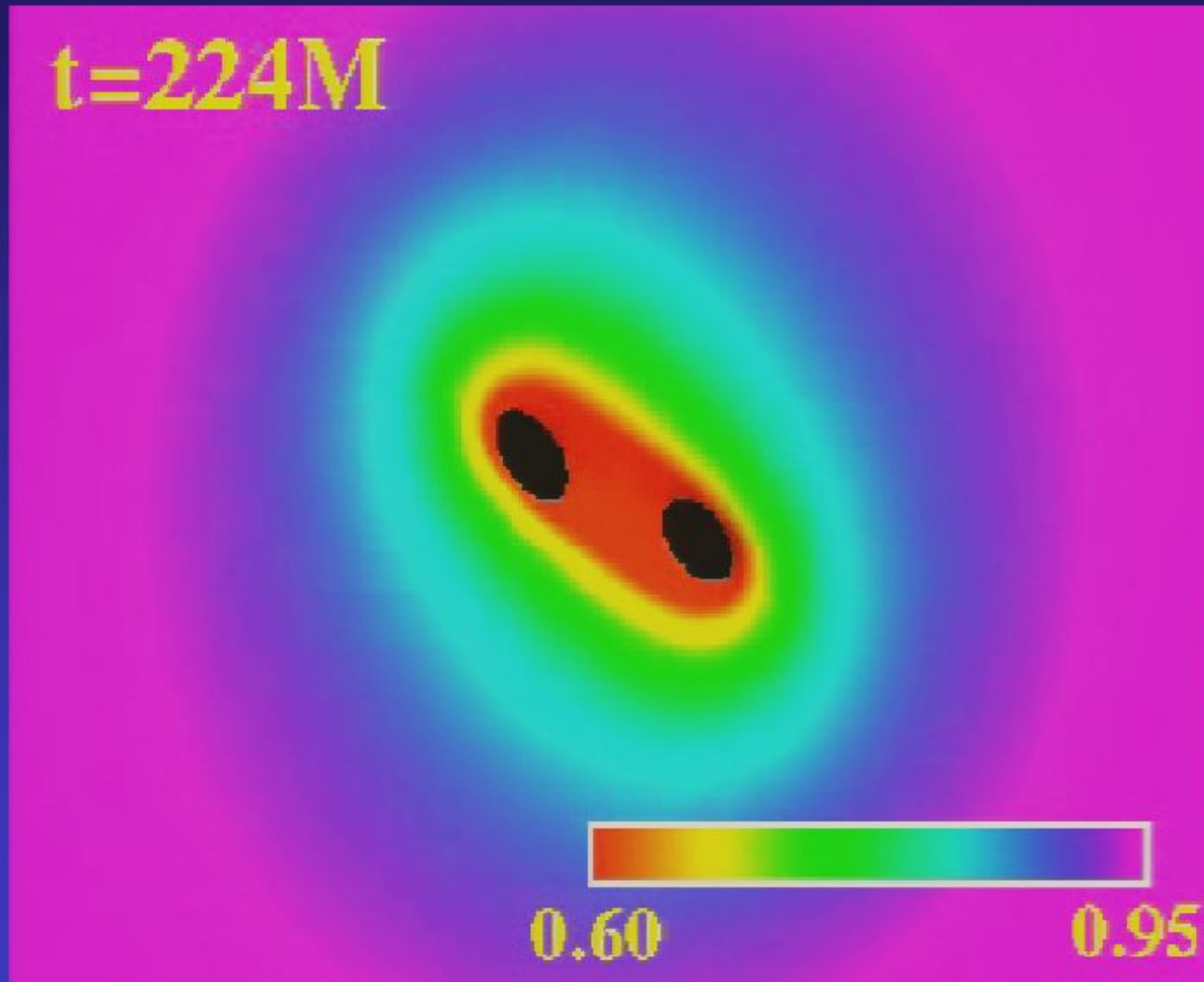


Lapse function α , orbital plane



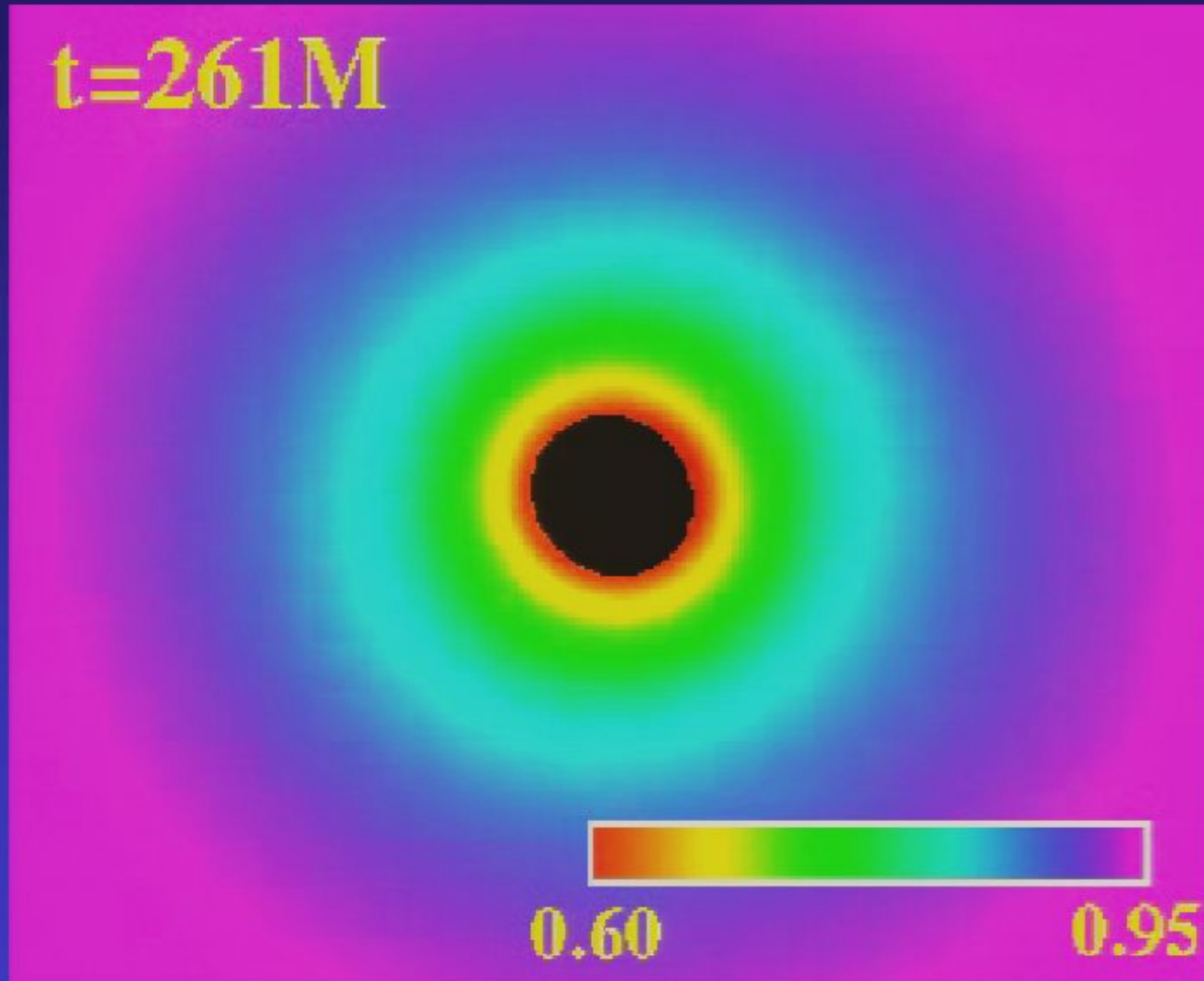
Lapse function α , orbital plane

$t=224M$



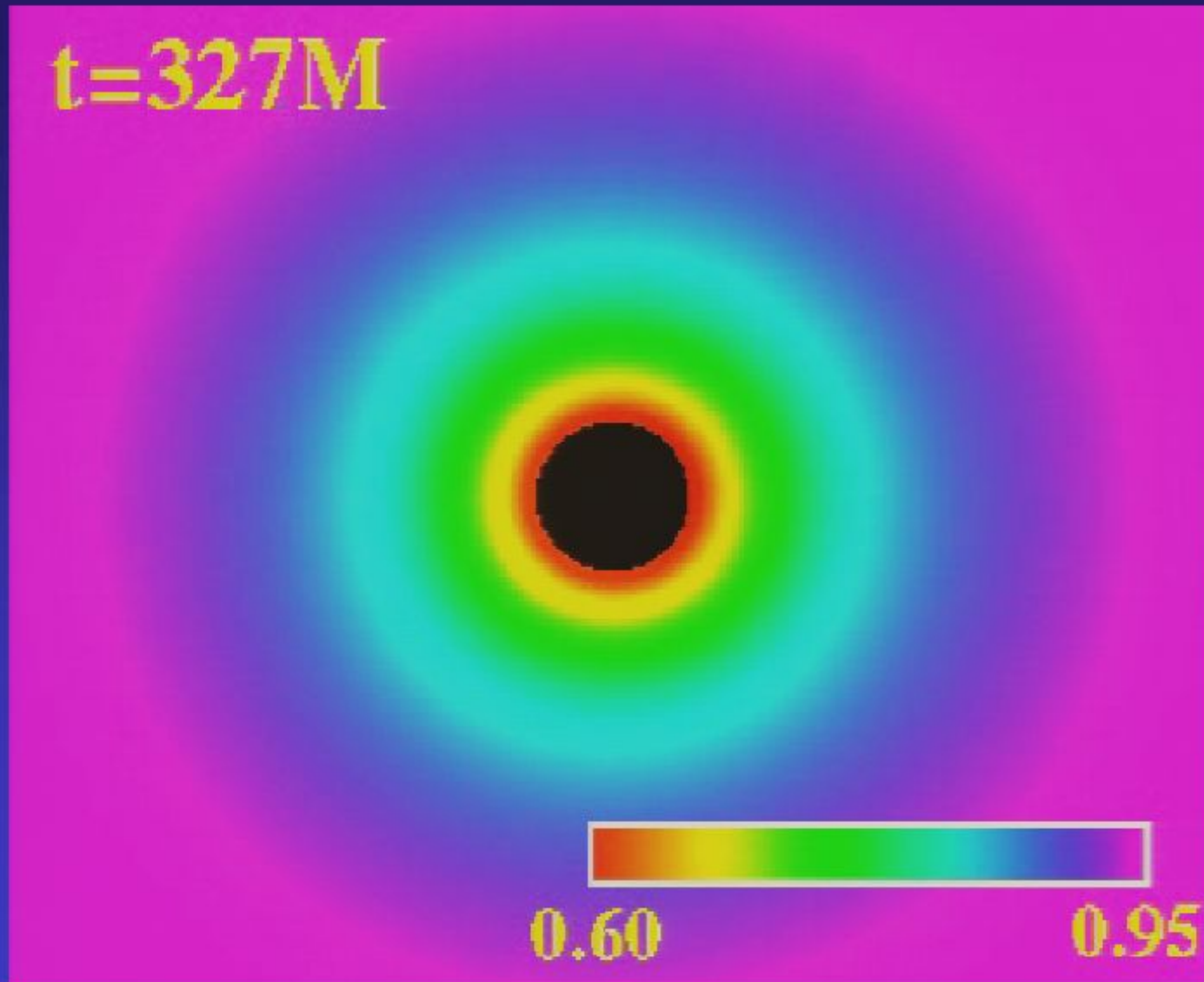
Lapse function α , orbital plane

t=261M

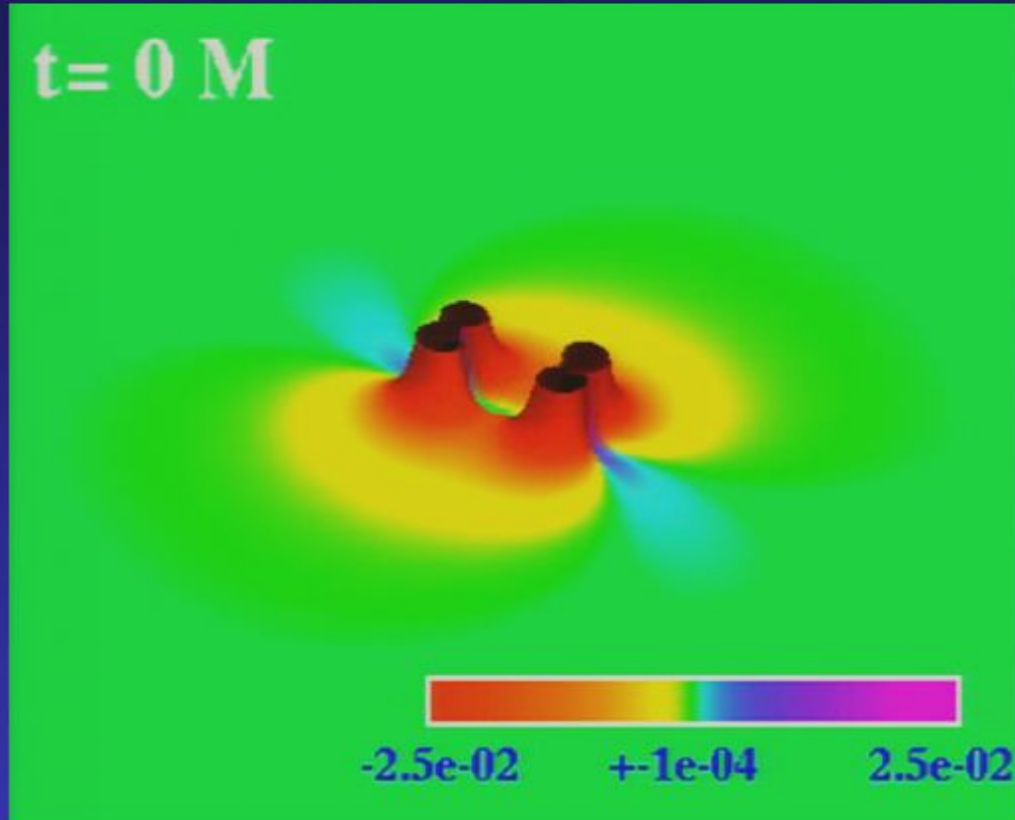


Lapse function α , orbital plane

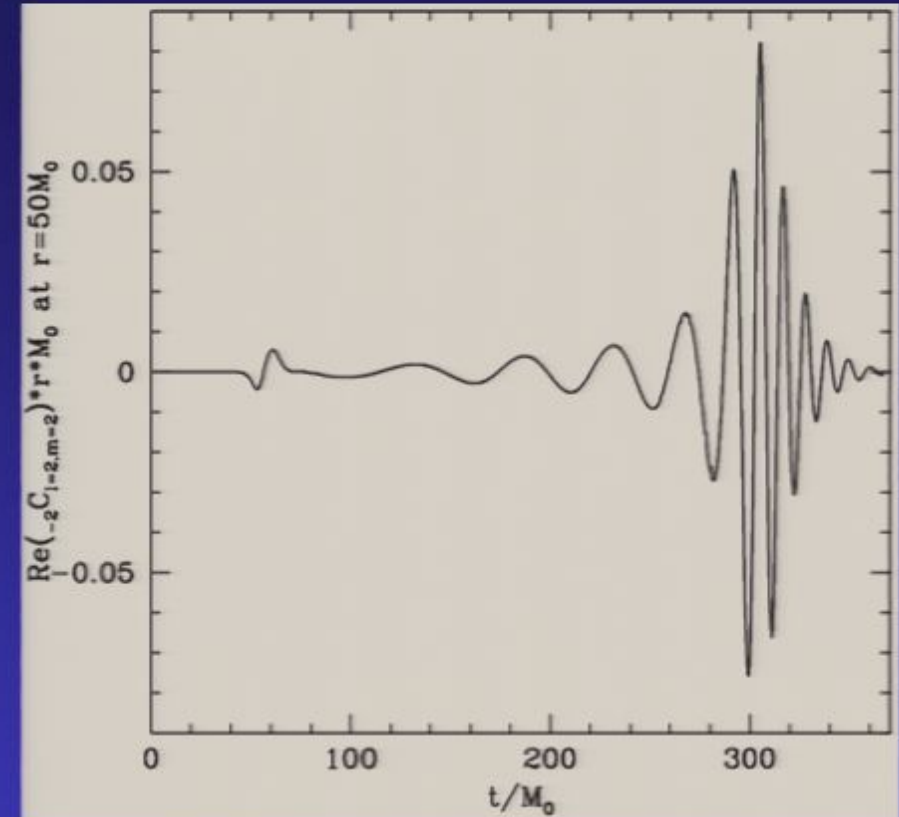
$t=327M$



Gravitational waves



Real component of the Newman-Penrose scalar Ψ_4 (times rM), orbital plane. Here, color and height of the surface represents the magnitude of Ψ_4 . Far from the source the real and imaginary components of Ψ_4 are just the second time derivatives of the "plus" and "cross" polarizations of the gravitational wave.

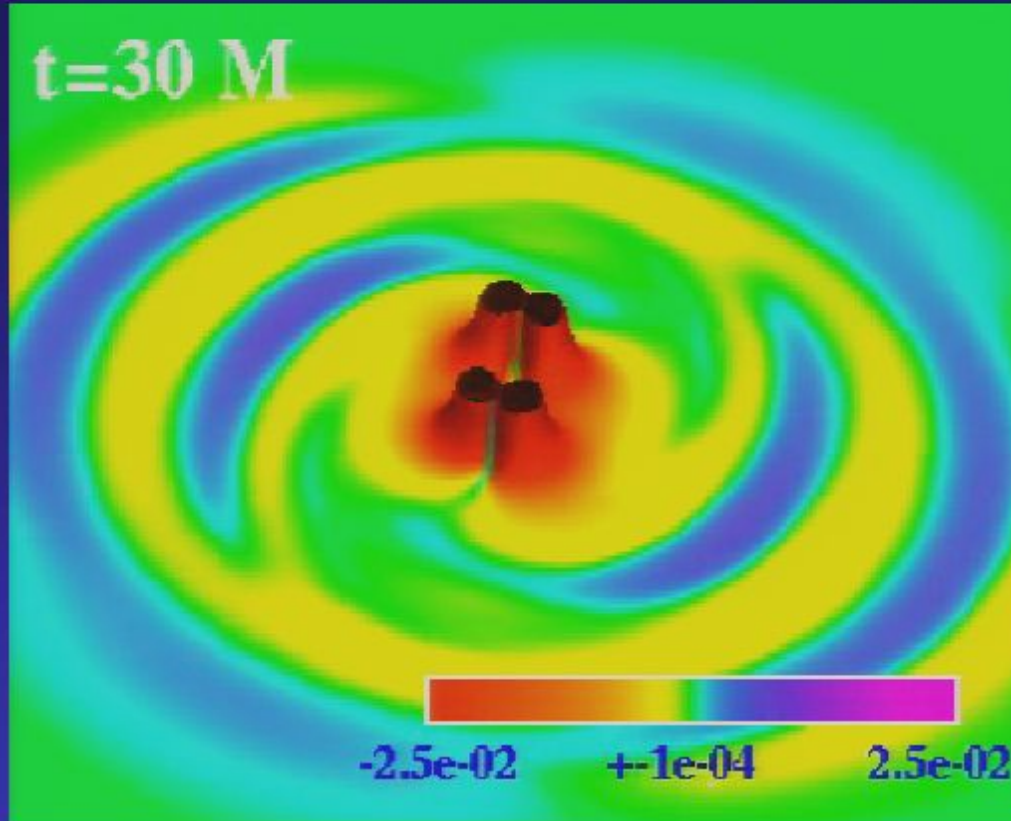


The real component of the spin -2 weight, $l=2$, $m=2$ spherical harmonic component of Ψ_4 times rM , measured at a coordinate distance of $50M$ from the center of the orbit.

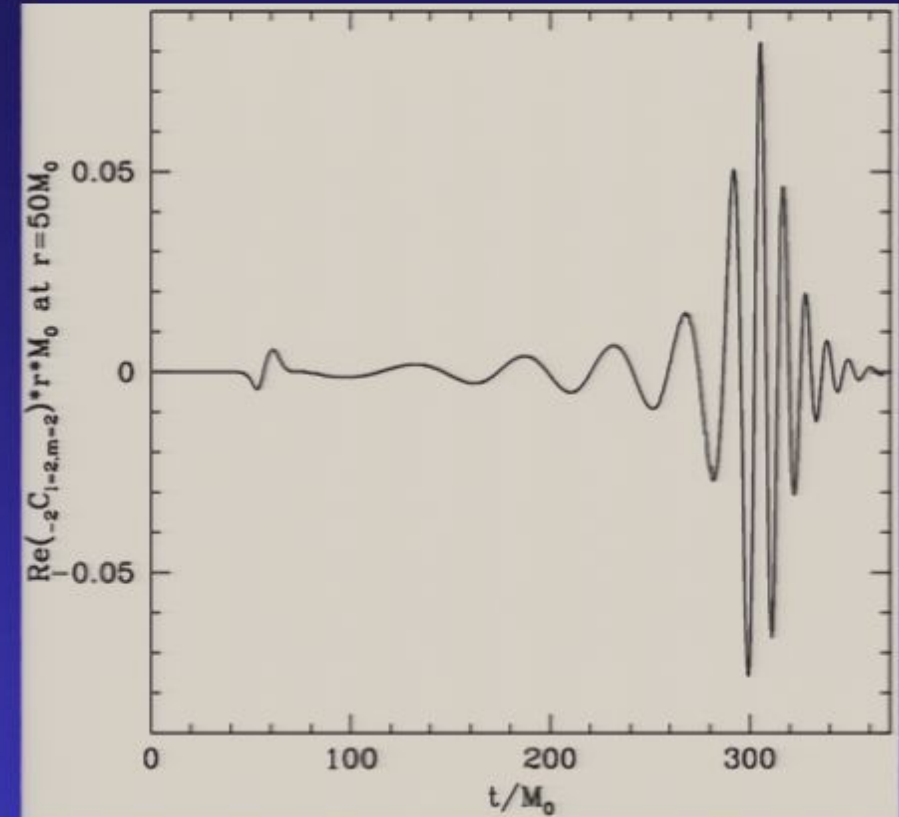
Convergence tests suggest dominant source of error is a near-linear drift in the phase of the waveform until a common horizon forms, which occurs $\sim 20M$ before the peak in amplitude.

Total phase error: $\pm 0.132\pi$

Gravitational waves



Real component of the Newman-Penrose scalar Ψ_4 (times rM), orbital plane. Here, color and height of the surface represents the magnitude of Ψ_4 . Far from the source the real and imaginary components of Ψ_4 are just the second time derivatives of the "plus" and "cross" polarizations of the gravitational wave.

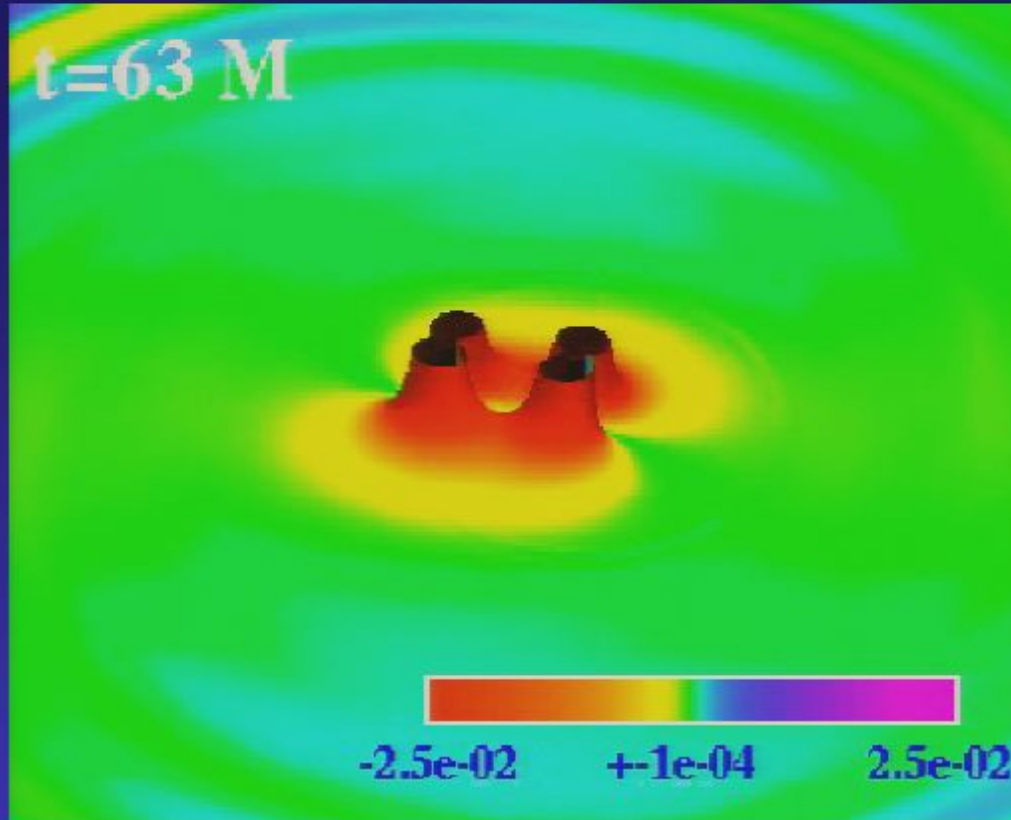


The real component of the spin -2 weight, $l=2$, $m=2$ spherical harmonic component of Ψ_4 times rM , measured at a coordinate distance of $50M$ from the center of the orbit.

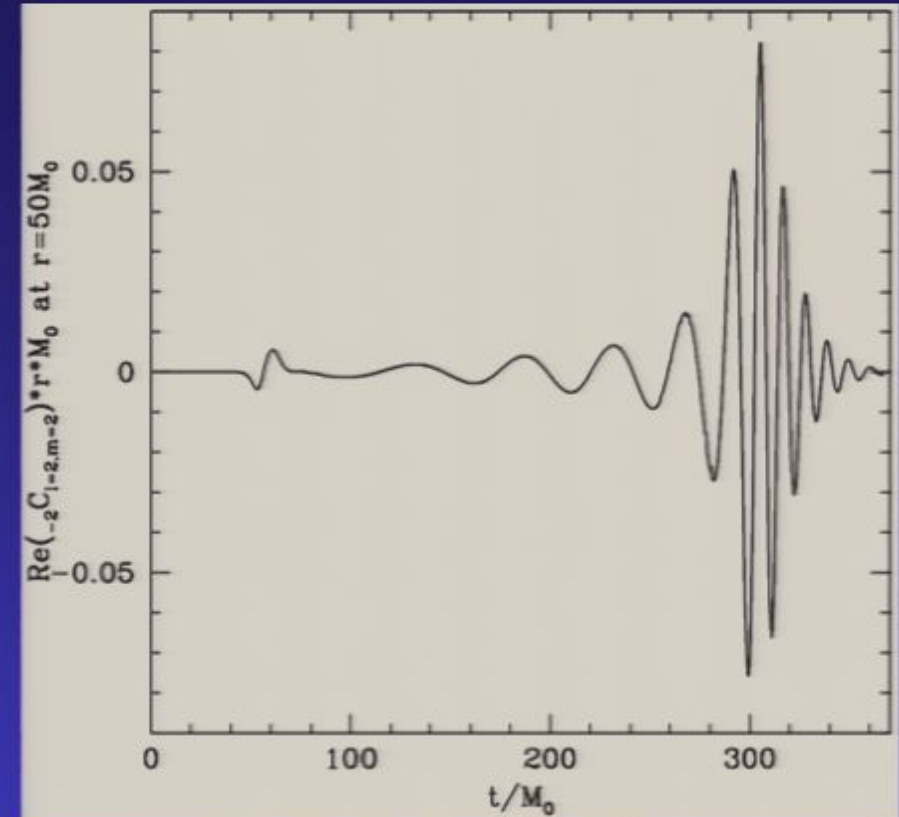
Convergence tests suggest dominant source of error is a near-linear drift in the phase of the waveform until a common horizon forms, which occurs $\sim 20M$ before the peak in amplitude.

Total phase error: $\pm 0.132\pi$

Gravitational waves



Real component of the Newman-Penrose scalar Ψ_4 (times rM), orbital plane. Here, color and height of the surface represents the magnitude of Ψ_4 . Far from the source the real and imaginary components of Ψ_4 are just the second time derivatives of the "plus" and "cross" polarizations of the gravitational wave.

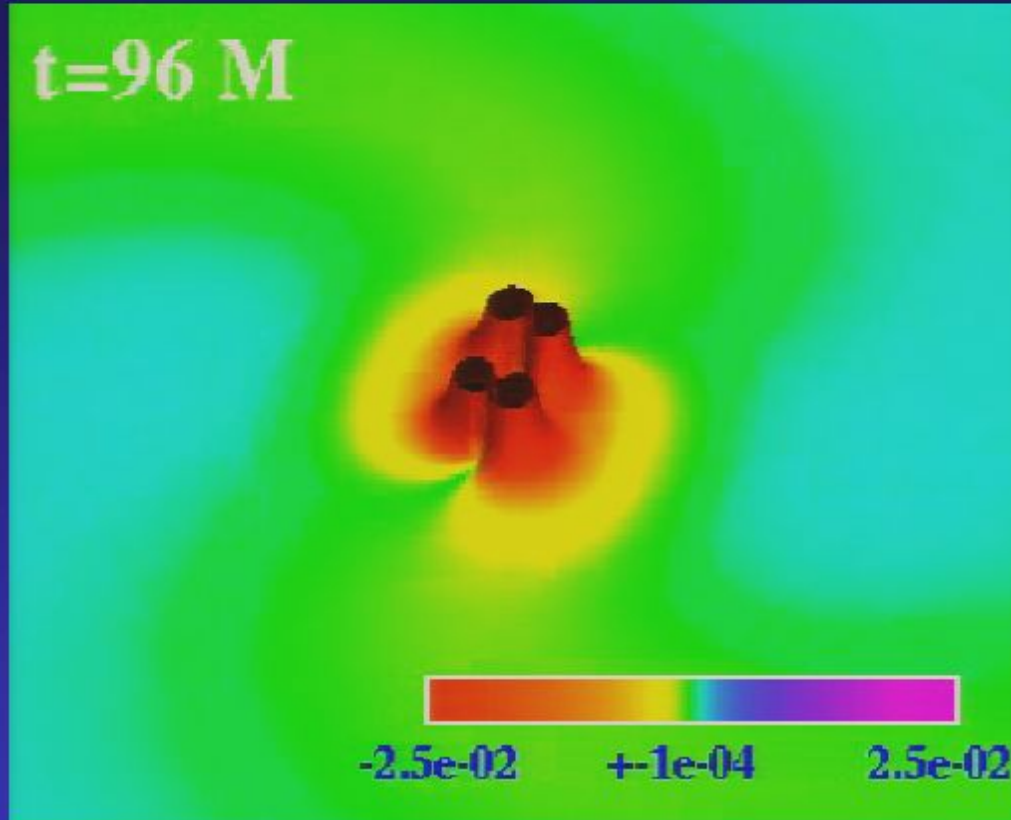


The real component of the spin -2 weight, $l=2$, $m=2$ spherical harmonic component of Ψ_4 times rM , measured at a coordinate distance of $50M$ from the center of the orbit.

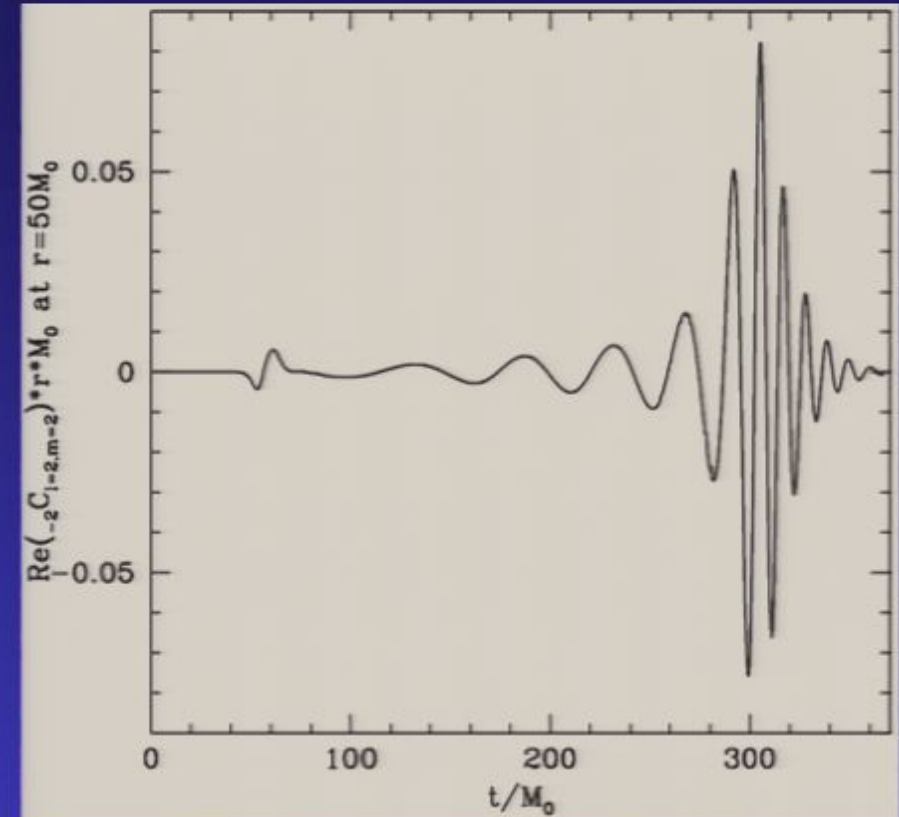
Convergence tests suggest dominant source of error is a near-linear drift in the phase of the waveform until a common horizon forms, which occurs $\sim 20M$ before the peak in amplitude.

Total phase error: $\pm 0.132\pi$

Gravitational waves



Real component of the Newman-Penrose scalar Ψ_4 (times rM), orbital plane. Here, color and height of the surface represents the magnitude of Ψ_4 . Far from the source the real and imaginary components of Ψ_4 are just the second time derivatives of the "plus" and "cross" polarizations of the gravitational wave.

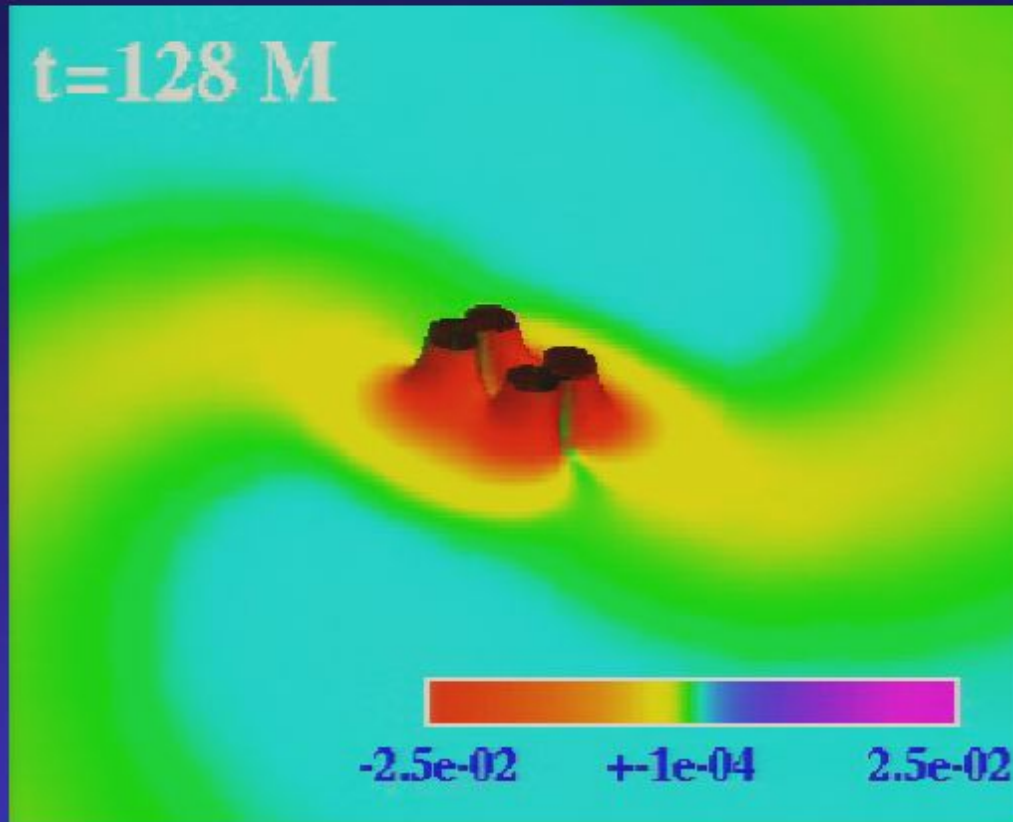


The real component of the spin -2 weight, $l=2$, $m=2$ spherical harmonic component of Ψ_4 times rM , measured at a coordinate distance of $50M$ from the center of the orbit.

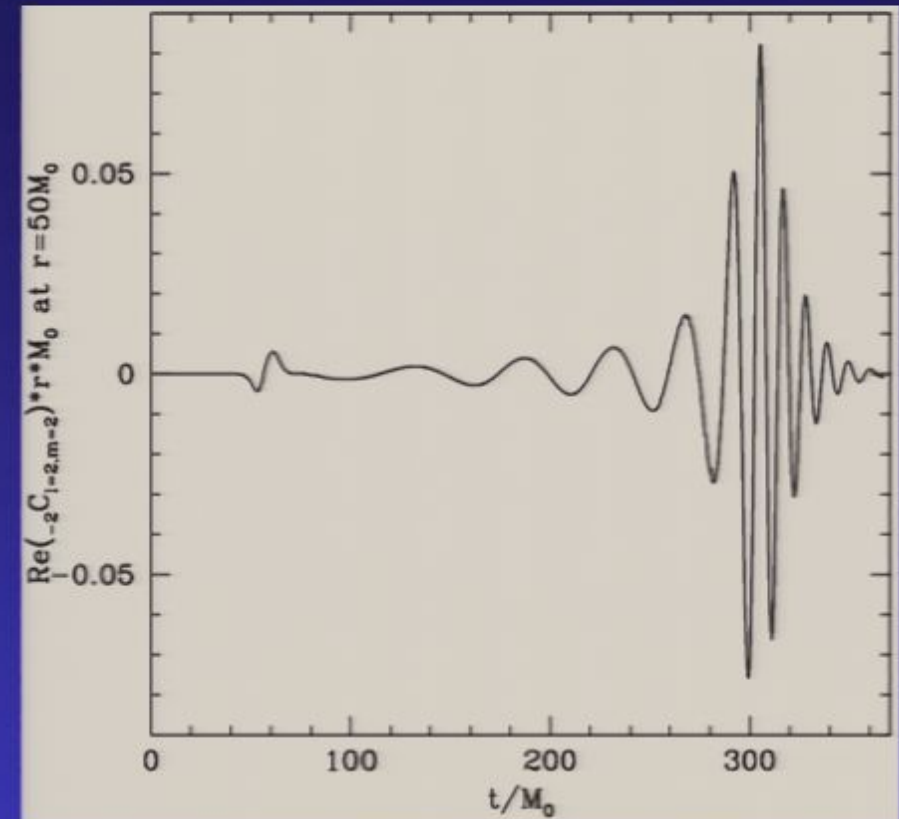
Convergence tests suggest dominant source of error is a near-linear drift in the phase of the waveform until a common horizon forms, which occurs $\sim 20M$ before the peak in amplitude.

Total phase error: $\pm 0.132\pi$

Gravitational waves



Real component of the Newman-Penrose scalar Ψ_4 (times rM), orbital plane. Here, color and height of the surface represents the magnitude of Ψ_4 . Far from the source the real and imaginary components of Ψ_4 are just the second time derivatives of the "plus" and "cross" polarizations of the gravitational wave.

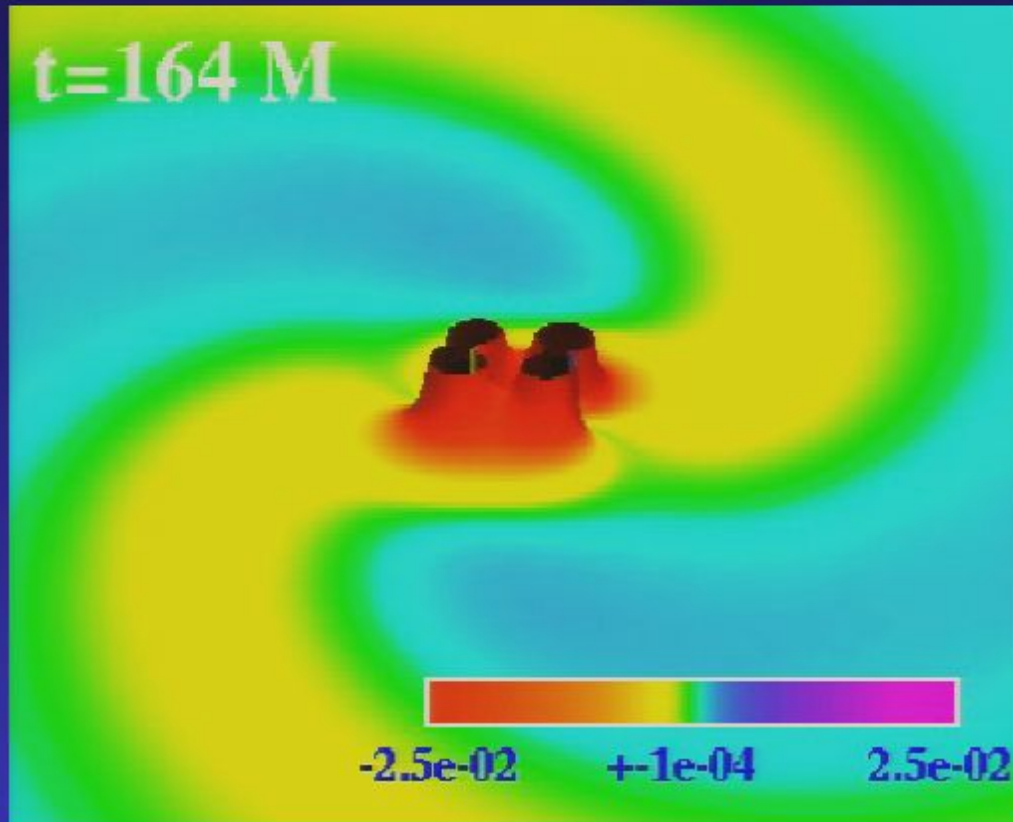


The real component of the spin -2 weight, $l=2$, $m=2$ spherical harmonic component of Ψ_4 times rM , measured at a coordinate distance of $50M$ from the center of the orbit.

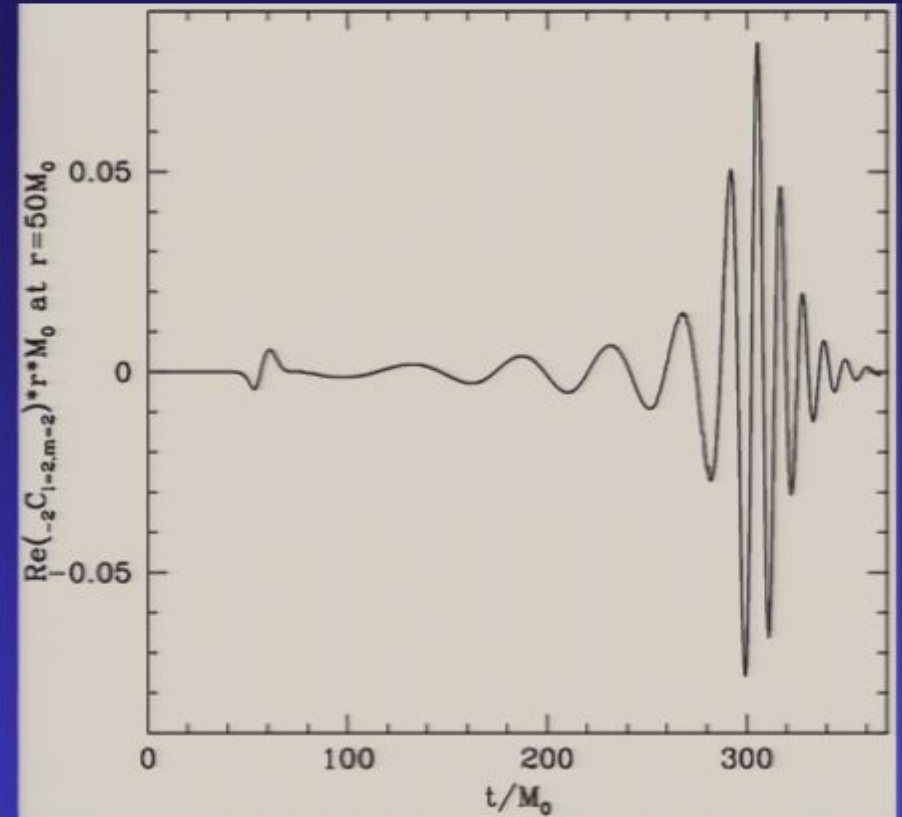
Convergence tests suggest dominant source of error is a near-linear drift in the phase of the waveform until a common horizon forms, which occurs $\sim 20M$ before the peak in amplitude.

Total phase error: $\pm 0.132\pi$

Gravitational waves



Real component of the Newman-Penrose scalar Ψ_4 (times rM), orbital plane. Here, color and height of the surface represents the magnitude of Ψ_4 . Far from the source the real and imaginary components of Ψ_4 are just the second time derivatives of the "plus" and "cross" polarizations of the gravitational wave.

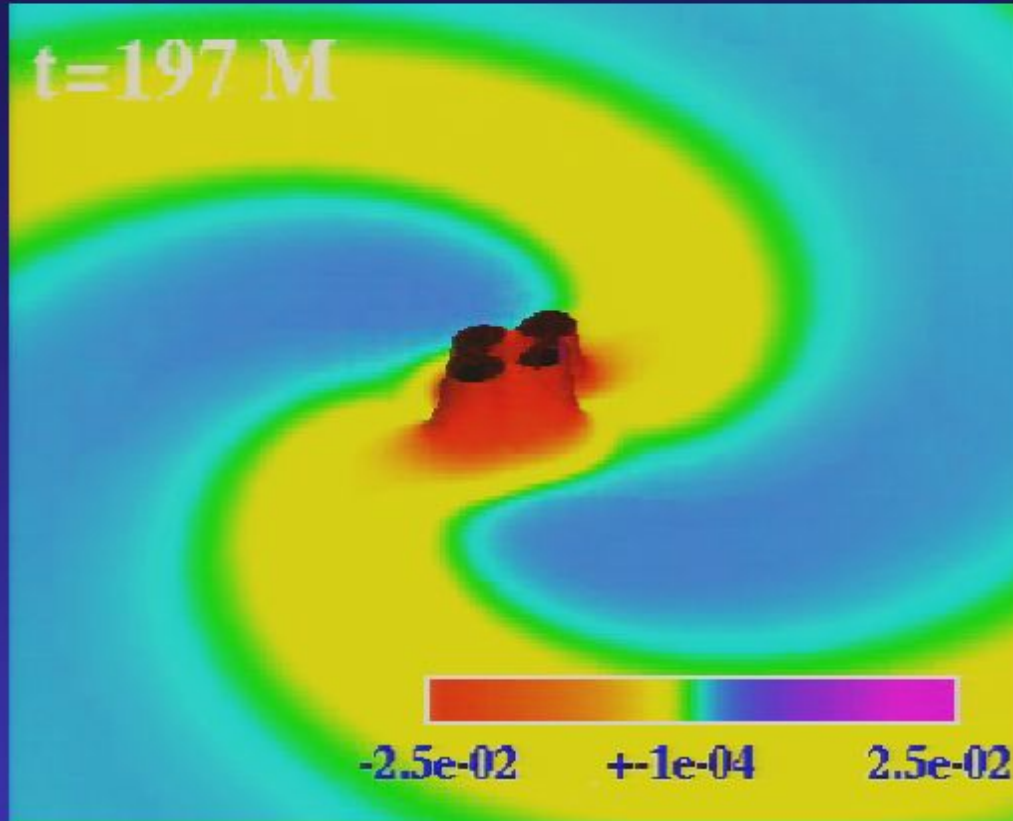


The real component of the spin -2 weight, $l=2$, $m=2$ spherical harmonic component of Ψ_4 times rM , measured at a coordinate distance of $50M$ from the center of the orbit.

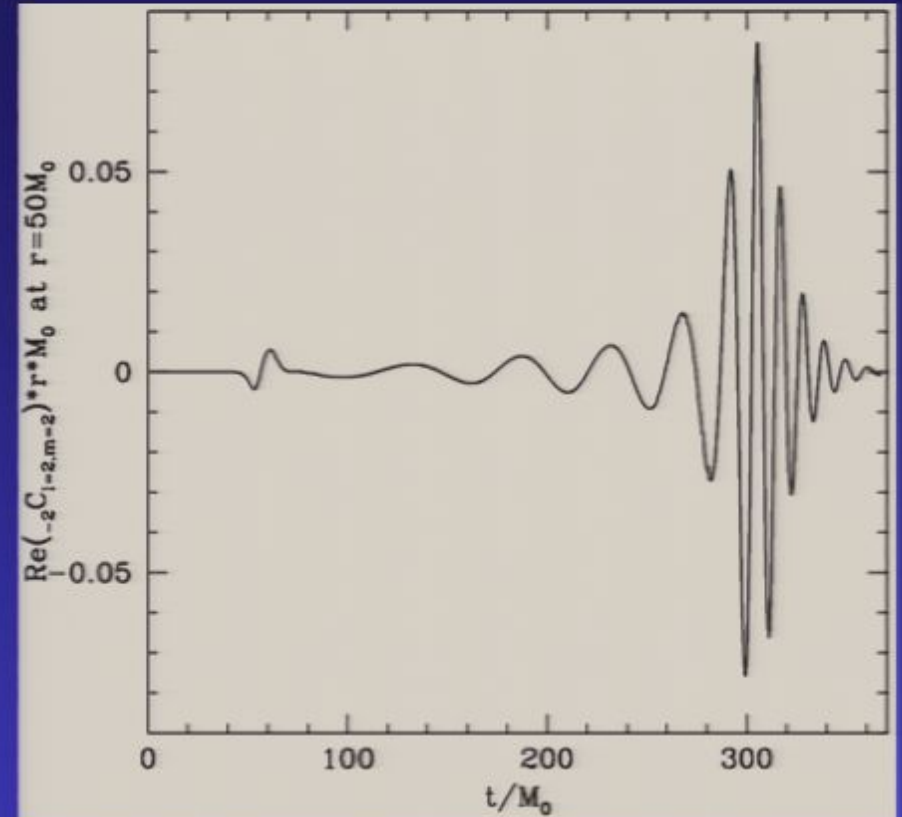
Convergence tests suggest dominant source of error is a near-linear drift in the phase of the waveform until a common horizon forms, which occurs $\sim 20M$ before the peak in amplitude.

Total phase error: $\pm 0.132\pi$

Gravitational waves



Real component of the Newman-Penrose scalar Ψ_4 (times rM), orbital plane. Here, color and height of the surface represents the magnitude of Ψ_4 . Far from the source the real and imaginary components of Ψ_4 are just the second time derivatives of the "plus" and "cross" polarizations of the gravitational wave.

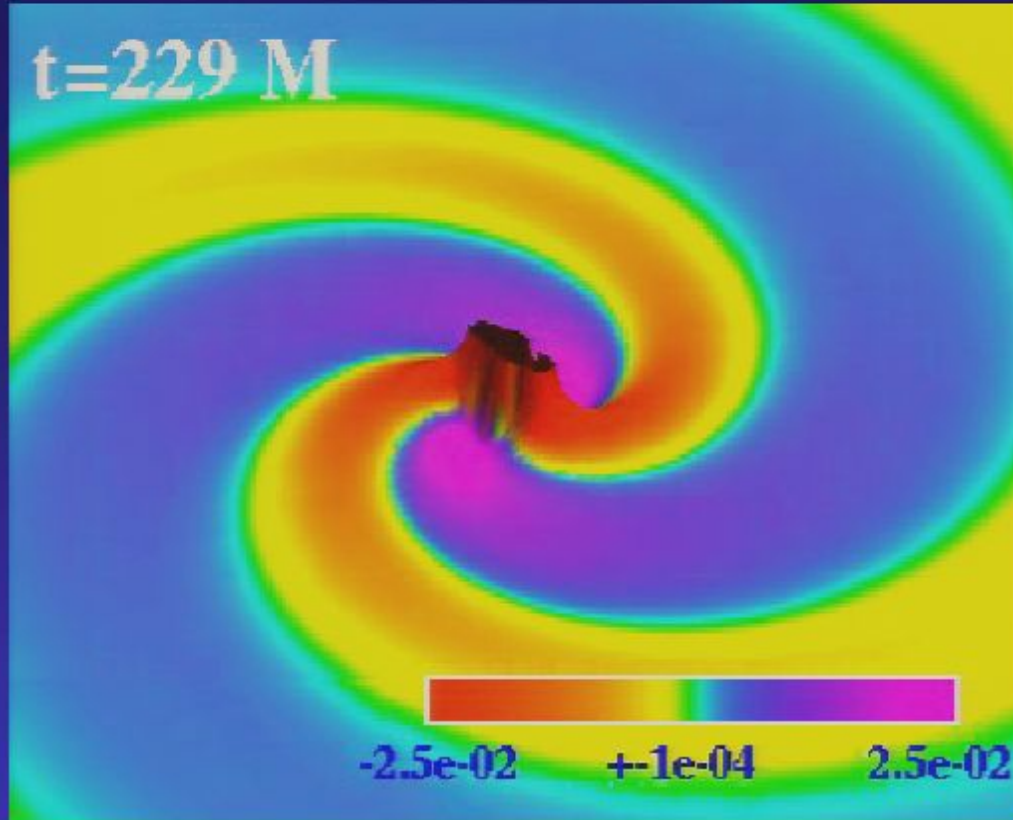


The real component of the spin -2 weight, $l=2$, $m=2$ spherical harmonic component of Ψ_4 times rM , measured at a coordinate distance of $50M$ from the center of the orbit.

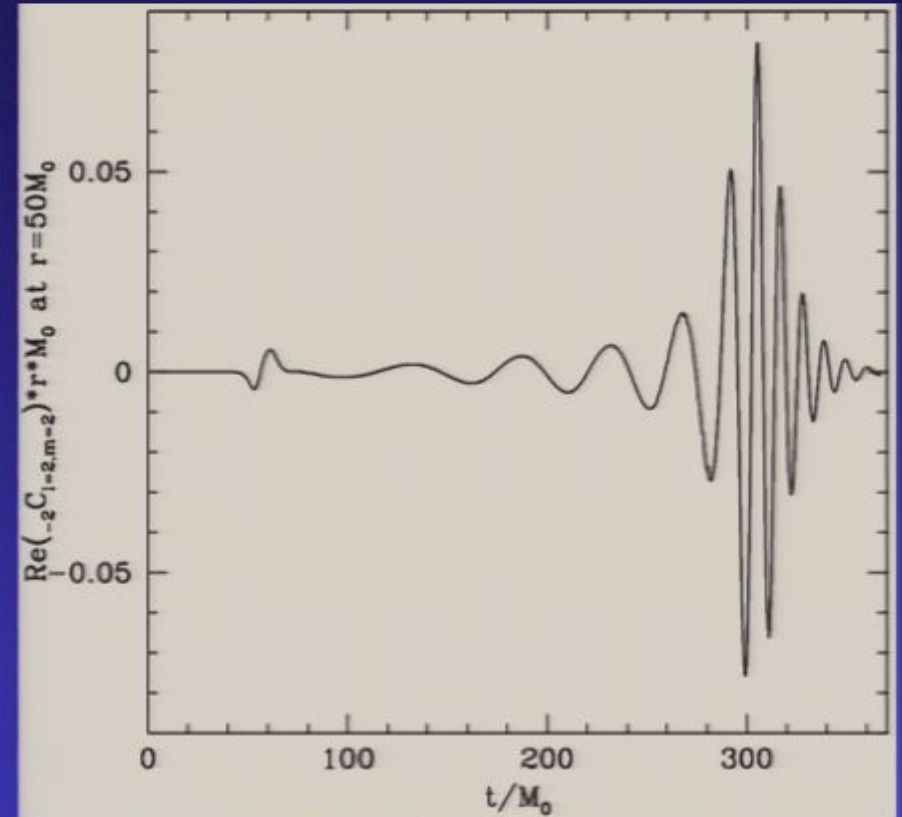
Convergence tests suggest dominant source of error is a near-linear drift in the phase of the waveform until a common horizon forms, which occurs $\sim 20M$ before the peak in amplitude.

Total phase error: $\pm 0.132\pi$

Gravitational waves



Real component of the Newman-Penrose scalar Ψ_4 (times rM), orbital plane. Here, color and height of the surface represents the magnitude of Ψ_4 . Far from the source the real and imaginary components of Ψ_4 are just the second time derivatives of the "plus" and "cross" polarizations of the gravitational wave.

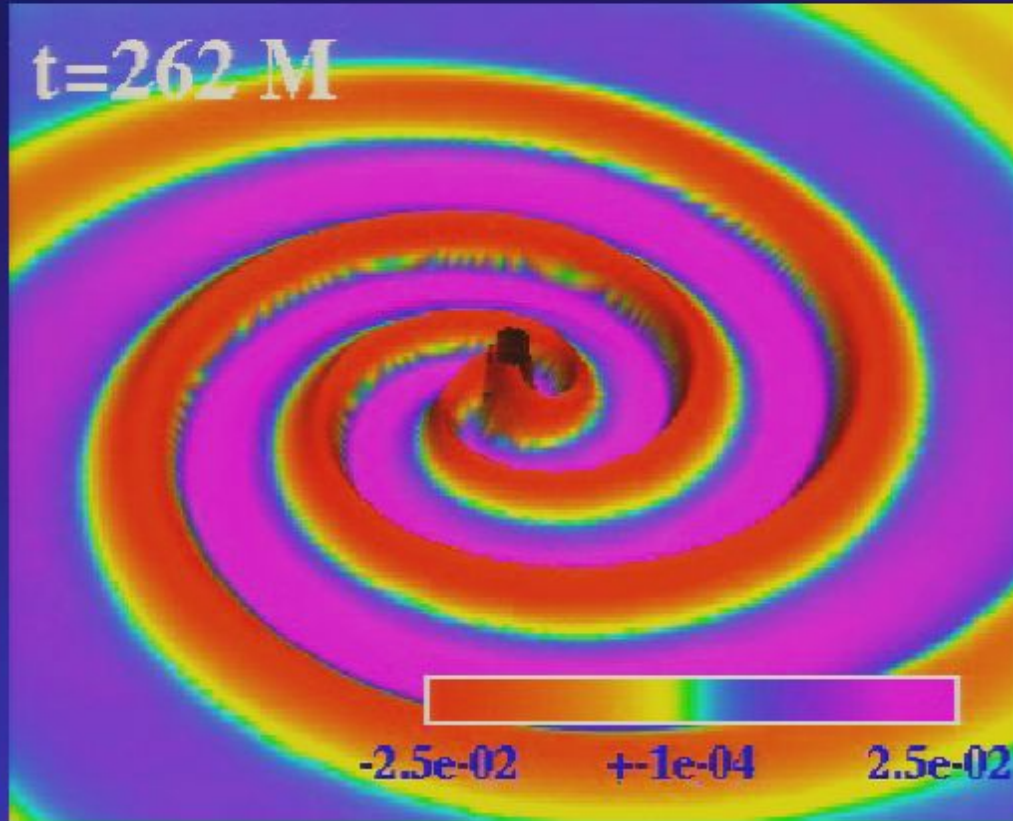


The real component of the spin -2 weight, $l=2$, $m=2$ spherical harmonic component of Ψ_4 times rM , measured at a coordinate distance of $50M$ from the center of the orbit.

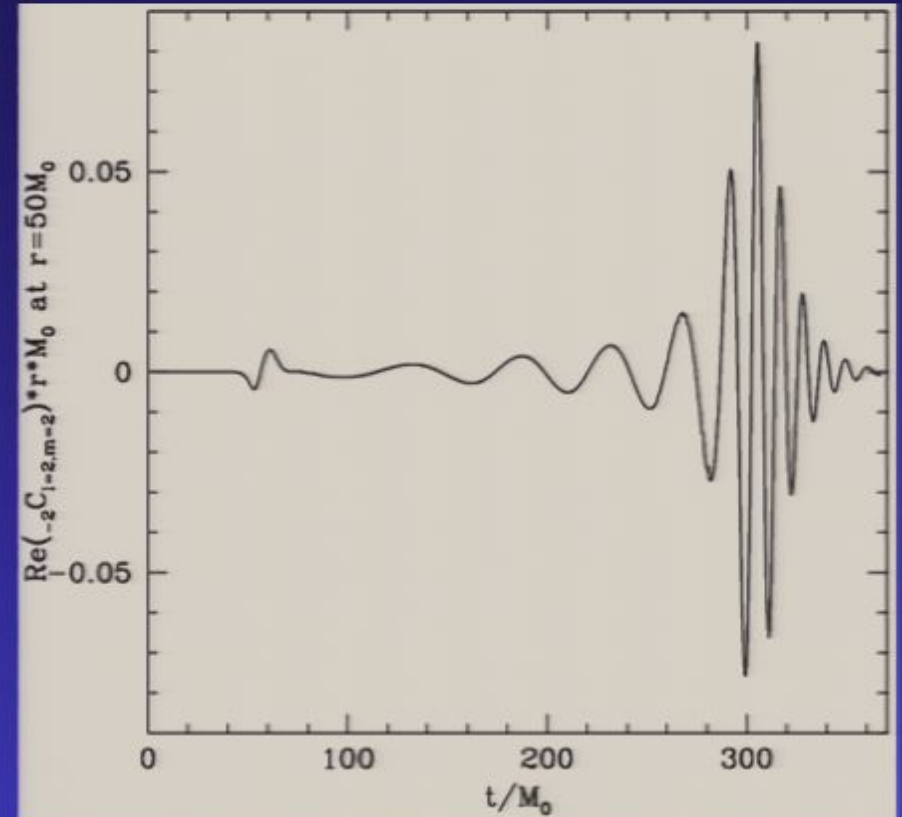
Convergence tests suggest dominant source of error is a near-linear drift in the phase of the waveform until a common horizon forms, which occurs $\sim 20M$ before the peak in amplitude.

Total phase error: $\pm 0.132\pi$

Gravitational waves



Real component of the Newman-Penrose scalar Ψ_4 (times rM), orbital plane. Here, color and height of the surface represents the magnitude of Ψ_4 . Far from the source the real and imaginary components of Ψ_4 are just the second time derivatives of the "plus" and "cross" polarizations of the gravitational wave.

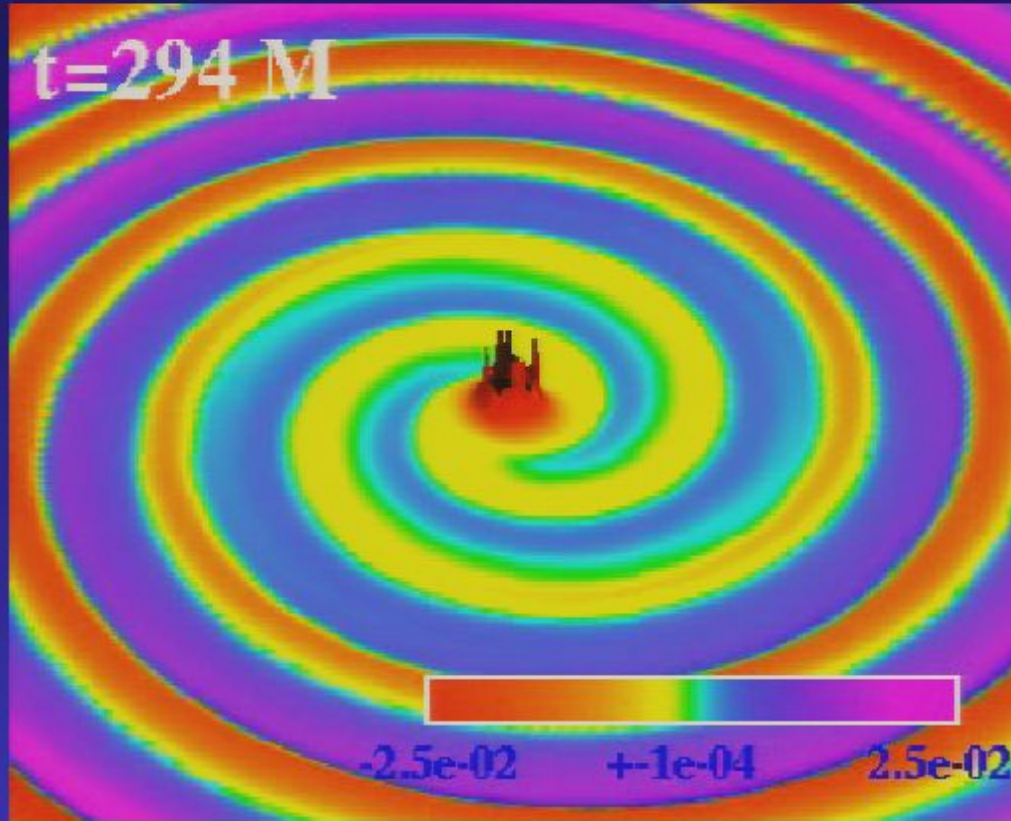


The real component of the spin -2 weight, $l=2$, $m=2$ spherical harmonic component of Ψ_4 times rM , measured at a coordinate distance of $50M$ from the center of the orbit.

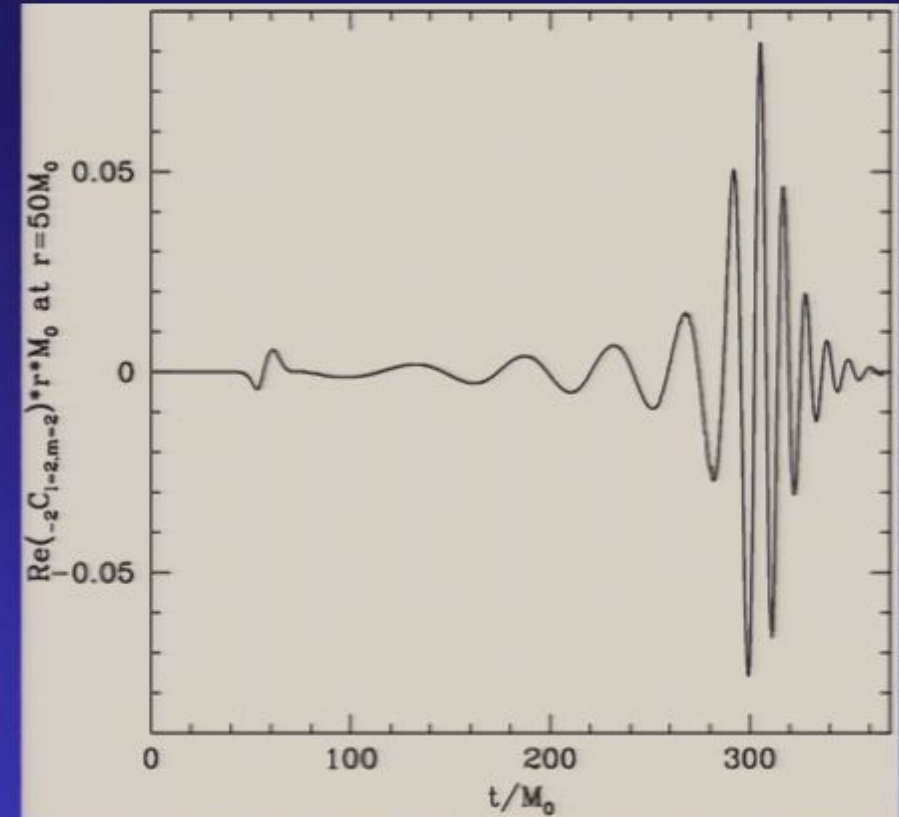
Convergence tests suggest dominant source of error is a near-linear drift in the phase of the waveform until a common horizon forms, which occurs $\sim 20M$ before the peak in amplitude.

Total phase error: $\pm 0.132\pi$

Gravitational waves



Real component of the Newman-Penrose scalar Ψ_4 (times rM), orbital plane. Here, color and height of the surface represents the magnitude of Ψ_4 . Far from the source the real and imaginary components of Ψ_4 are just the second time derivatives of the "plus" and "cross" polarizations of the gravitational wave.

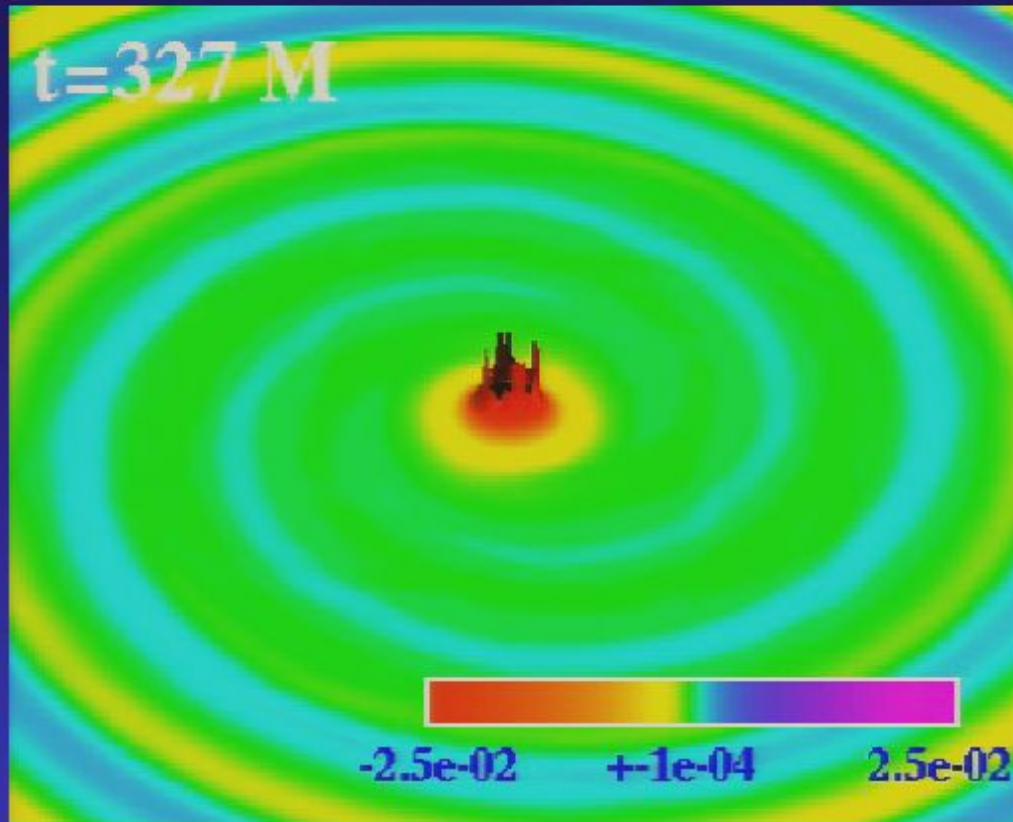


The real component of the spin -2 weight, $l=2$, $m=2$ spherical harmonic component of Ψ_4 times rM , measured at a coordinate distance of $50M$ from the center of the orbit.

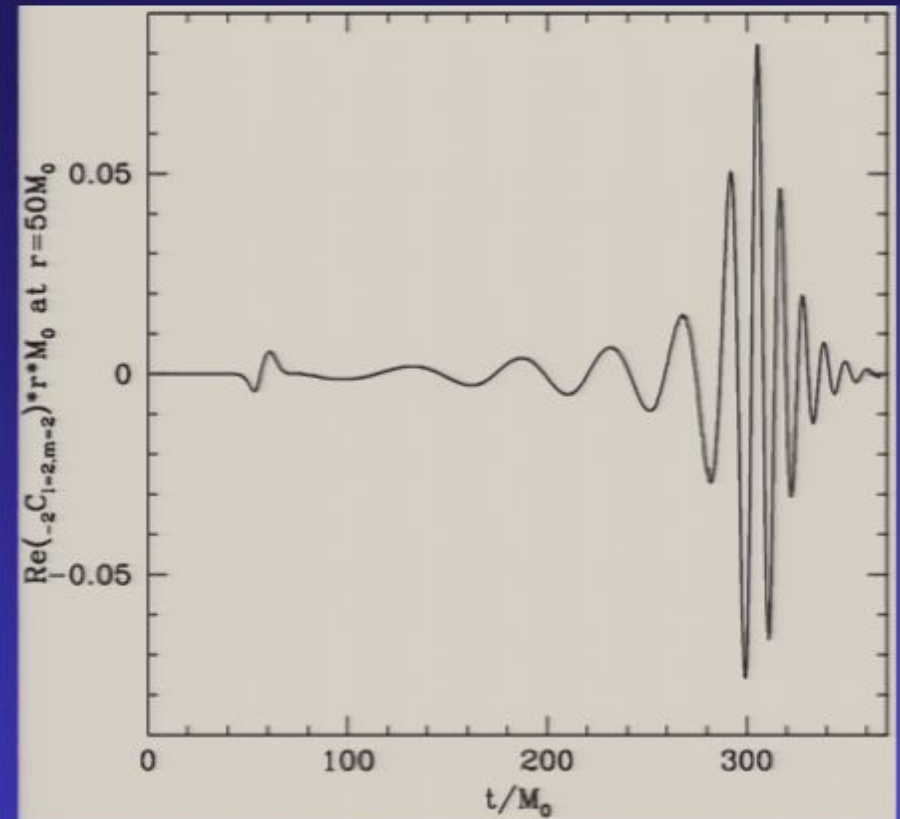
Convergence tests suggest dominant source of error is a near-linear drift in the phase of the waveform until a common horizon forms, which occurs $\sim 20M$ before the peak in amplitude.

Total phase error: $\pm 0.132\pi$

Gravitational waves



Real component of the Newman-Penrose scalar Ψ_4 (times rM), orbital plane. Here, color and height of the surface represents the magnitude of Ψ_4 . Far from the source the real and imaginary components of Ψ_4 are just the second time derivatives of the "plus" and "cross" polarizations of the gravitational wave.

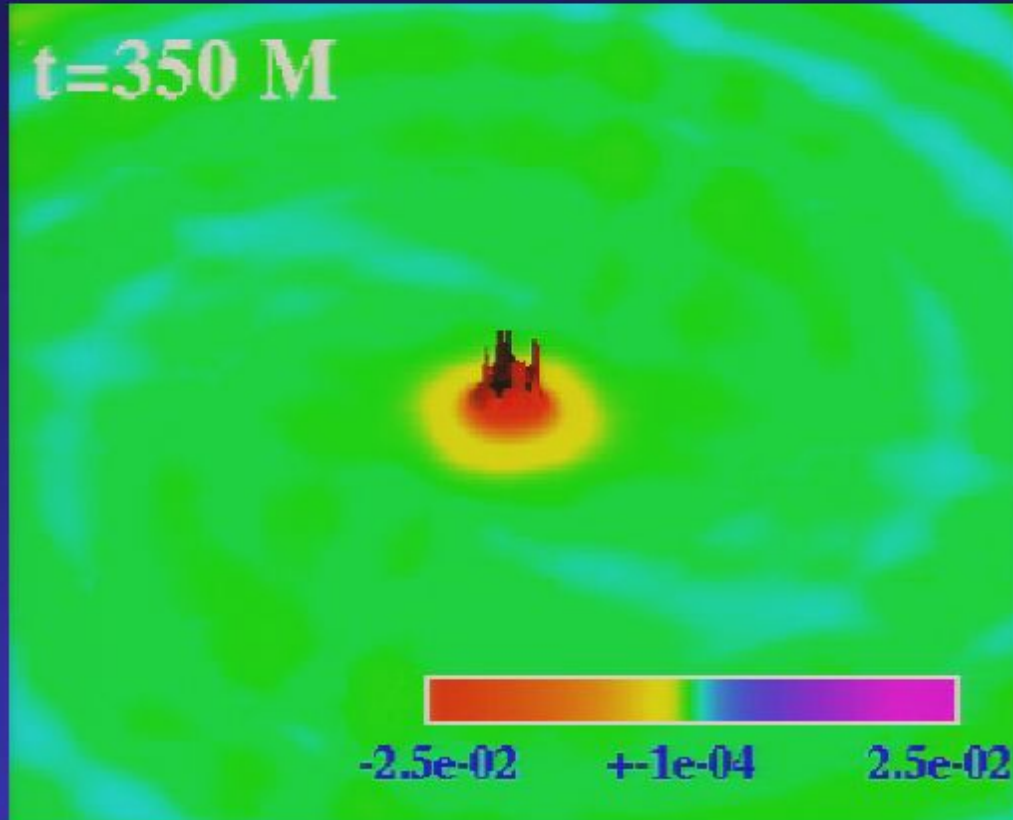


The real component of the spin -2 weight, $l=2$, $m=2$ spherical harmonic component of Ψ_4 times rM , measured at a coordinate distance of $50M$ from the center of the orbit.

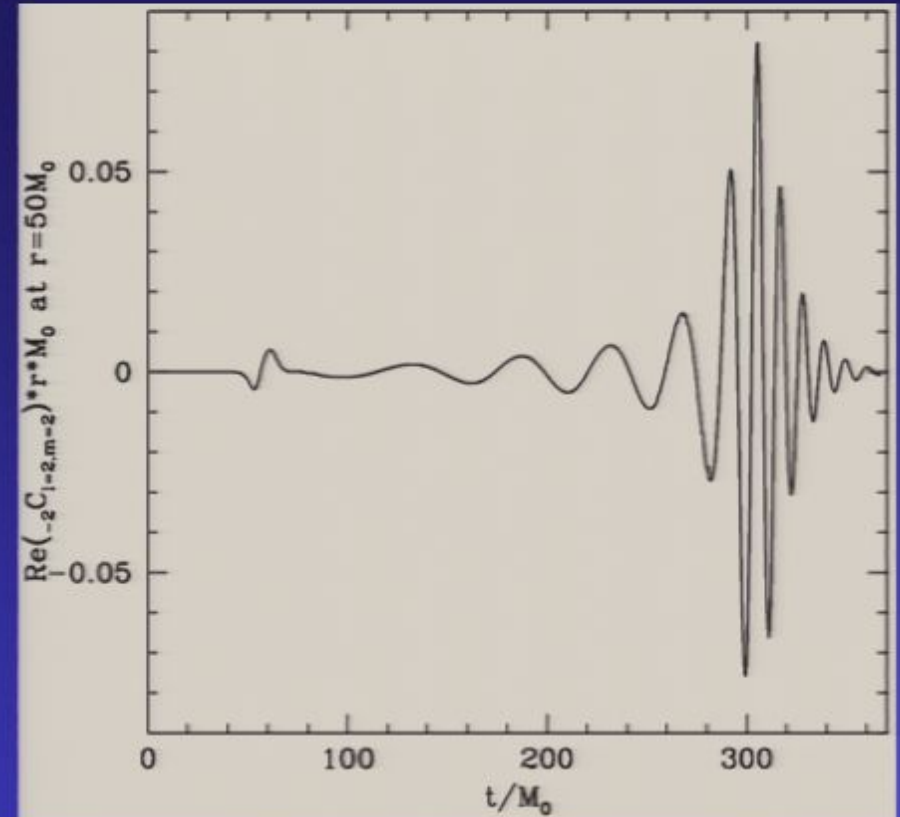
Convergence tests suggest dominant source of error is a near-linear drift in the phase of the waveform until a common horizon forms, which occurs $\sim 20M$ before the peak in amplitude.

Total phase error: $\pm 0.132\pi$

Gravitational waves



Real component of the Newman-Penrose scalar Ψ_4 (times rM), orbital plane. Here, color and height of the surface represents the magnitude of Ψ_4 . Far from the source the real and imaginary components of Ψ_4 are just the second time derivatives of the "plus" and "cross" polarizations of the gravitational wave.



The real component of the spin -2 weight, $l=2$, $m=2$ spherical harmonic component of Ψ_4 times rM , measured at a coordinate distance of $50M$ from the center of the orbit.

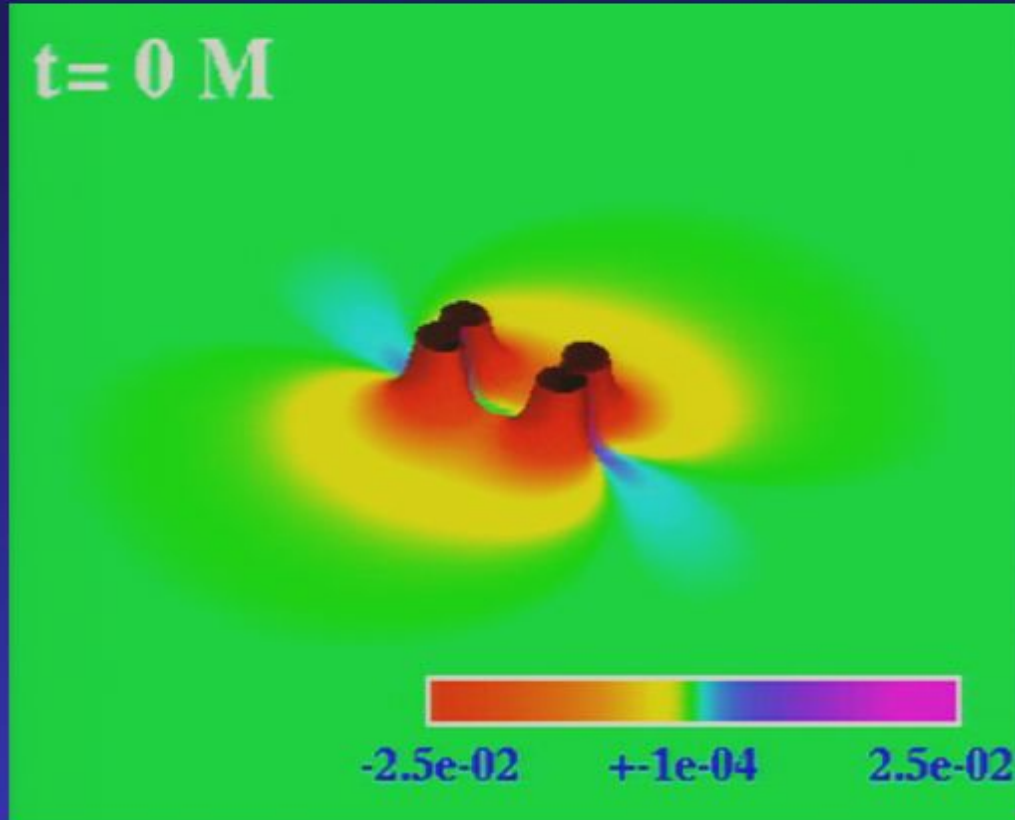
Convergence tests suggest dominant source of error is a near-linear drift in the phase of the waveform until a common horizon forms, which occurs $\sim 20M$ before the peak in amplitude.

Total phase error: $\pm 0.132\pi$

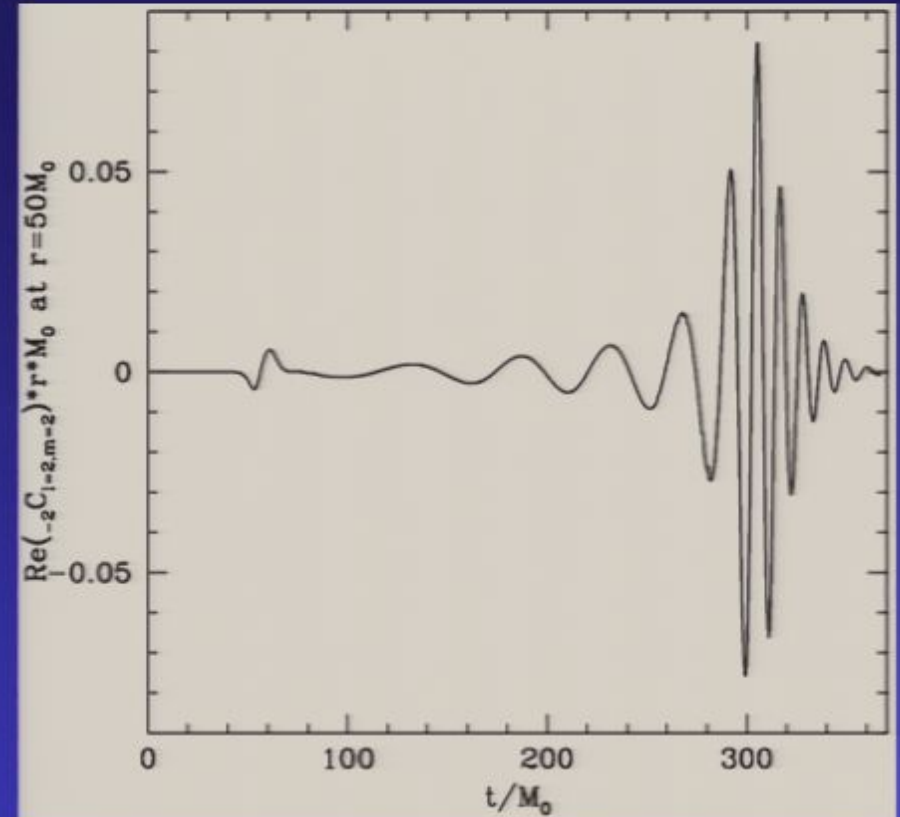
What does this wave represent?

- Scale the system to two **10 solar mass** ($\sim 2 \times 10^{31}$ kg) BHs
 - radius of each black hole in the binary is ~ 30 km
 - radius of final black hole is ~ 60 km
 - distance from the final black hole where the wave was measured ~ 1500 km
 - frequency of the wave ~ 200 Hz (early inspiral) - 800Hz (ring-down)
 - fractional oscillatory “distortion” in space induced by the wave transverse to the direction of propagation has a *maximum* amplitude $\Delta L/L \sim 3 \times 10^{-3}$
 - a 2m tall person will get stretched/squeezed by ~ 6 mm as the wave passes
 - LIGO’s arm length would change by ~ 12 m. Wave amplitude decays like 1/distance from source; e.g. at 10Mpc the change in arms $\sim 5 \times 10^{-17}$ m (1/20 the radius of a proton, which is well within the ballpark of what LIGO is trying to measure!!)
 - despite the seemingly small amplitude for the wave, the energy it carries is enormous — around $10^{30} \text{ kg } c^2 \sim 10^{47} \text{ J} \sim 10^{54} \text{ ergs}$ (peak luminosity is about 1/100th the Planck luminosity of 10^{59} ergs/s !!)

Gravitational waves



Real component of the Newman-Penrose scalar Ψ_4 (times rM), orbital plane. Here, color and height of the surface represents the magnitude of Ψ_4 . Far from the source the real and imaginary components of Ψ_4 are just the second time derivatives of the "plus" and "cross" polarizations of the gravitational wave.



The real component of the spin -2 weight, $l=2$, $m=2$ spherical harmonic component of Ψ_4 times rM , measured at a coordinate distance of $50M$ from the center of the orbit.

Convergence tests suggest dominant source of error is a near-linear drift in the phase of the waveform until a common horizon forms, which occurs $\sim 20M$ before the peak in amplitude.

Total phase error: $\pm 0.132\pi$

What does this wave represent?

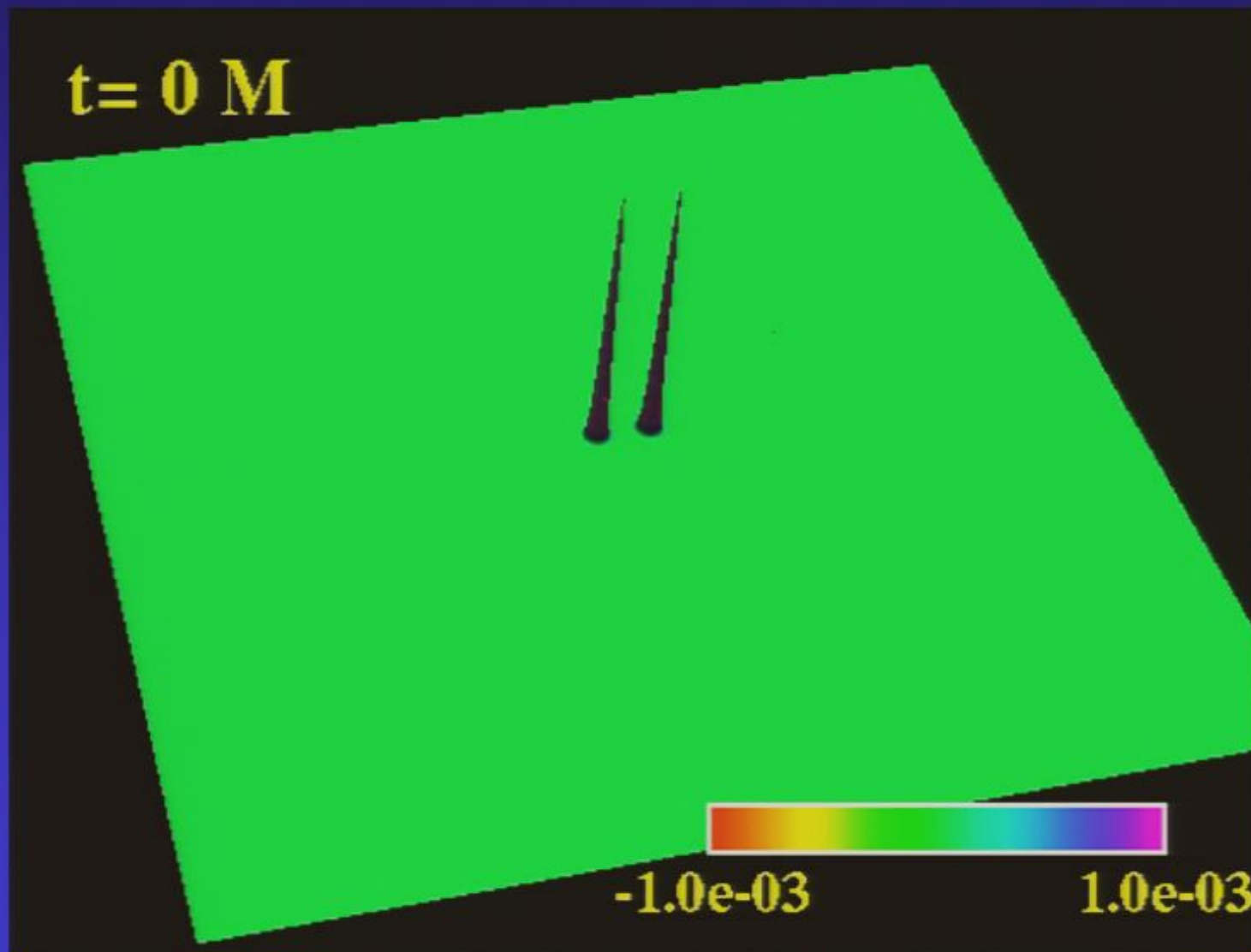
- Scale the system to two **10 solar mass** ($\sim 2 \times 10^{31}$ kg) BHs
 - radius of each black hole in the binary is ~ 30 km
 - radius of final black hole is ~ 60 km
 - distance from the final black hole where the wave was measured ~ 1500 km
 - frequency of the wave ~ 200 Hz (early inspiral) - 800Hz (ring-down)
 - fractional oscillatory “distortion” in space induced by the wave transverse to the direction of propagation has a *maximum* amplitude $\Delta L/L \sim 3 \times 10^{-3}$
 - a 2m tall person will get stretched/squeezed by ~ 6 mm as the wave passes
 - LIGO’s arm length would change by ~ 12 m. Wave amplitude decays like 1/distance from source; e.g. at 10Mpc the change in arms $\sim 5 \times 10^{-17}$ m (1/20 the radius of a proton, which is well within the ballpark of what LIGO is trying to measure!!)
 - despite the seemingly small amplitude for the wave, the energy it carries is enormous — around 10^{30} kg $c^2 \sim 10^{47}$ J $\sim 10^{54}$ ergs (peak luminosity is about 1/100th the Planck luminosity of 10^{59} ergs/s !!)

Scalar field collapse driven binaries

- Look at equal mass mergers
 - initial scalar field pulses separated a coordinate (proper) distance $8.9M$ ($10.8M$) on the x-axis, one boosted by v in the $+y$ direction, the other by v in the $-y$ direction
 - note, resultant black hole velocities are related to, but not equal to v
- To find interesting orbital dynamics, tune the parameter v to get as many orbits as possible
 - in the limit as v goes to 0, get head-on collisions
 - in the large v limit, black holes are deflected but fly apart
- Generically these black hole binaries will have some eccentricity (not easy to define given how close they are initially), and so arguably of less astrophysical significance
 - want to explore the non-linear interaction of BH's in full general relativity

Scalar field $\phi.r$, compactified (code) coordinates

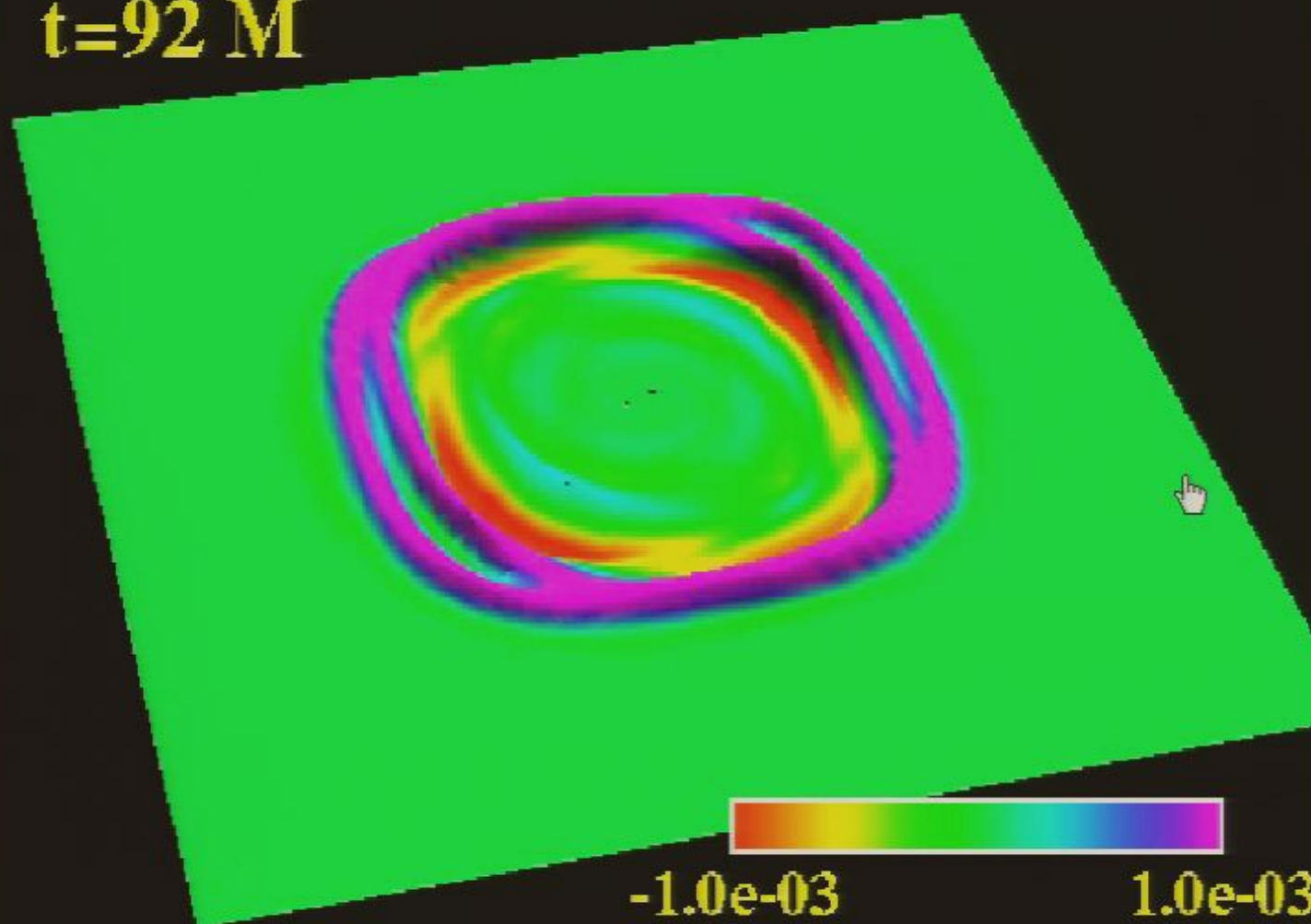
$$\bar{x} = \tan(x\pi/2), \bar{y} = \tan(y\pi/2), \bar{z} = \tan(z\pi/2)$$



Scalar field $\phi.r$, compactified (code) coordinates

$$\bar{x} = \tan(x\pi/2), \bar{y} = \tan(y\pi/2), \bar{z} = \tan(z\pi/2)$$

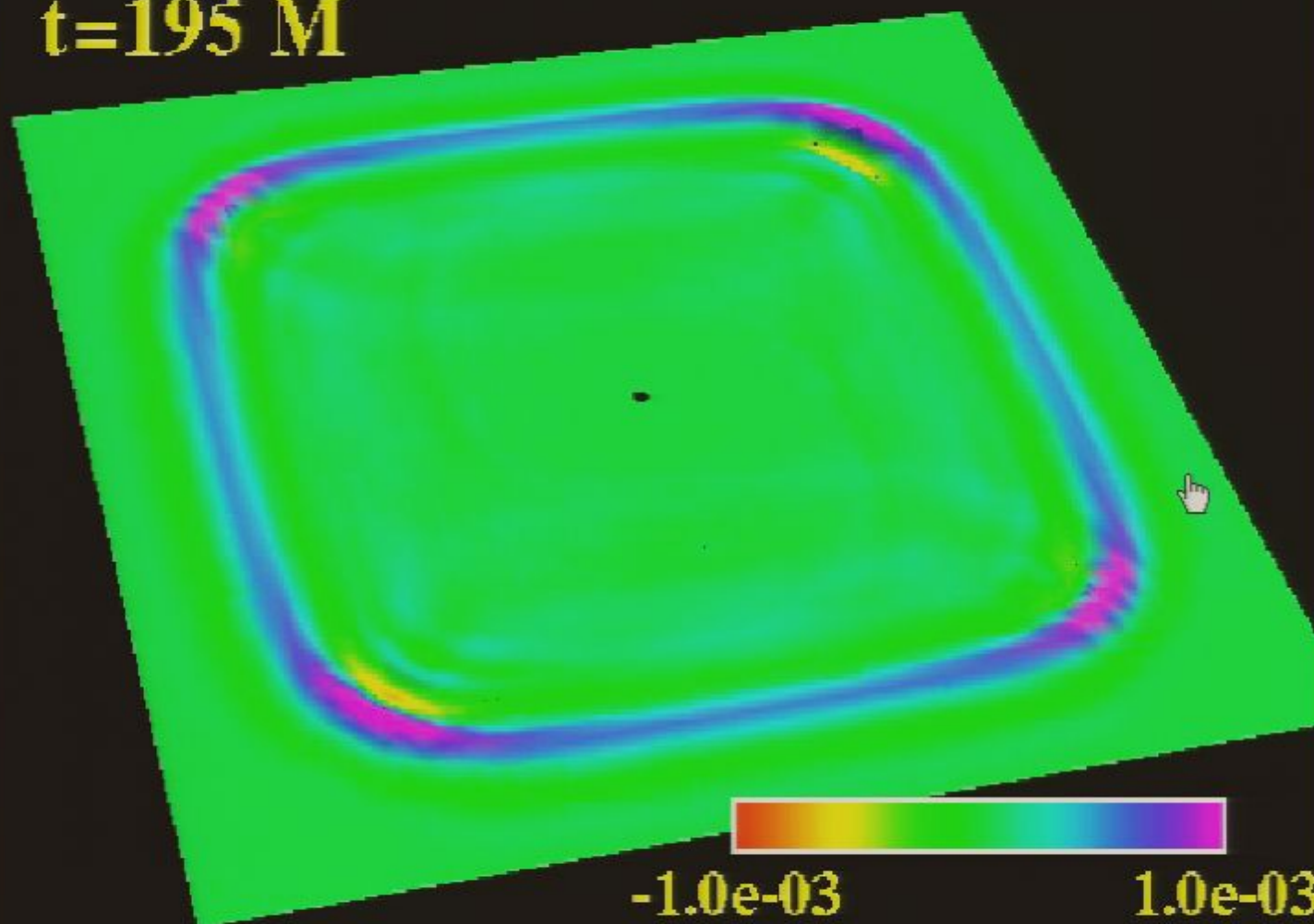
t=92 M



Scalar field $\phi.r$, compactified (code) coordinates

$$\bar{x} = \tan(x\pi/2), \bar{y} = \tan(y\pi/2), \bar{z} = \tan(z\pi/2)$$

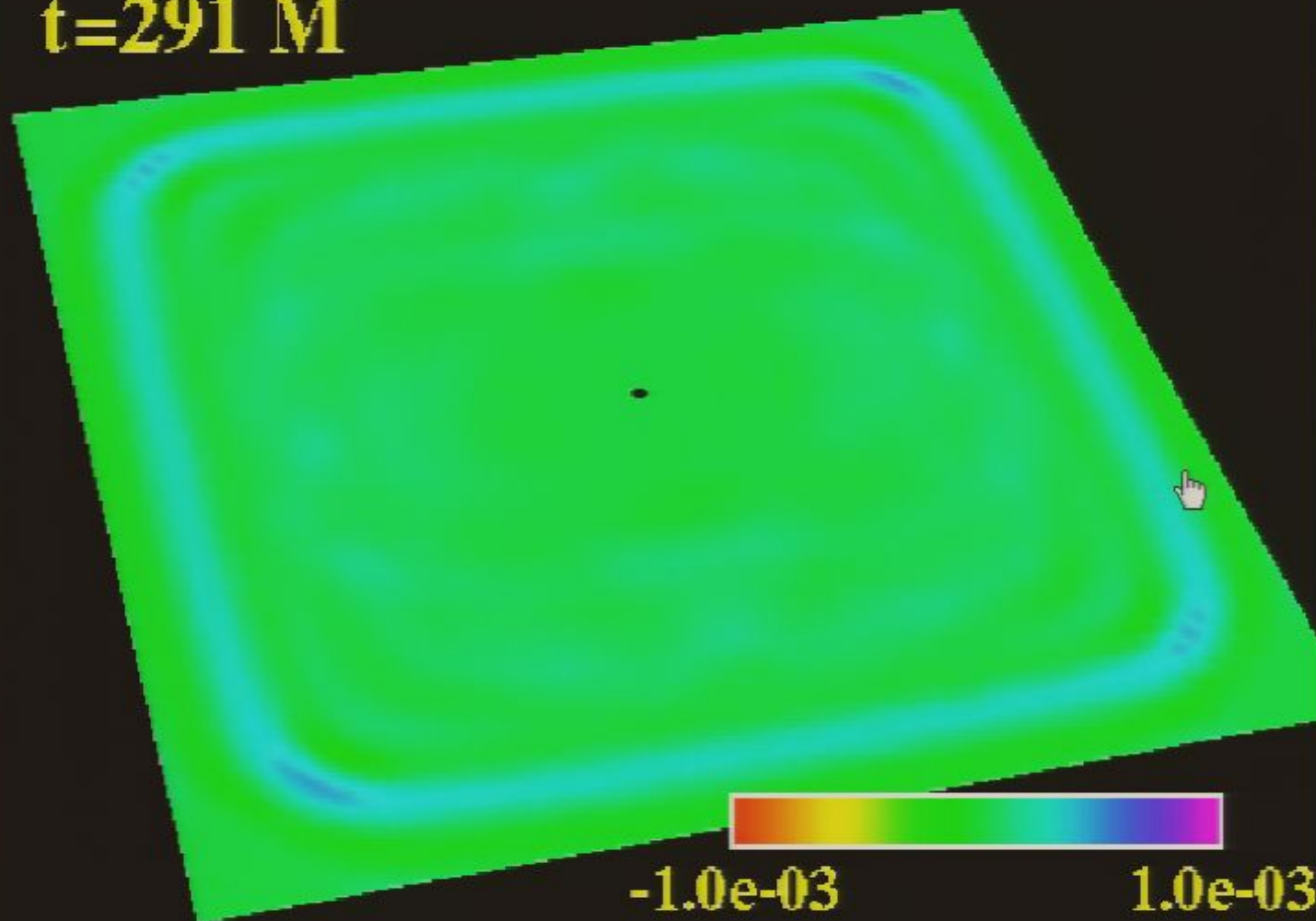
t=195 M



Scalar field $\phi.r$, compactified (code) coordinates

$$\bar{x} = \tan(x\pi/2), \bar{y} = \tan(y\pi/2), \bar{z} = \tan(z\pi/2)$$

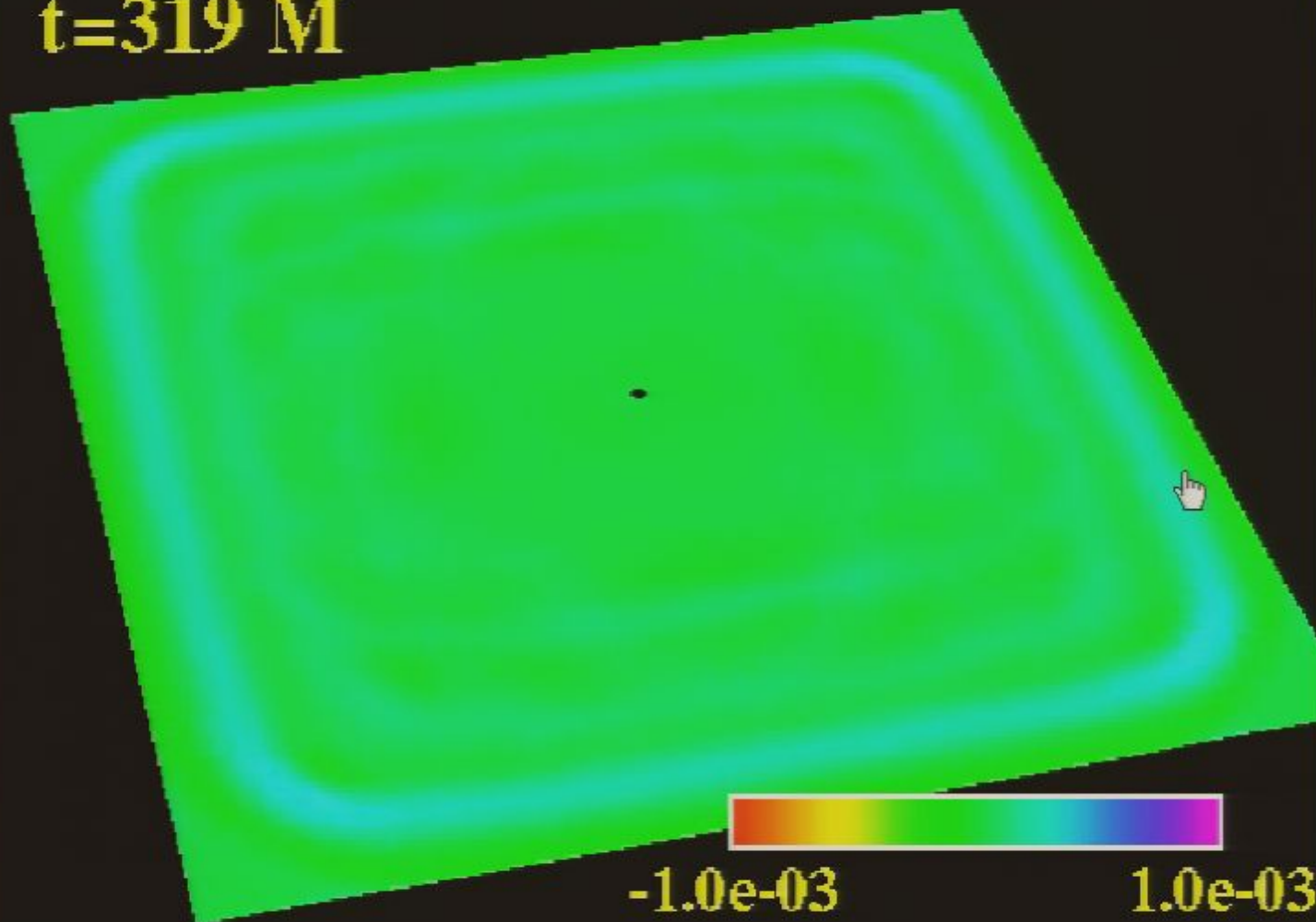
t=291 M



Scalar field $\phi.r$, compactified (code) coordinates

$$\bar{x} = \tan(x\pi/2), \bar{y} = \tan(y\pi/2), \bar{z} = \tan(z\pi/2)$$

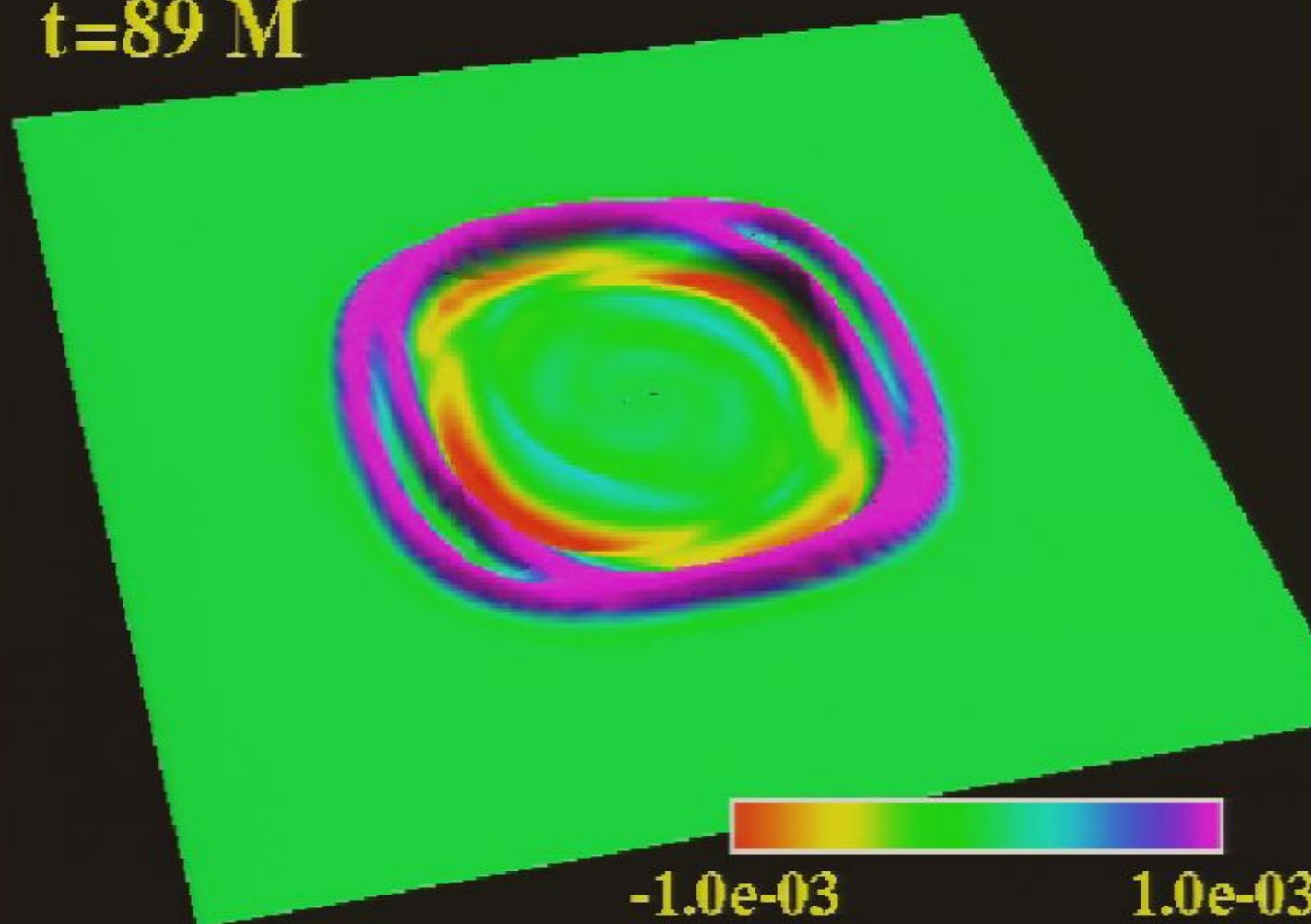
t=319 M



Scalar field $\phi.r$, compactified (code) coordinates

$$\bar{x} = \tan(x\pi/2), \bar{y} = \tan(y\pi/2), \bar{z} = \tan(z\pi/2)$$

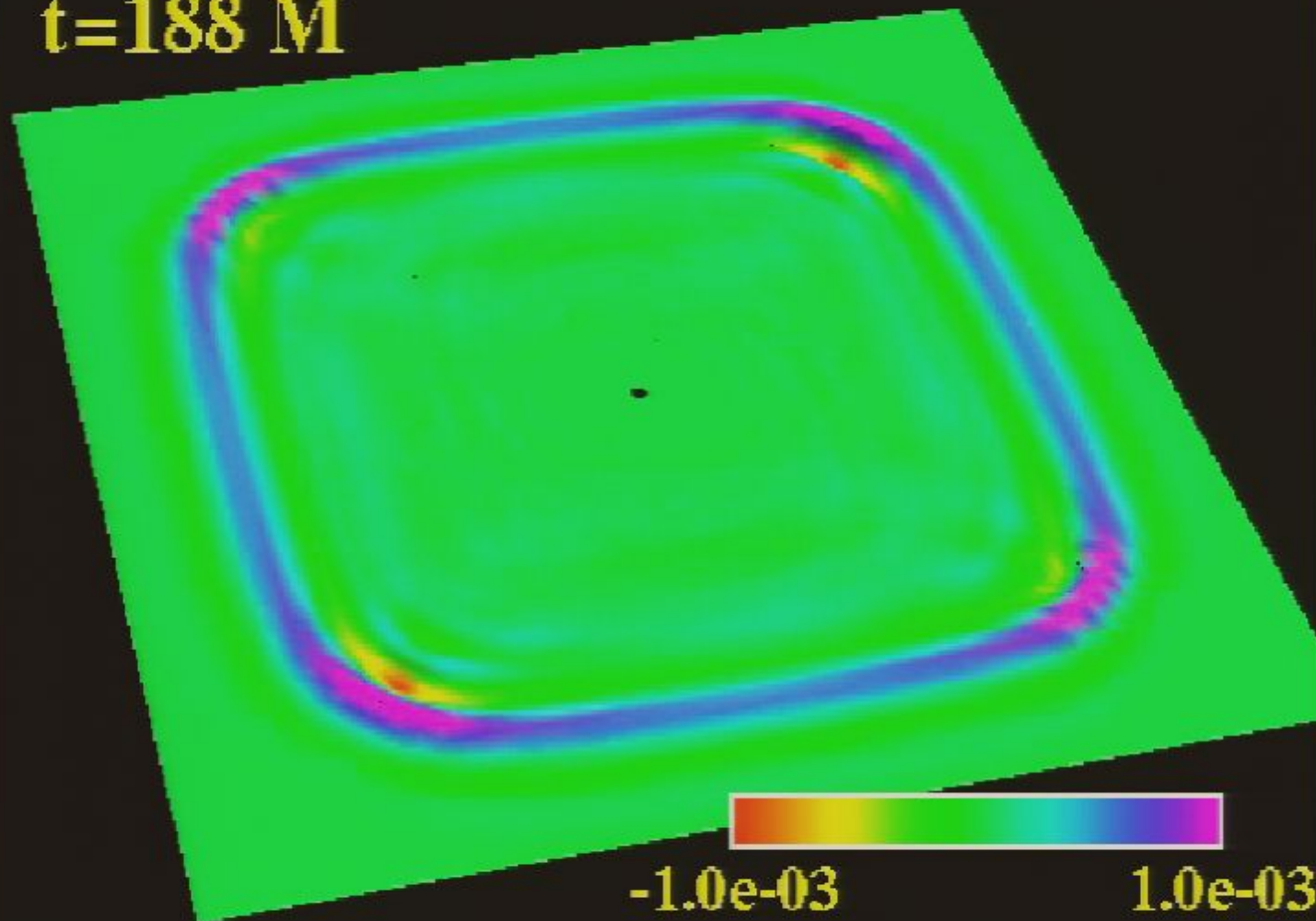
t=89 M



Scalar field $\phi.r$, compactified (code) coordinates

$$\bar{x} = \tan(x\pi/2), \bar{y} = \tan(y\pi/2), \bar{z} = \tan(z\pi/2)$$

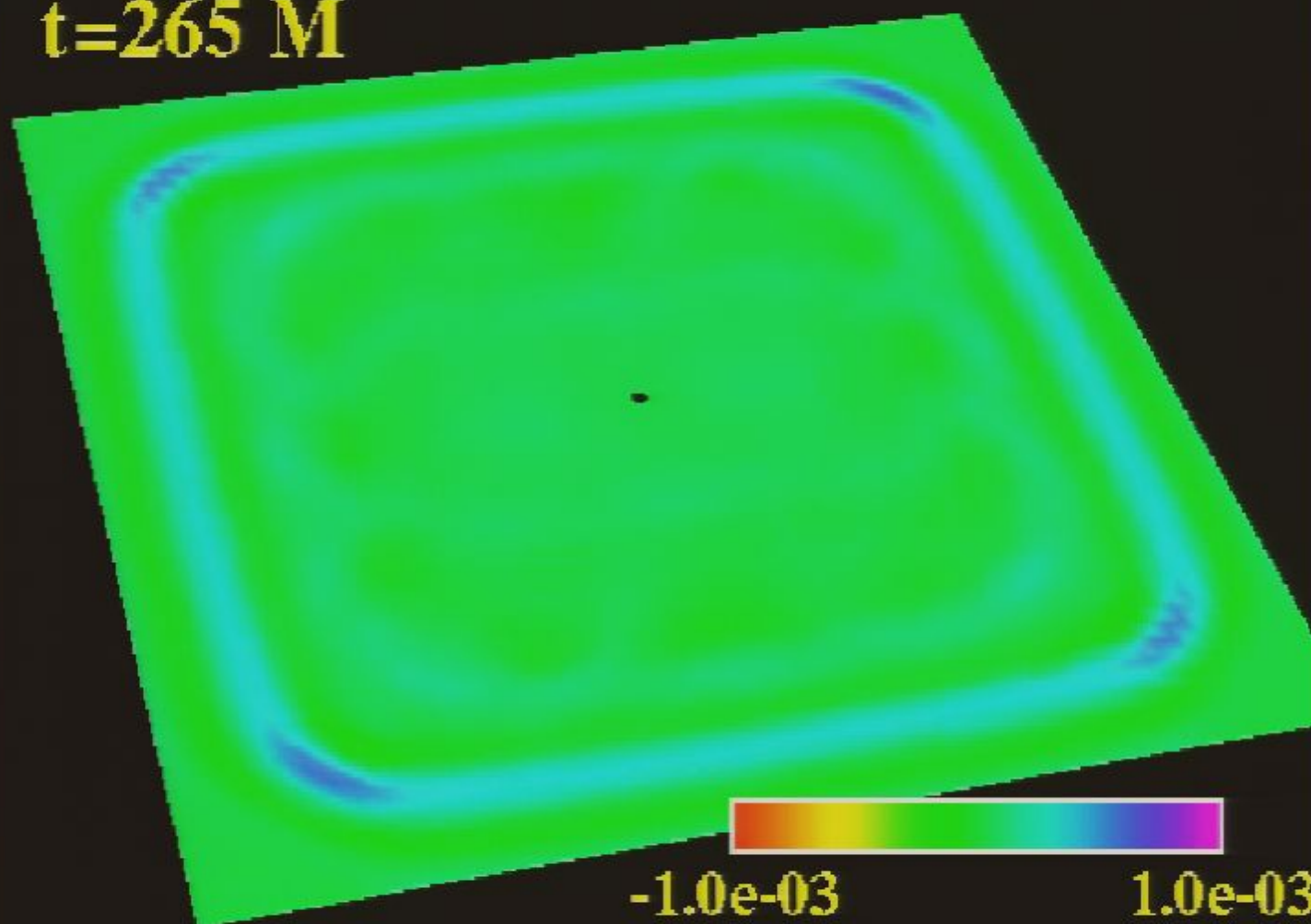
t=188 M



Scalar field $\phi.r$, compactified (code) coordinates

$$\bar{x} = \tan(x\pi/2), \bar{y} = \tan(y\pi/2), \bar{z} = \tan(z\pi/2)$$

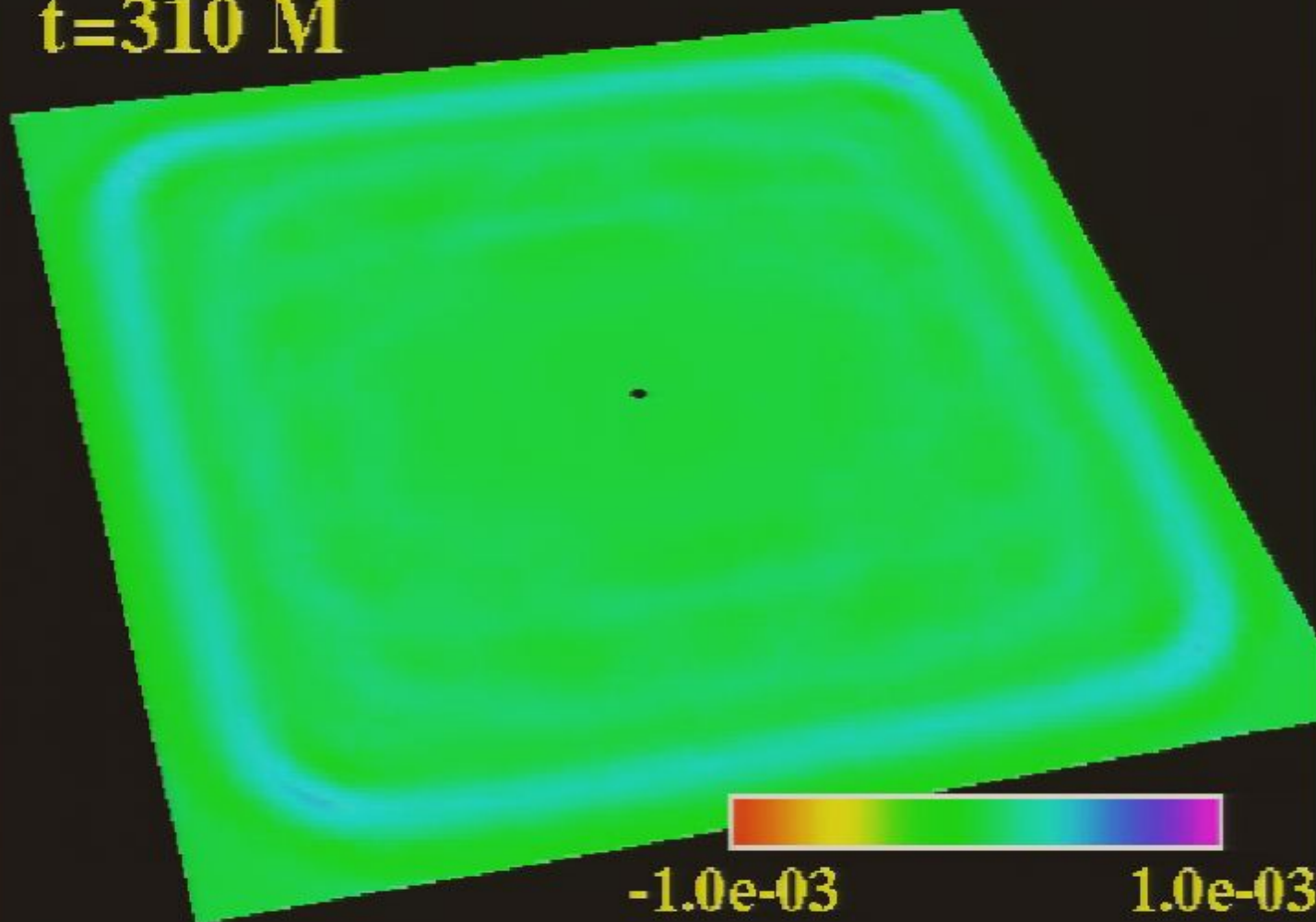
t=265 M



Scalar field $\phi.r$, compactified (code) coordinates

$$\bar{x} = \tan(x\pi/2), \bar{y} = \tan(y\pi/2), \bar{z} = \tan(z\pi/2)$$

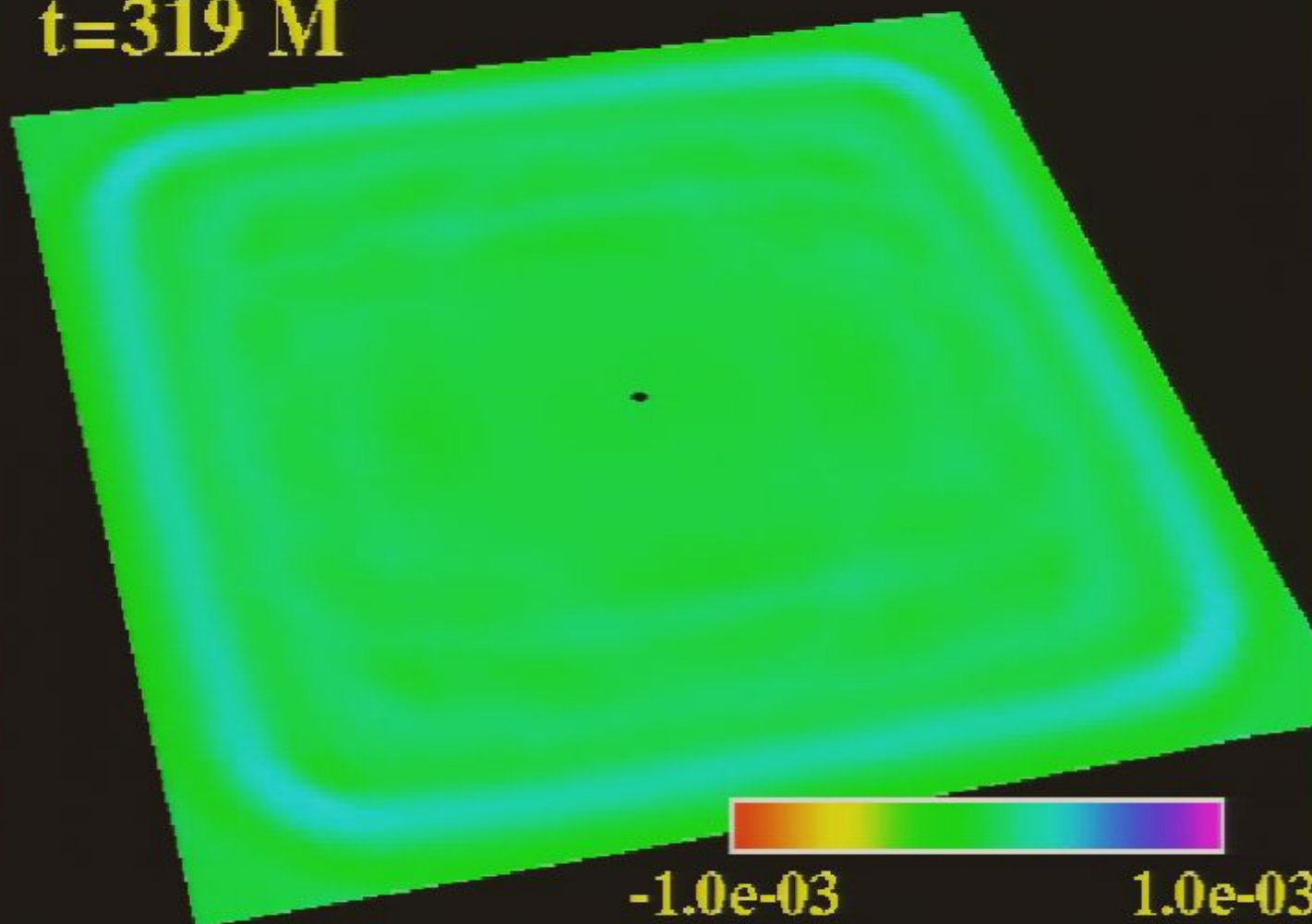
t=310 M



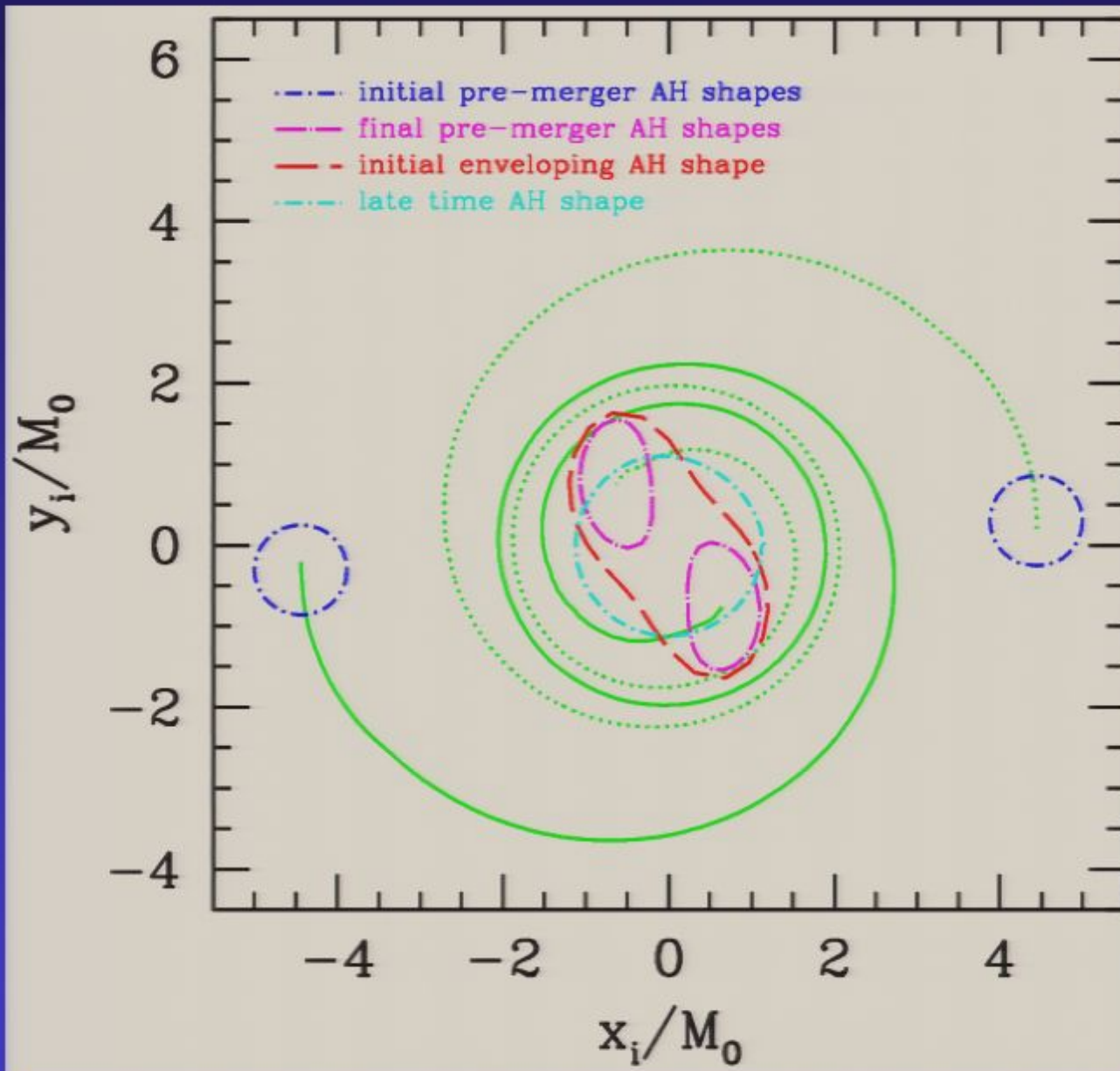
Scalar field $\phi.r$, compactified (code) coordinates

$$\bar{x} = \tan(x\pi/2), \bar{y} = \tan(y\pi/2), \bar{z} = \tan(z\pi/2)$$

t=319 M



Sample Orbit



h-resolution runs

v	n	p_m/M_0	d_m/M_0	m_f/M_0	a/m_f	(E/M_0)
0.21000	1.3	-	-	0.89 ± 0.03	0.75 ± 0.05	0.032
0.21125	1.4	-	-	0.88 ± 0.03	0.74 ± 0.05	0.035
0.21234	2.3	-	-	0.83 ± 0.03	0.73 ± 0.05	?
0.21250	2.7	4.0	3.6	-	-	0.020
0.21500	1.5	5.5	4.6	-	-	0.006
0.22000	1.0	7.2	5.8	-	-	0.005

6/8 h-resolution runs

v	n	p_m/M_0	d_m/M_0	m_f/M_0	a/m_f	(E/M_0)
0.20960	0.9	-	-	0.97 ± 0.01	0.65 ± 0.03	0.028
0.21750	1.4	-	-	0.92 ± 0.01	0.72 ± 0.03	0.037
0.21875	2.0	-	-	0.88 ± 0.01	0.70 ± 0.03	0.046
0.21906	2.4	-	-	0.86 ± 0.01	0.70 ± 0.03	0.052
0.219180	2.8	-	-	0.82 ± 0.02	0.70 ± 0.05	0.063
0.219200	3.0	-	-	0.80 ± 0.02	0.75 ± 0.05	0.064
0.219209	3.3	-	-	0.78 ± 0.02	0.71 ± 0.05	0.067
0.219214	3.7	-	-	0.75 ± 0.02	0.71 ± 0.05	0.074
0.219219	4.9	3.2	3.0	-	-	0.058
0.21938	2.5	4.8	4.2	-	-	0.019
0.22000	1.9	5.3	4.4	-	-	0.014

4/8 h-resolution runs

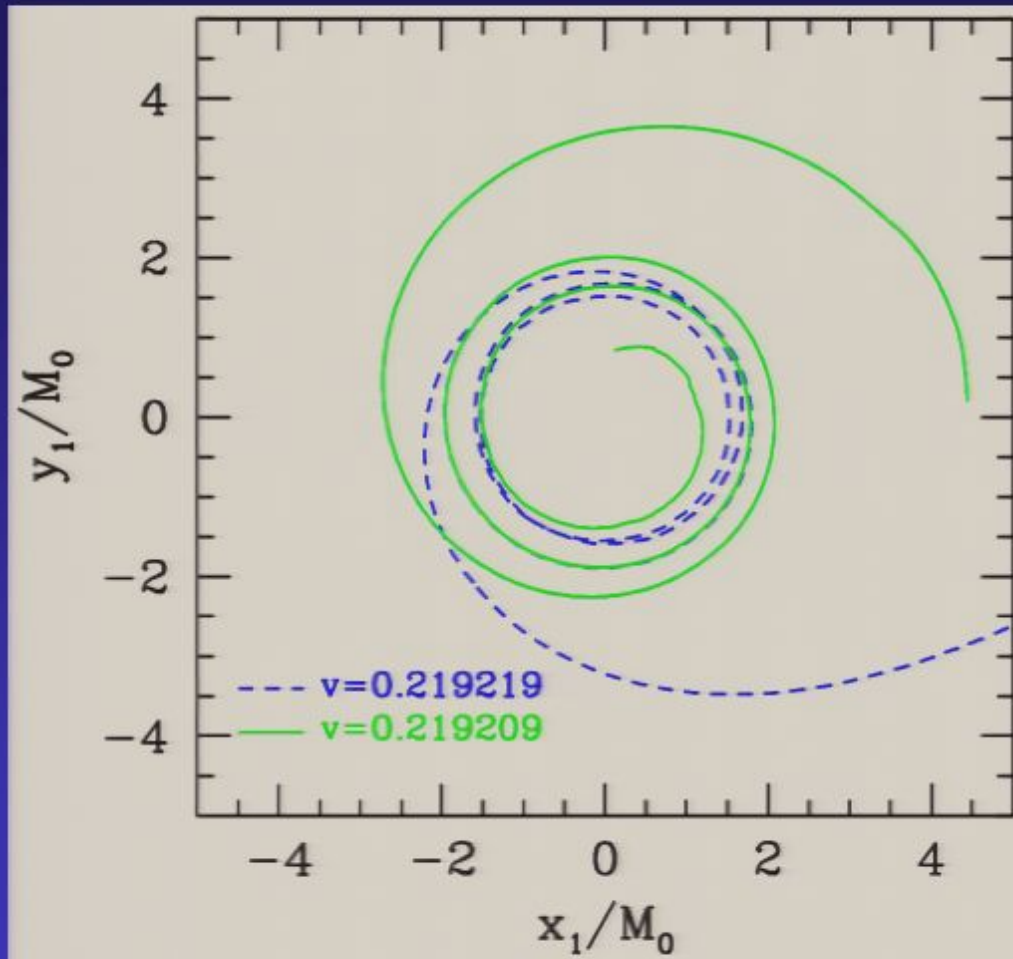
v	n	p_m/M_0	d_m/M_0	m_f/M_0	a/m_f	(E/M_0)
0.21500	1.4	-	-	0.945 ± 0.005	0.71 ± 0.02	0.042
0.22000	2.1	5.7	4.8	-	-	?

Pirsa: 06040024

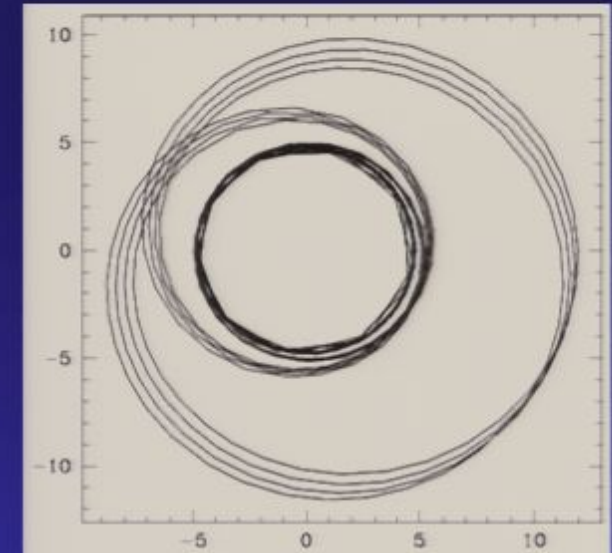
Early indications of “extreme” sensitivity to initial conditions

- What’s going on??
 - **warning:** large cumulative numerical errors, especially for the lower resolutions (though does not necessarily mean qualitative features are wrong, c.f. critical gravitational collapse)
 - could be the fully non-linear analogue of “zoom-whirl” behavior in test particle orbits

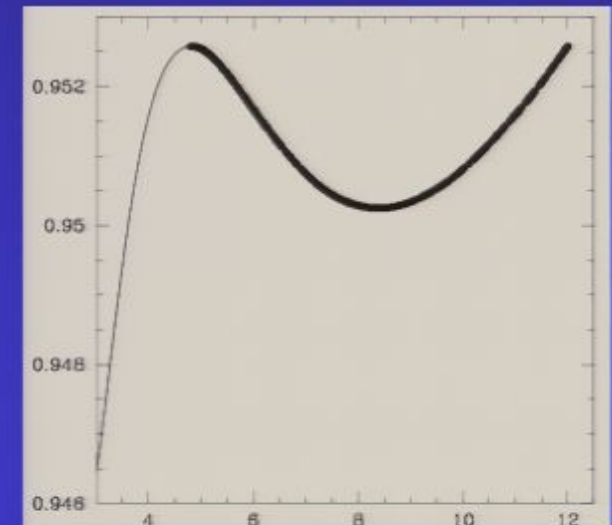
Orbits



- two sample orbits from the $6/8h$ resolution runs
- tuning v we are approaching the equivalent of a *homoclinic orbit*
- here the separation is close to $3M$ in the whirl part, which in the test-particle limit corresponds to the innermost stable circular *photon* orbit



example of a homoclinic particle orbit in Schwarzschild (above) and the corresponding effective potential (below)



Lapse and Gravitational Waves

6/8h resolution, $v=0.21909$ merger example

t= 0 M



Lapse function α , orbital plane

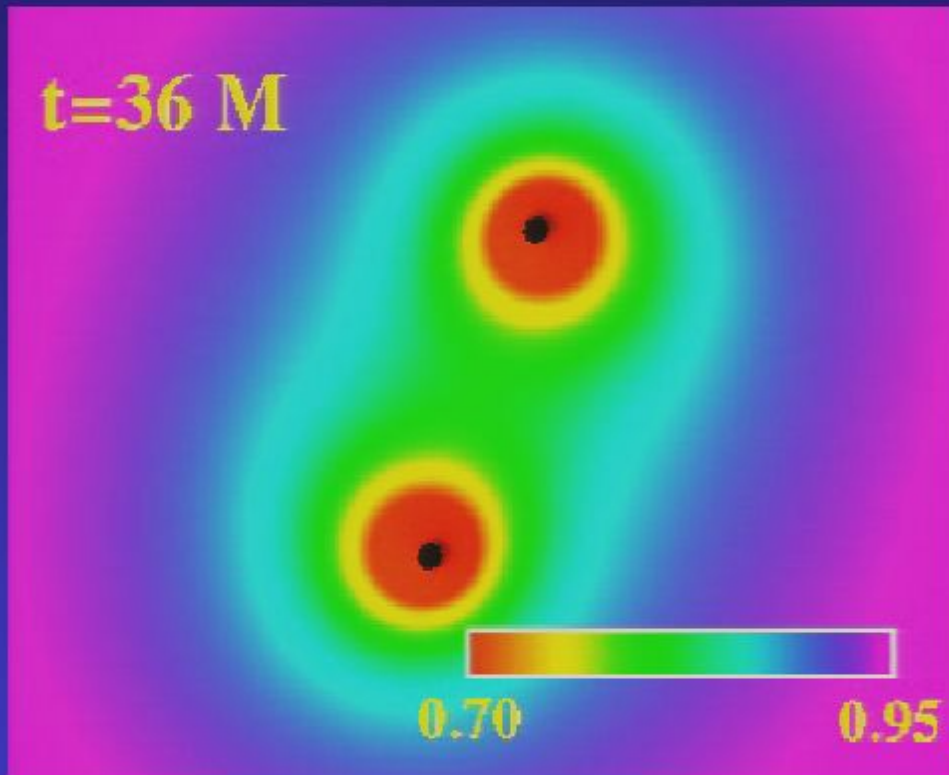
t= 1 M



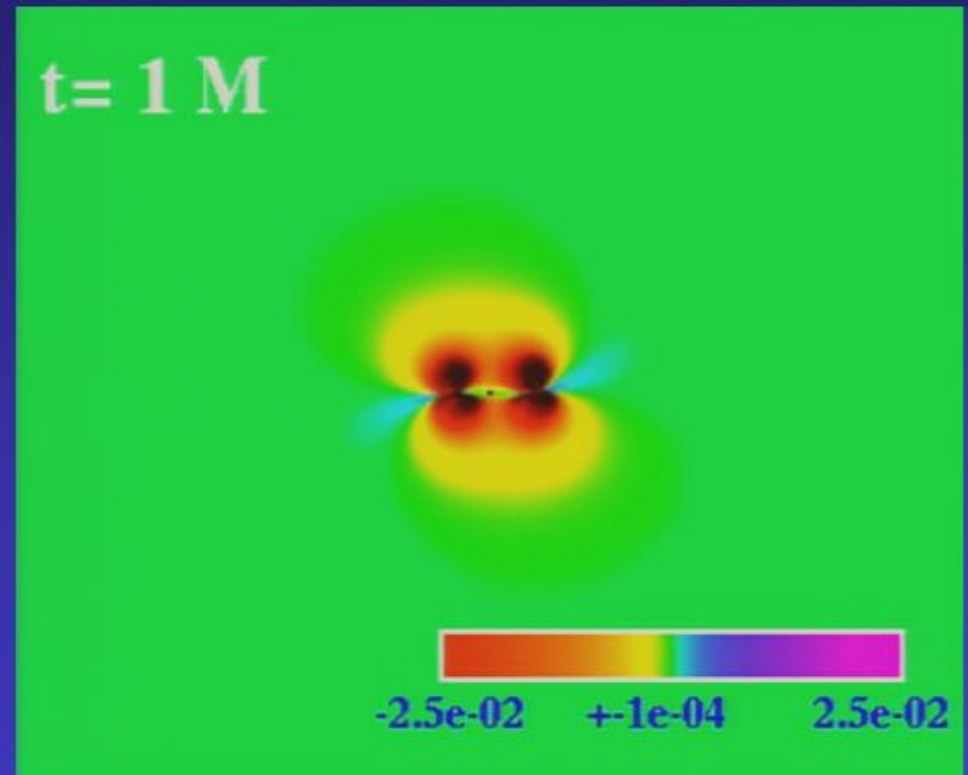
Real component of the Newman-Penrose scalar Ψ_4 (times rM), orbital plane

Lapse and Gravitational Waves

6/8h resolution, $v=0.21909$ merger example



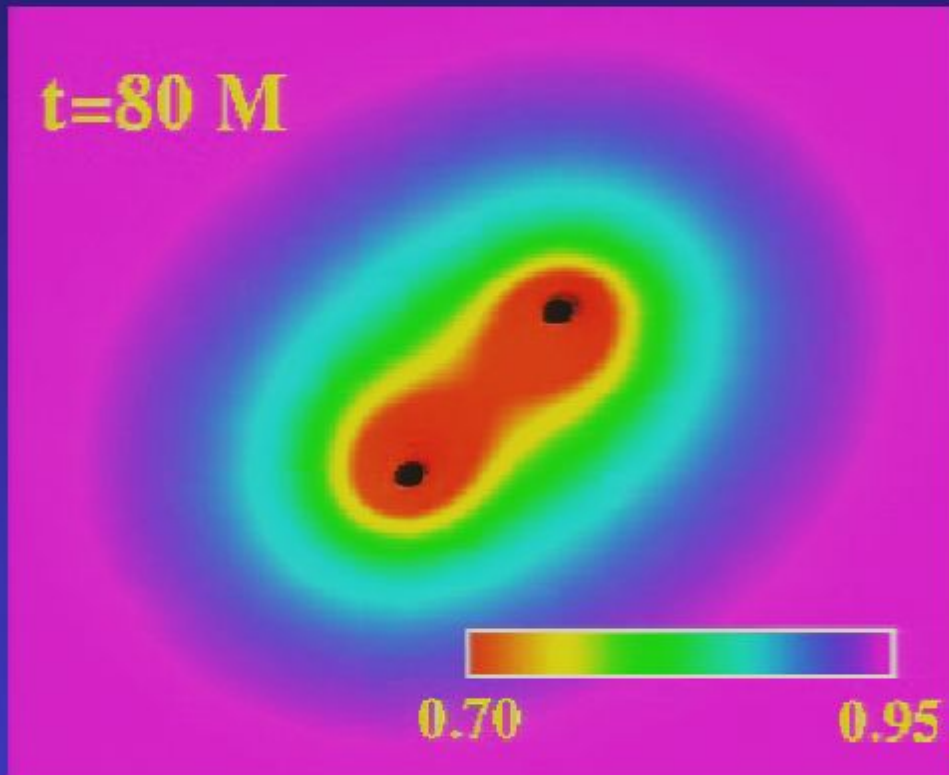
Lapse function α , orbital plane



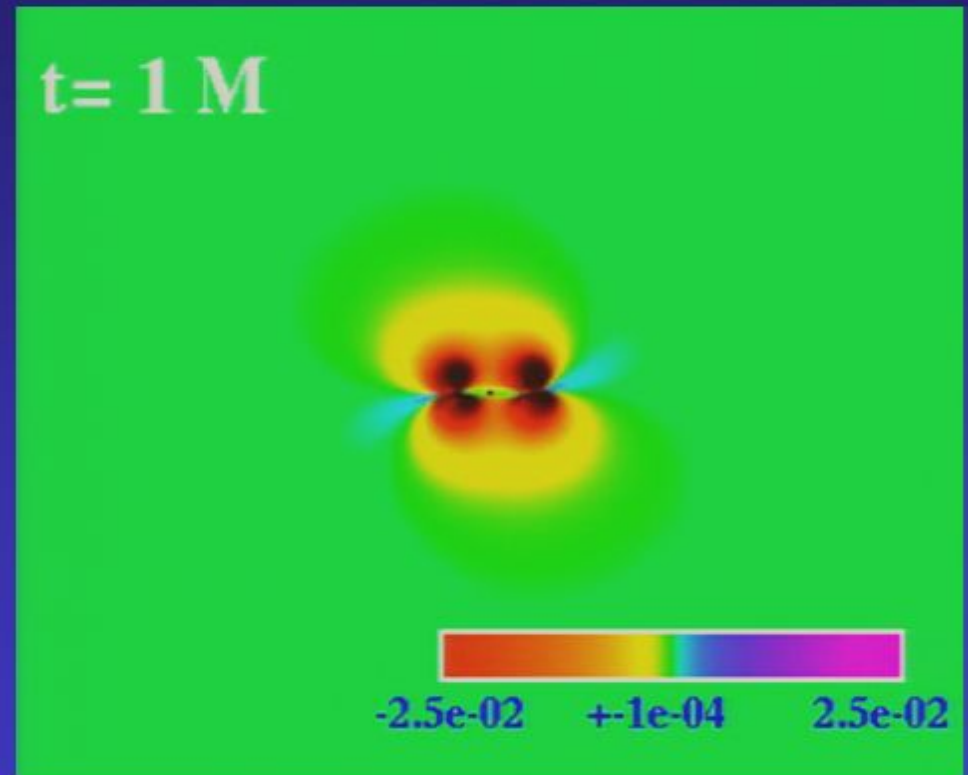
Real component of the Newman-Penrose scalar Ψ_4 (times rM), orbital plane

Lapse and Gravitational Waves

6/8h resolution, $v=0.21909$ merger example



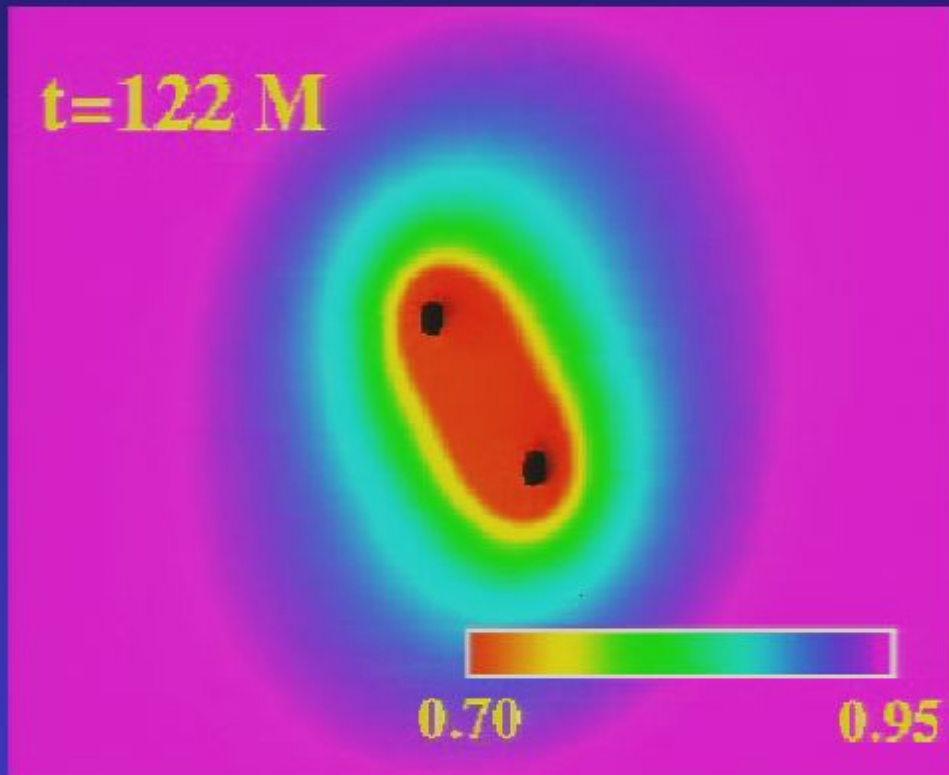
Lapse function α , orbital plane



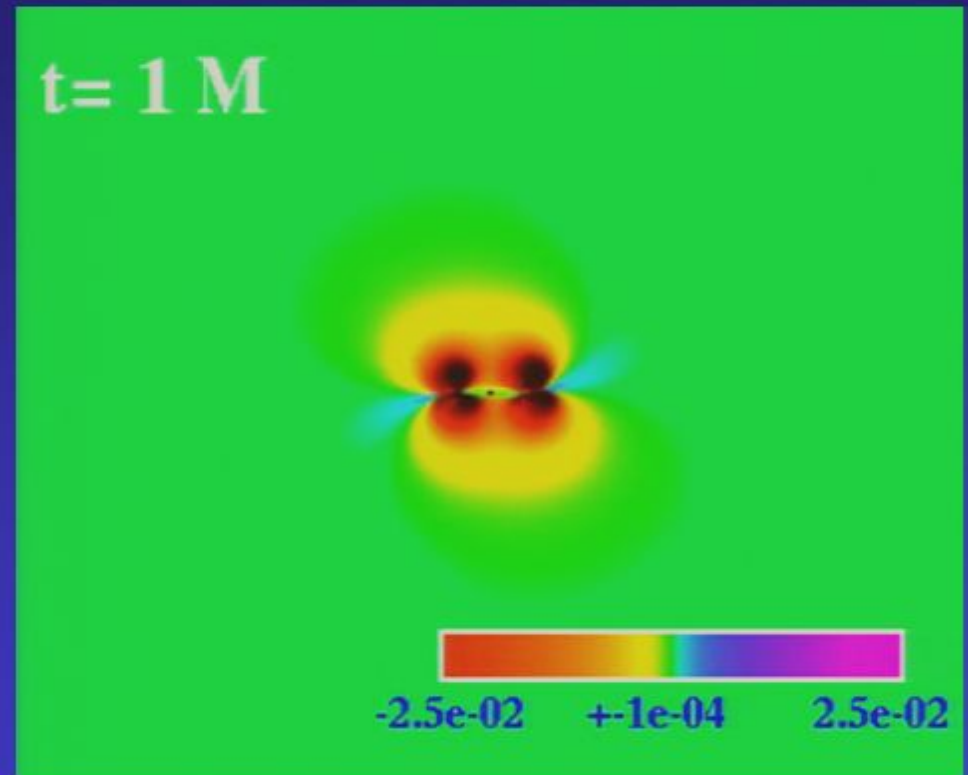
Real component of the Newman-Penrose scalar Ψ_4 (times rM), orbital plane

Lapse and Gravitational Waves

6/8h resolution, $v=0.21909$ merger example



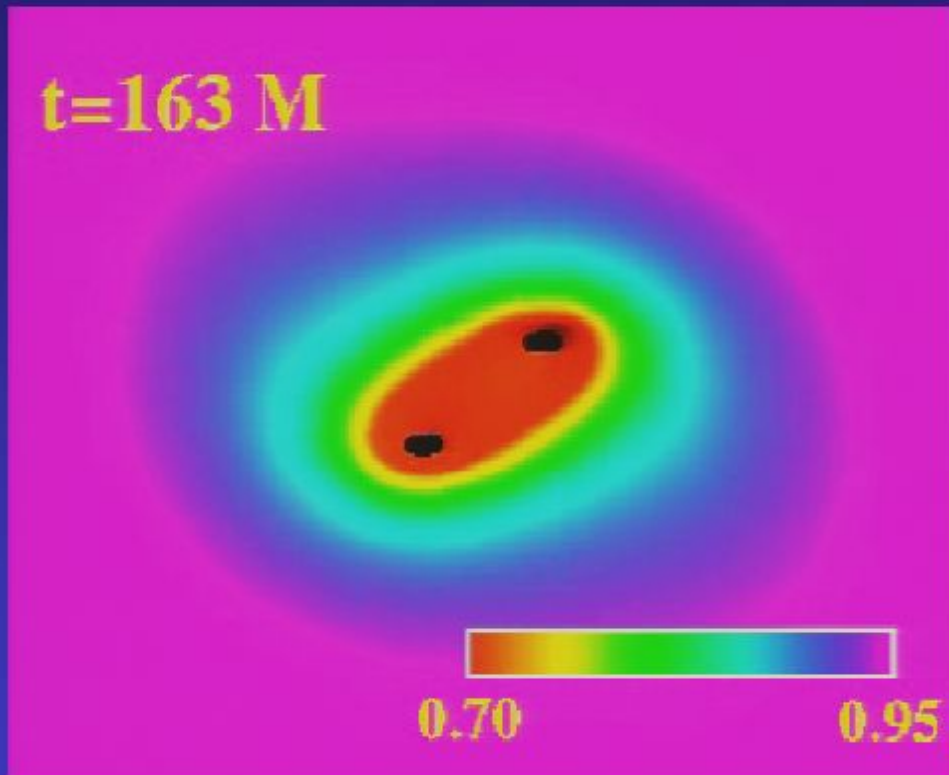
Lapse function α , orbital plane



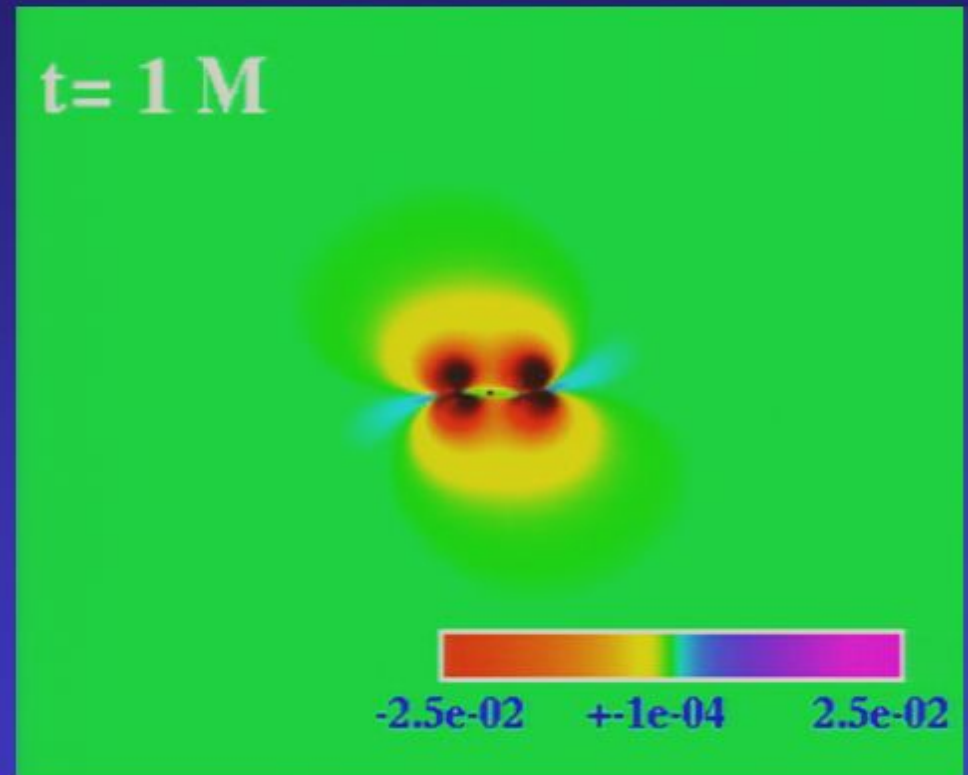
Real component of the Newman-Penrose scalar Ψ_4 (times rM), orbital plane

Lapse and Gravitational Waves

6/8h resolution, $v=0.21909$ merger example



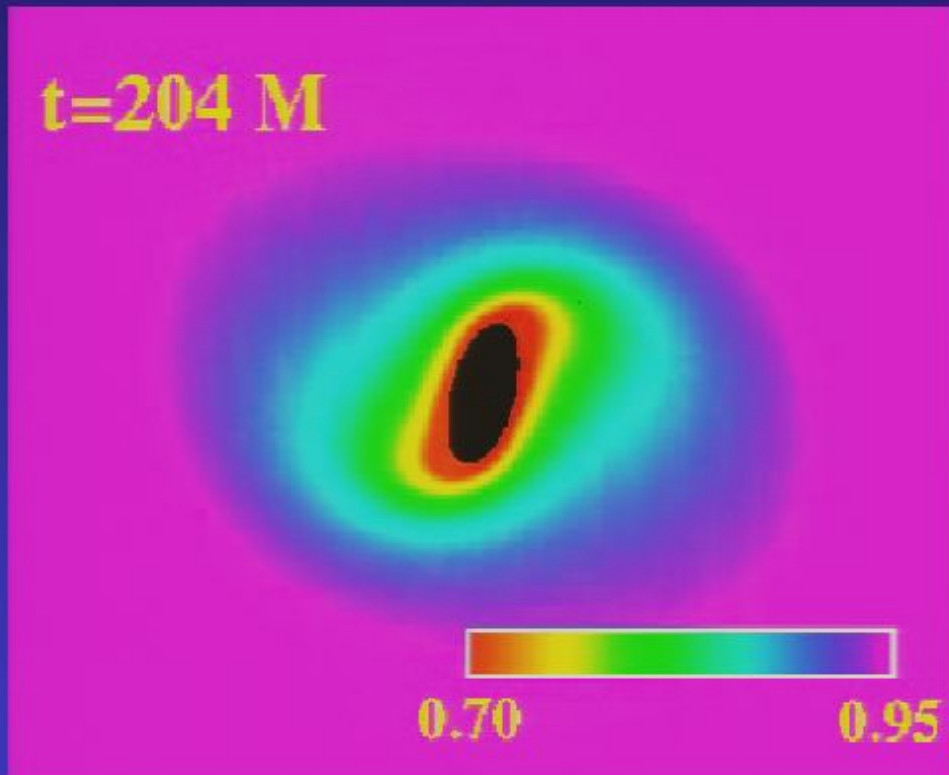
Lapse function α , orbital plane



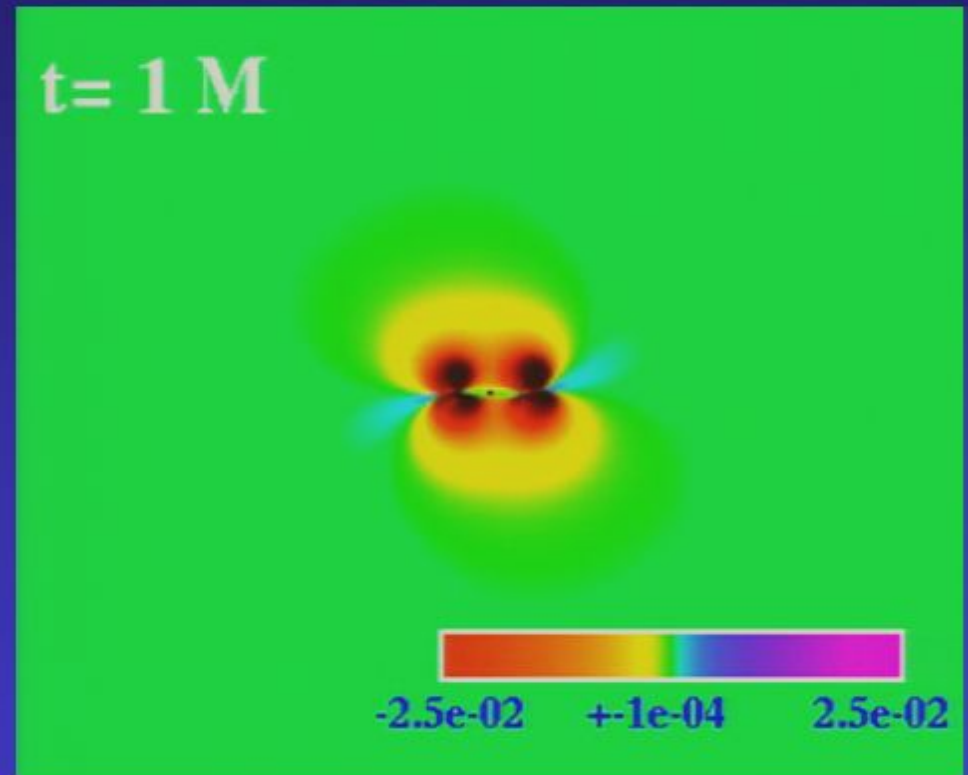
Real component of the Newman-Penrose scalar Ψ_4 (times rM), orbital plane

Lapse and Gravitational Waves

6/8h resolution, $v=0.21909$ merger example



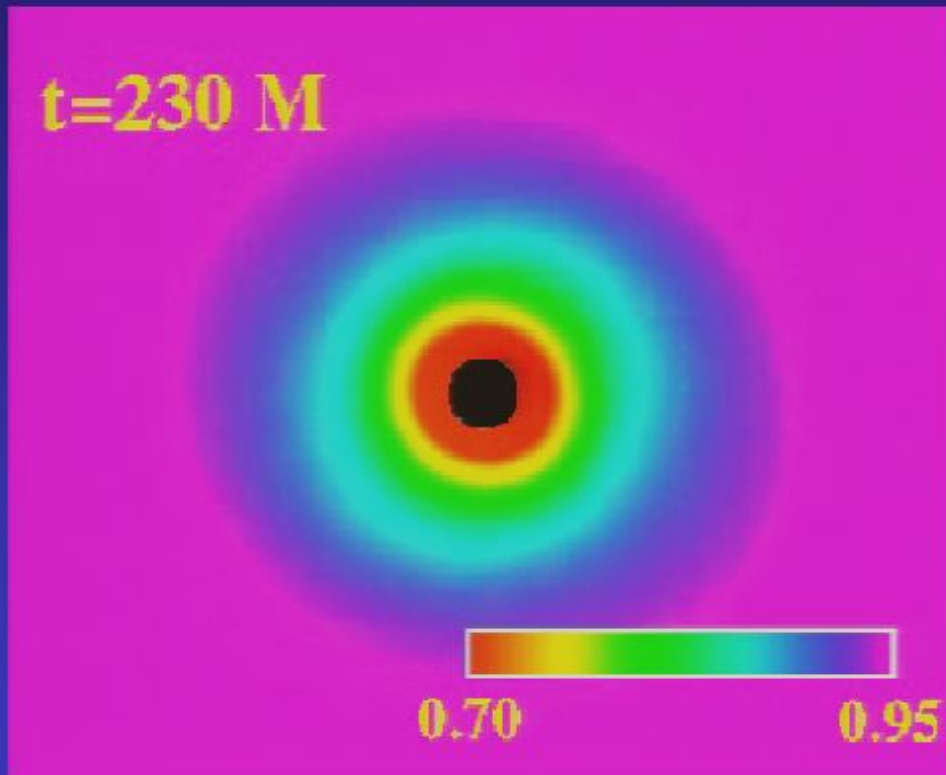
Lapse function α , orbital plane



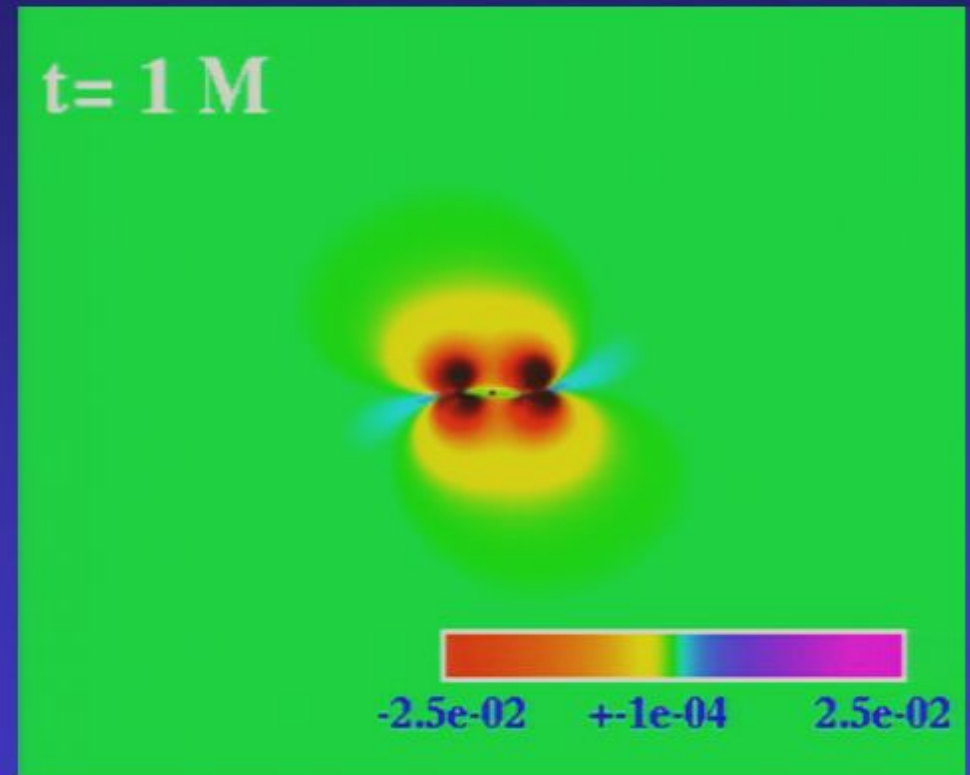
Real component of the Newman-Penrose scalar Ψ_4 (times rM), orbital plane

Lapse and Gravitational Waves

6/8h resolution, $v=0.21909$ merger example



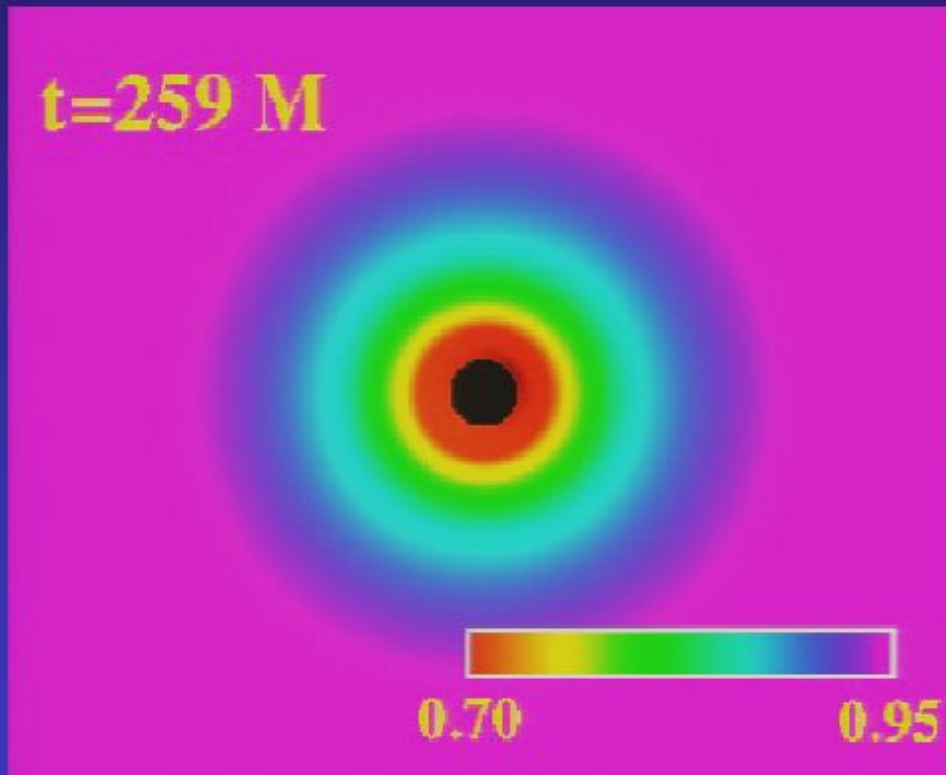
Lapse function α , orbital plane



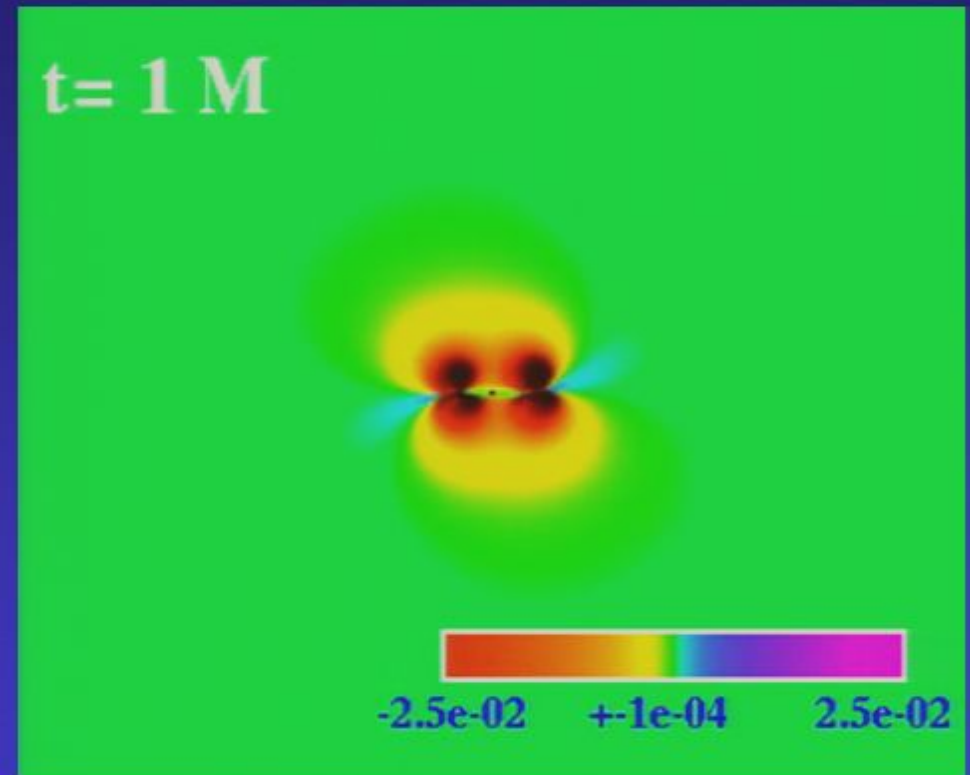
Real component of the Newman-Penrose scalar Ψ_4 (times rM), orbital plane

Lapse and Gravitational Waves

6/8h resolution, $v=0.21909$ merger example



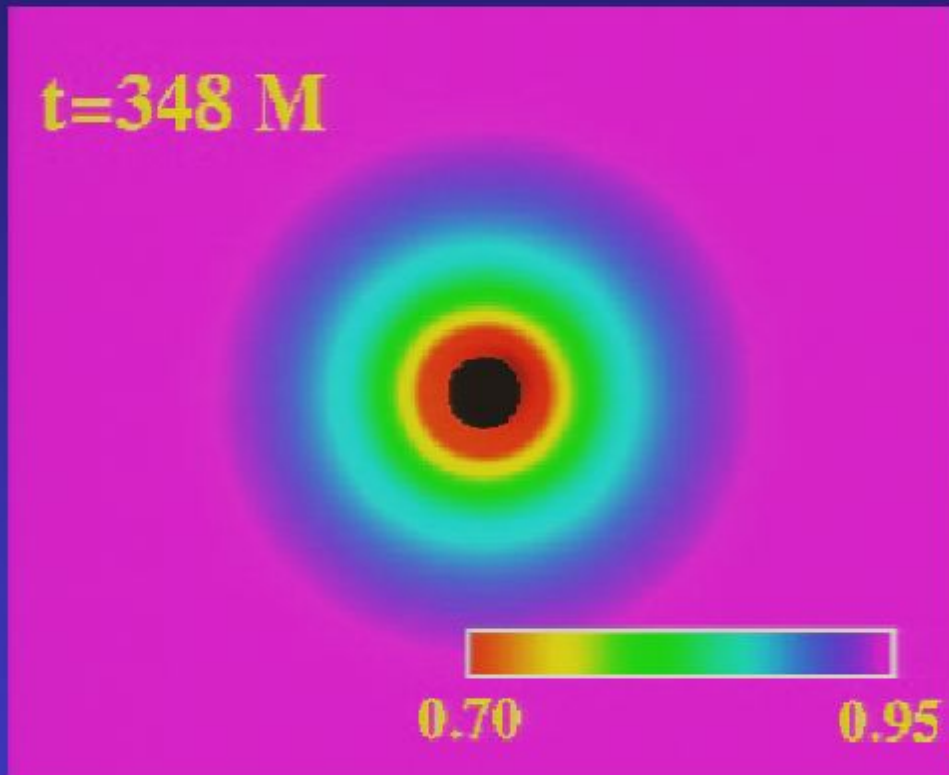
Lapse function α , orbital plane



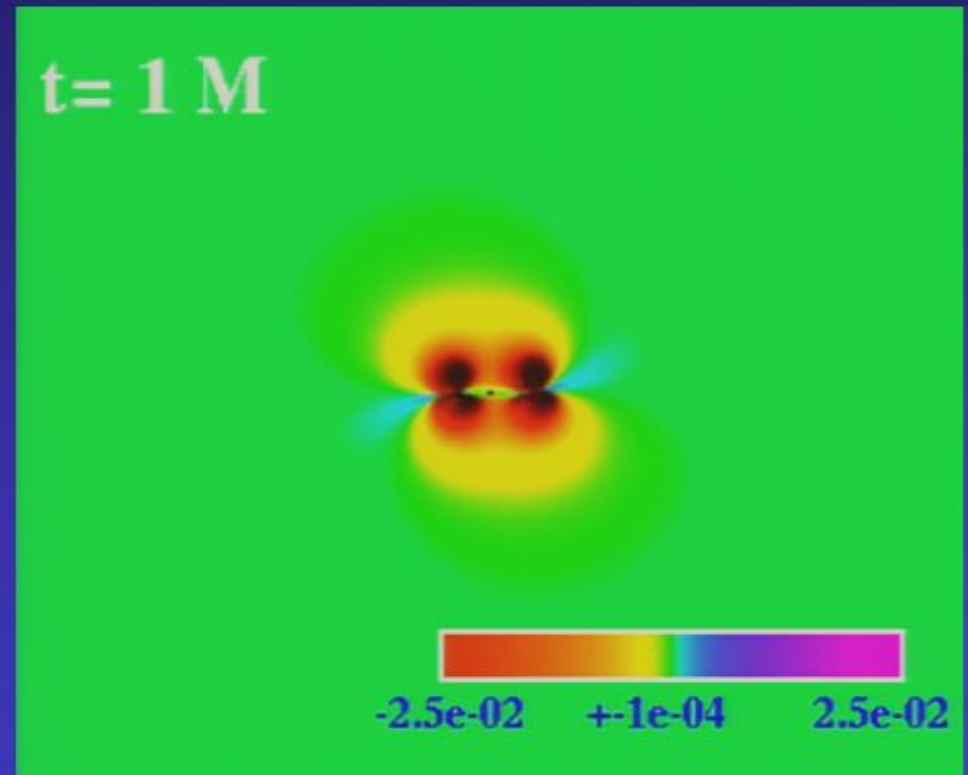
Real component of the Newman-Penrose scalar Ψ_4 (times rM), orbital plane

Lapse and Gravitational Waves

6/8h resolution, $v=0.21909$ merger example



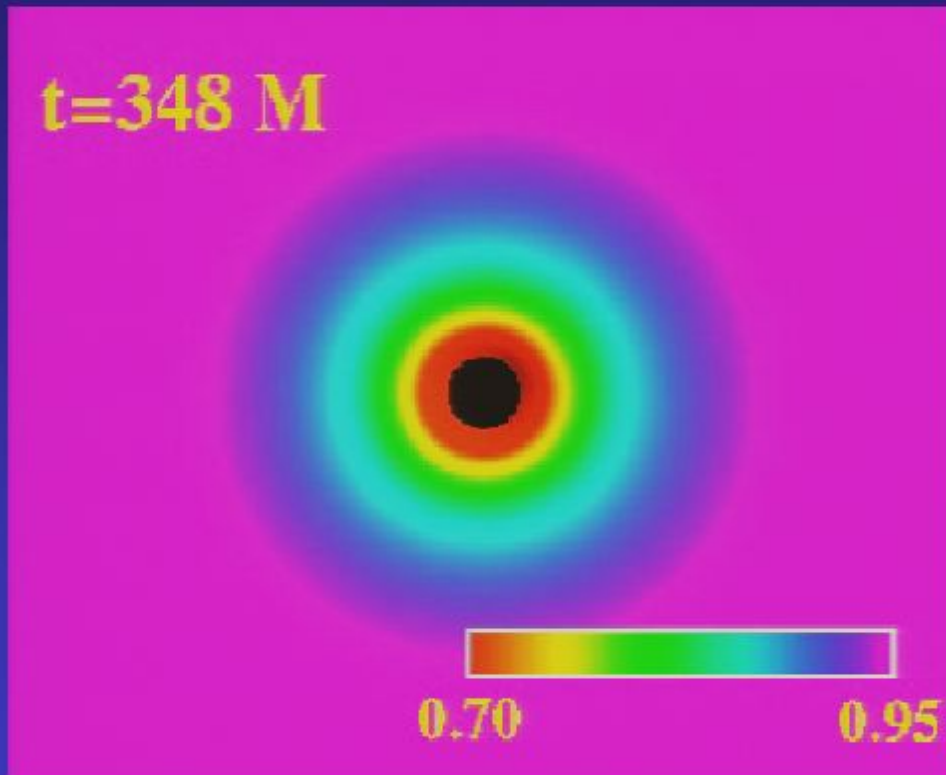
Lapse function α , orbital plane



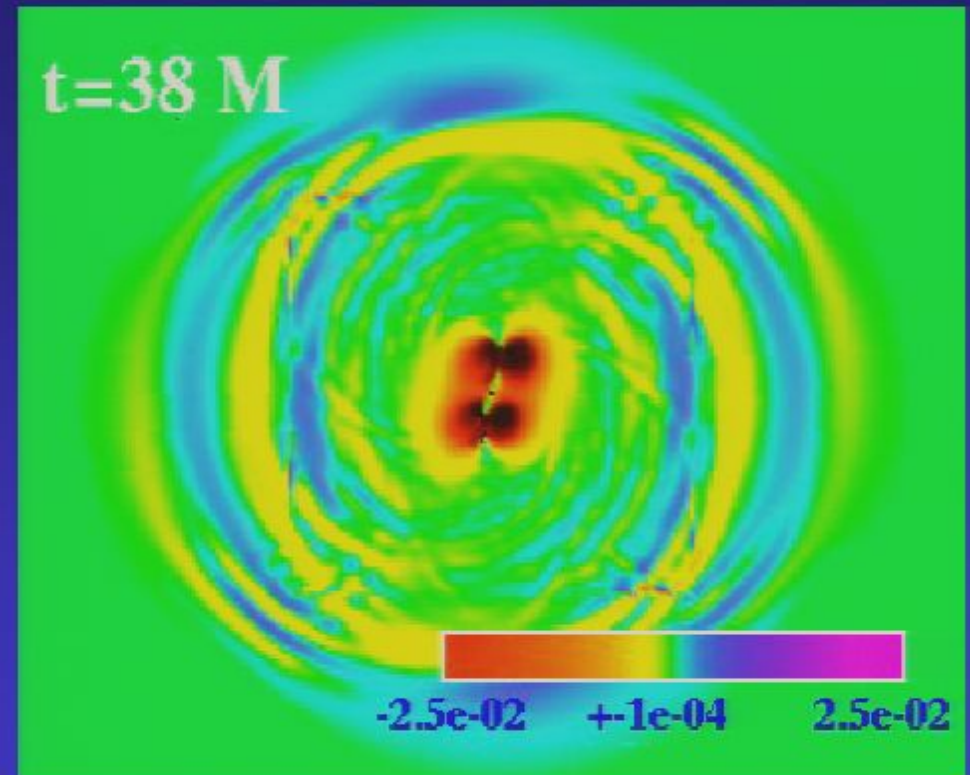
Real component of the Newman-Penrose scalar Ψ_4 (times rM), orbital plane

Lapse and Gravitational Waves

6/8h resolution, $v=0.21909$ merger example



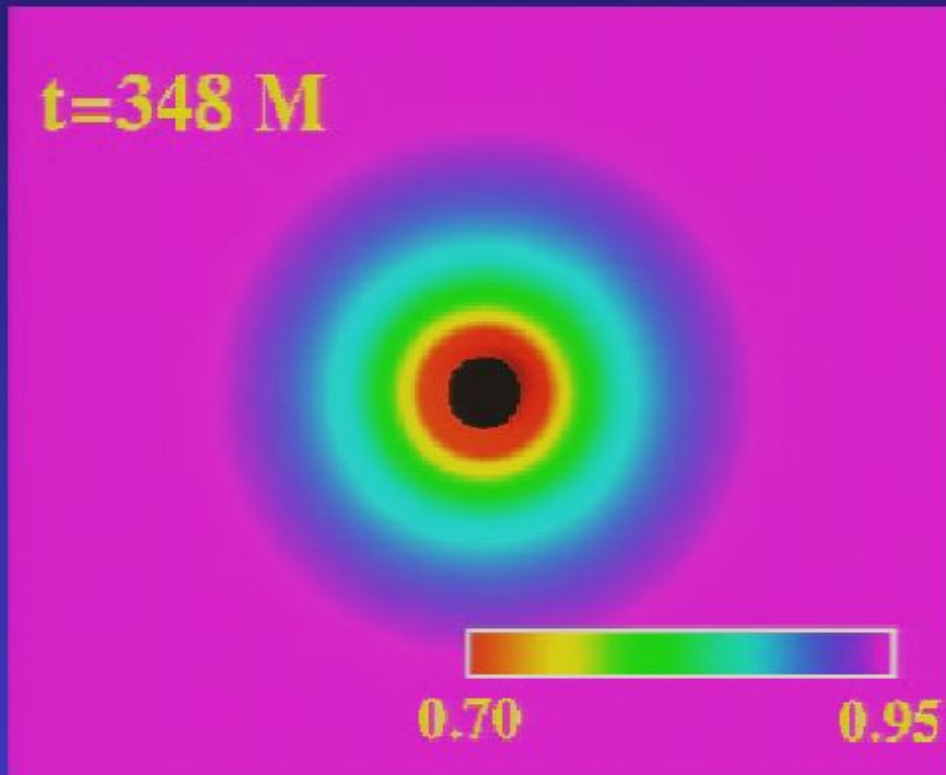
Lapse function α , orbital plane



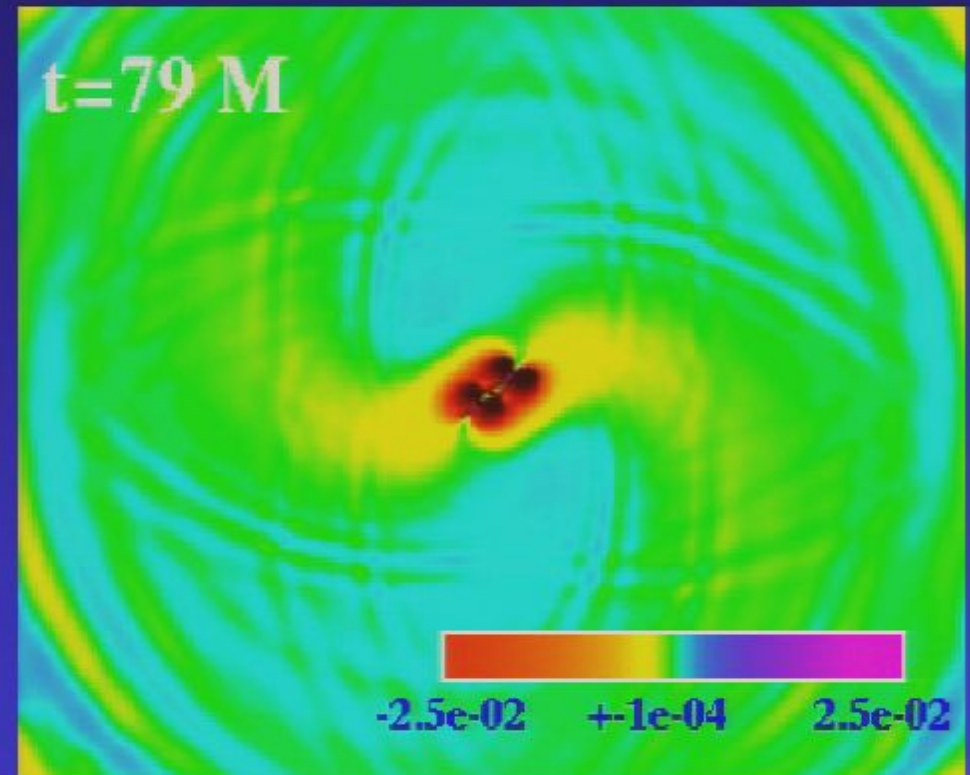
Real component of the Newman-Penrose scalar Ψ_4 (times rM), orbital plane

Lapse and Gravitational Waves

6/8h resolution, $v=0.21909$ merger example



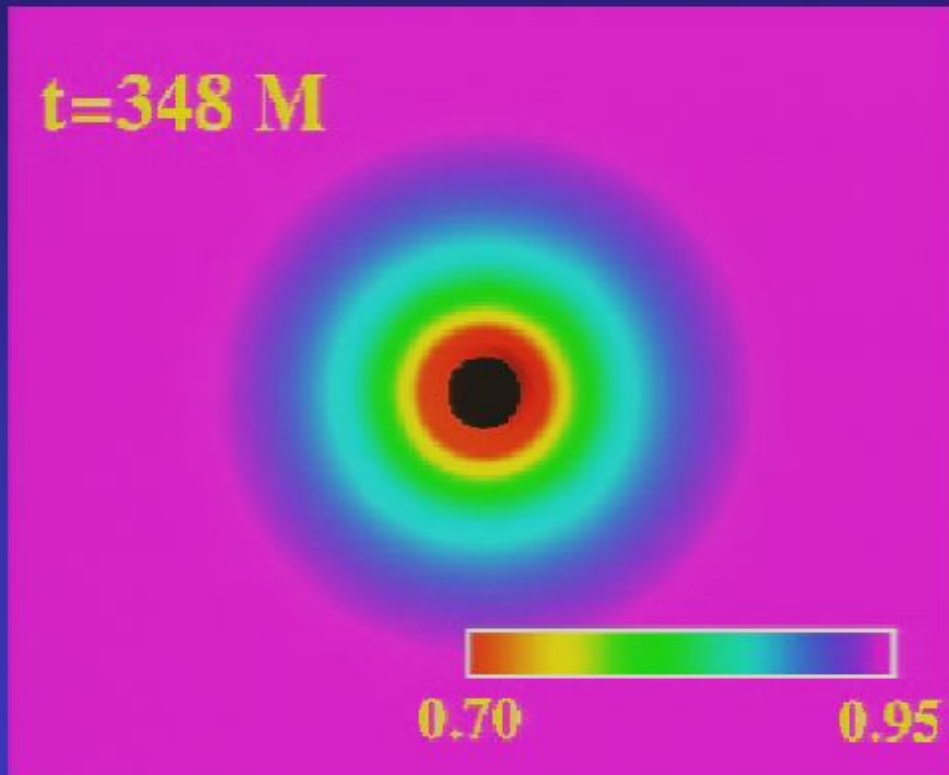
Lapse function α , orbital plane



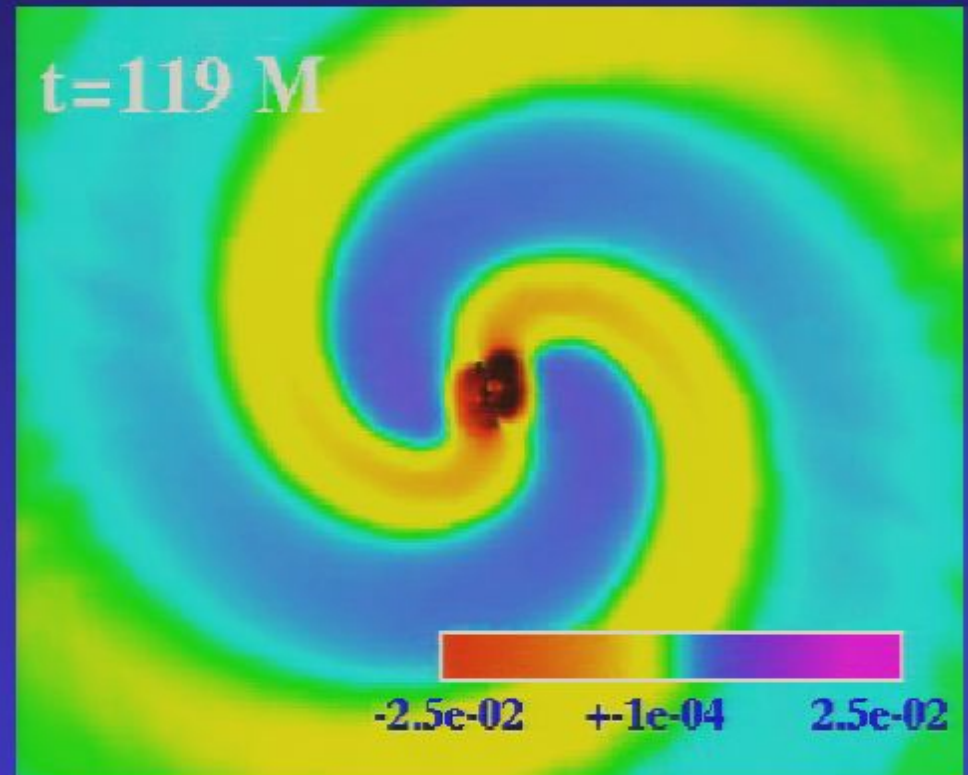
Real component of the Newman-Penrose scalar Ψ_4 (times rM), orbital plane

Lapse and Gravitational Waves

6/8h resolution, $v=0.21909$ merger example



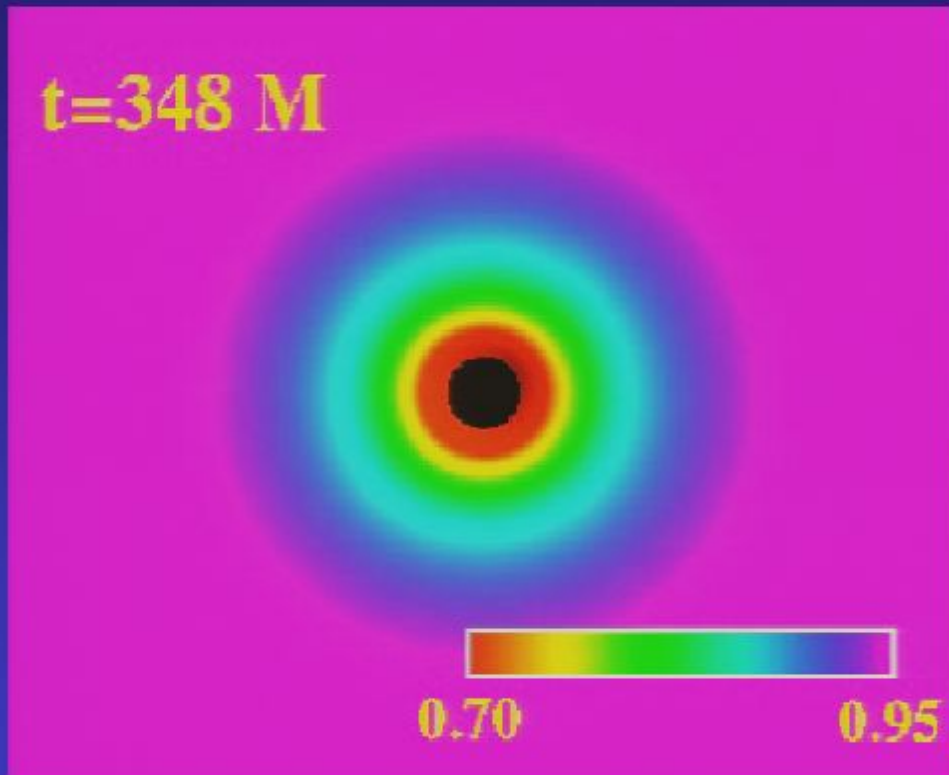
Lapse function α , orbital plane



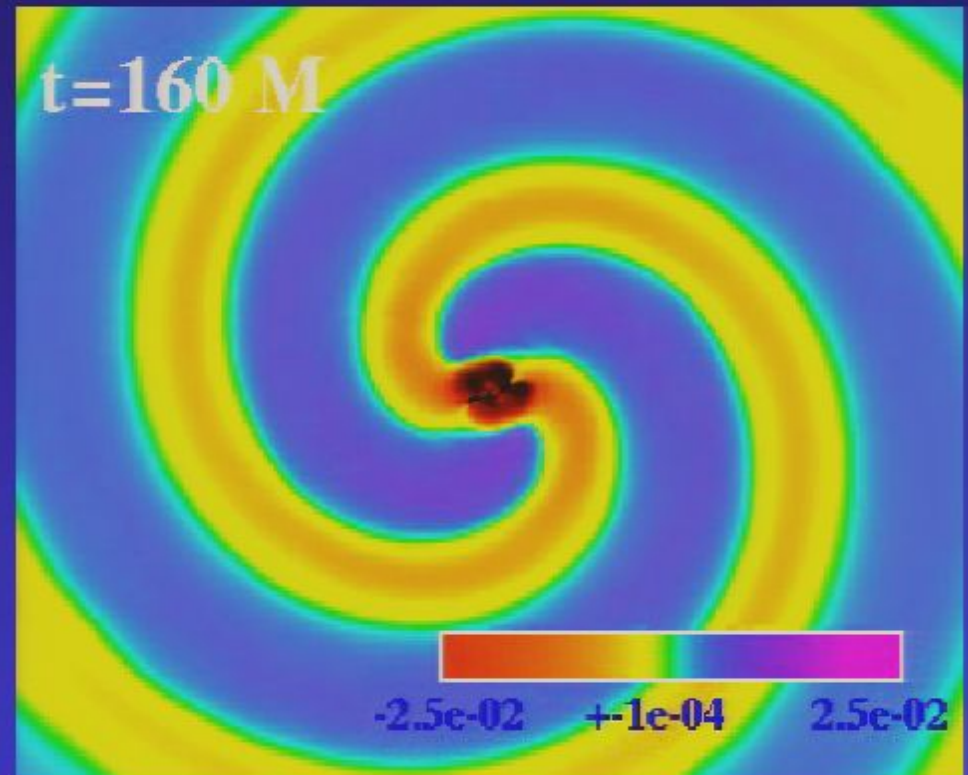
Real component of the Newman-Penrose scalar Ψ_4 (times rM), orbital plane

Lapse and Gravitational Waves

6/8h resolution, $v=0.21909$ merger example



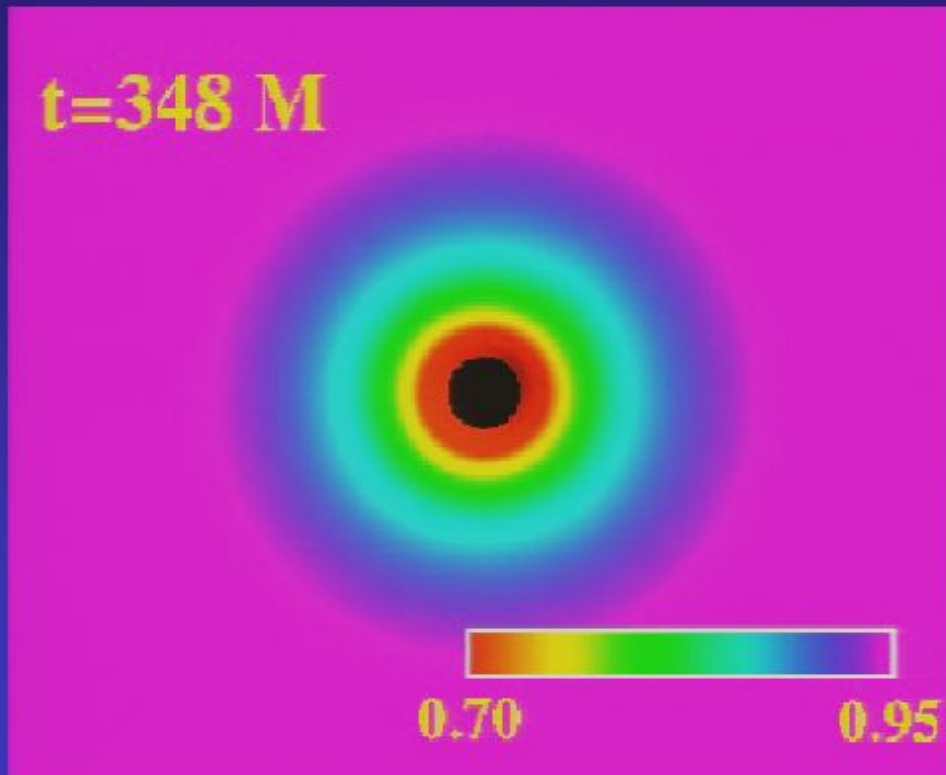
Lapse function α , orbital plane



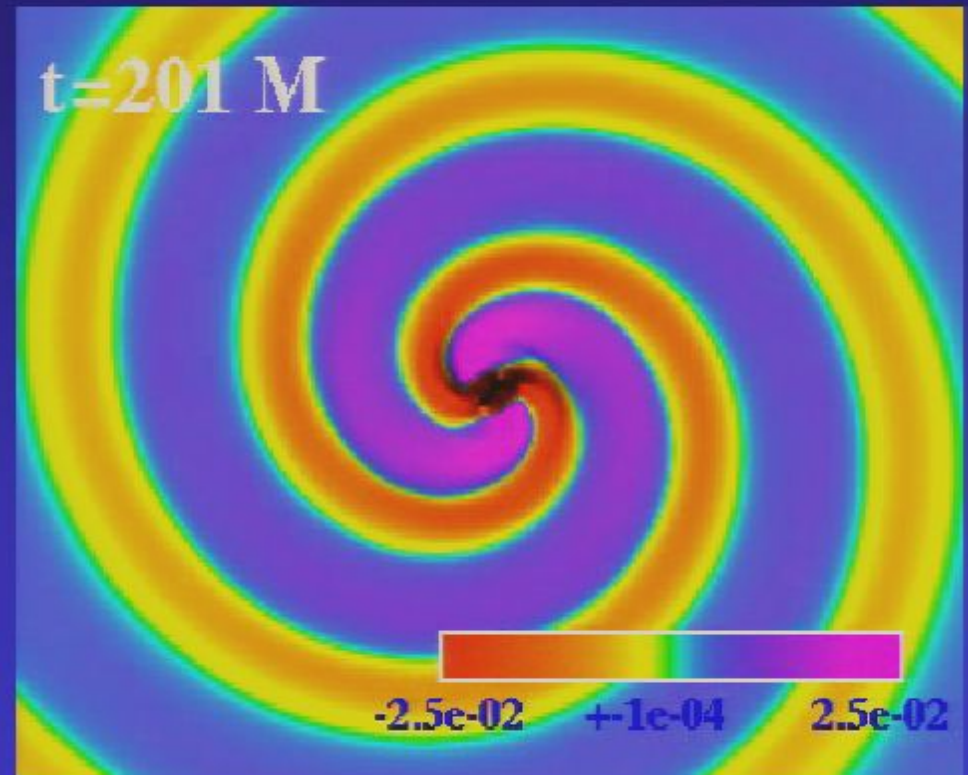
Real component of the Newman-Penrose scalar Ψ_4 (times rM), orbital plane

Lapse and Gravitational Waves

6/8h resolution, $v=0.21909$ merger example



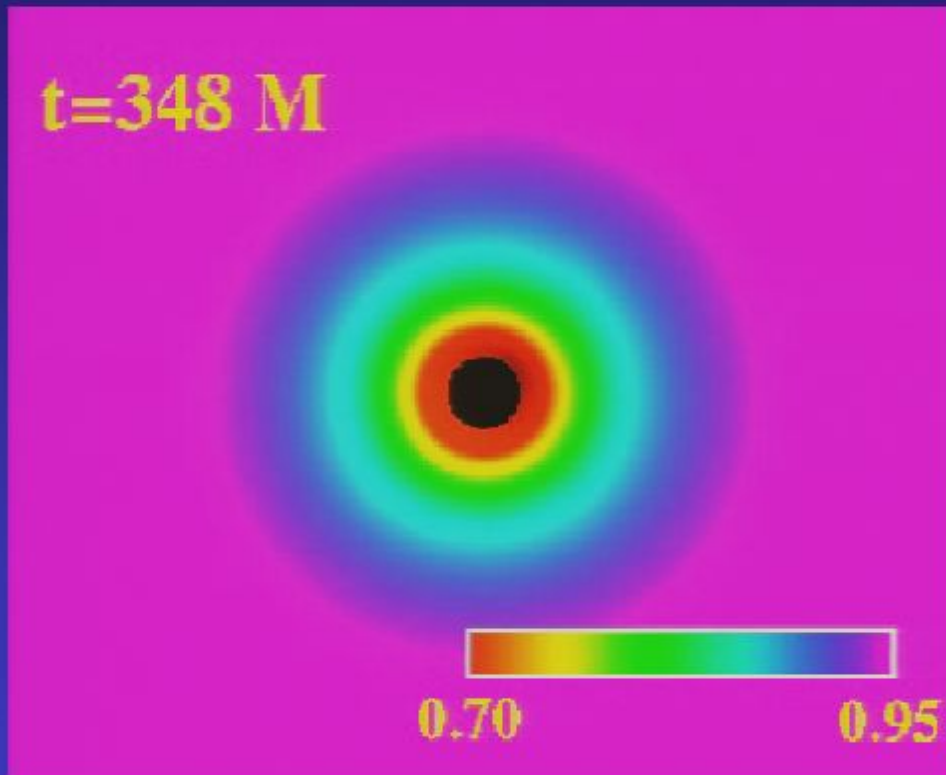
Lapse function α , orbital plane



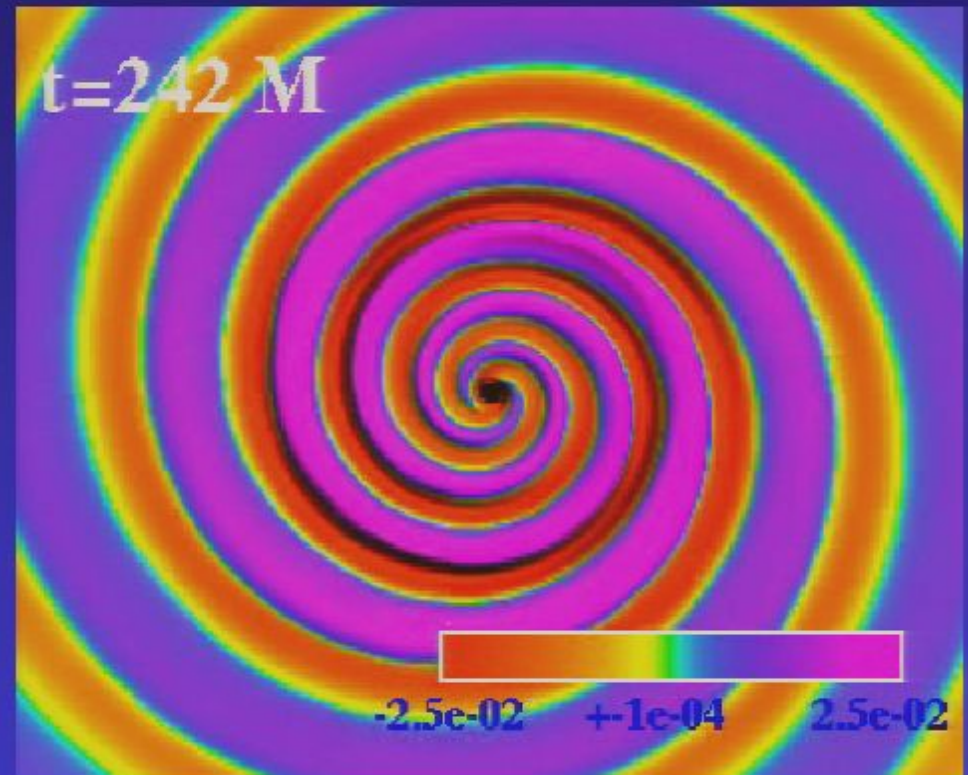
Real component of the Newman-Penrose scalar Ψ_4 (times rM), orbital plane

Lapse and Gravitational Waves

6/8h resolution, $v=0.21909$ merger example



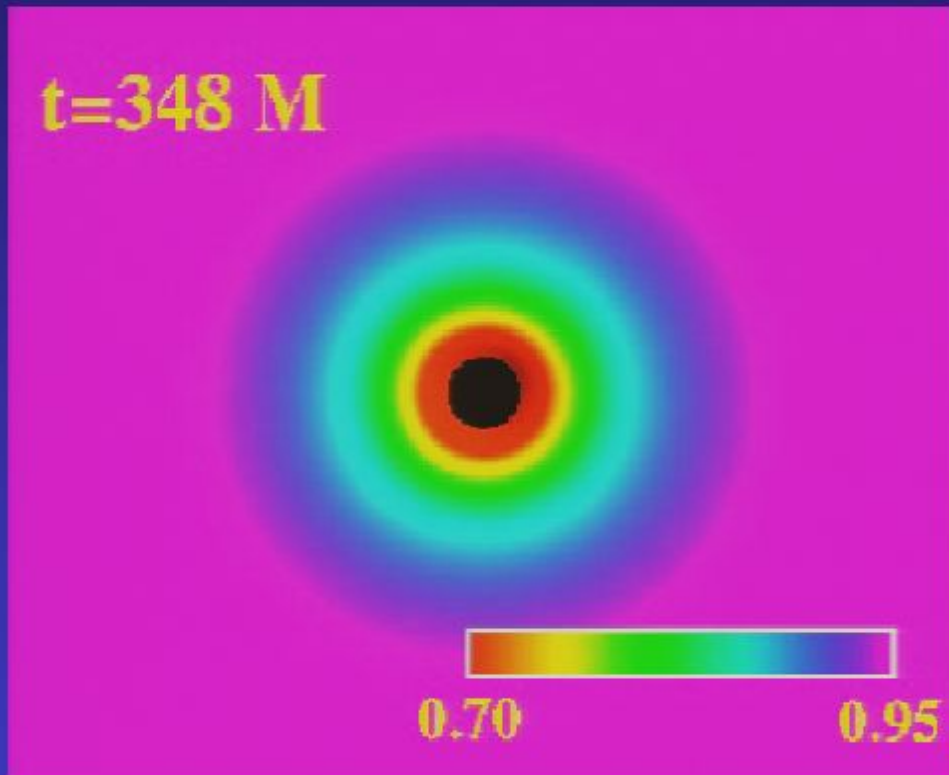
Lapse function α , orbital plane



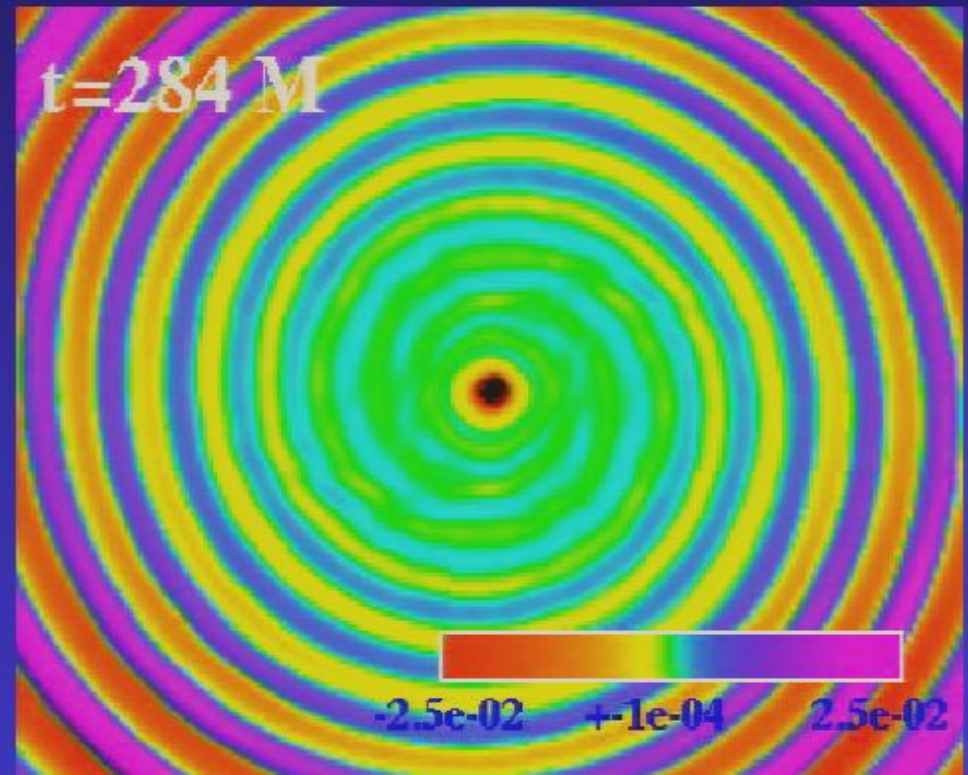
Real component of the Newman-Penrose scalar Ψ_4 (times rM), orbital plane

Lapse and Gravitational Waves

6/8h resolution, $v=0.21909$ merger example



Lapse function α , orbital plane

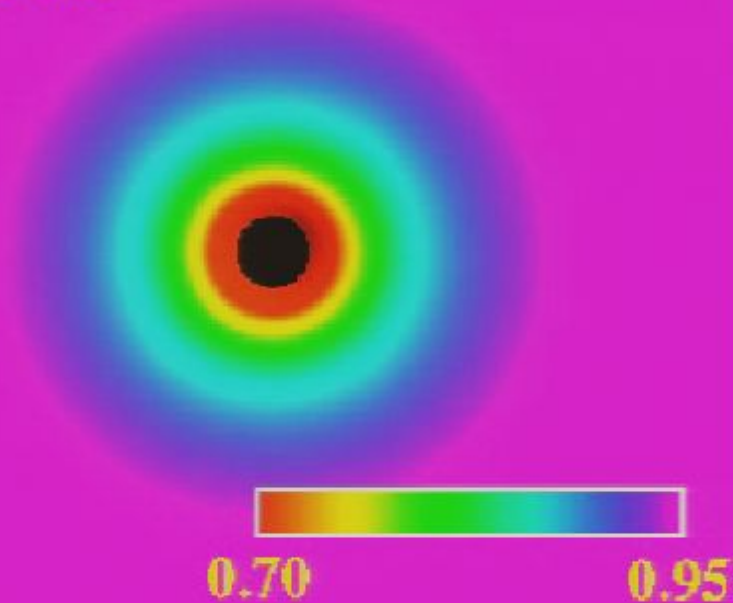


Real component of the Newman-Penrose scalar Ψ_4 (times rM), orbital plane

Lapse and Gravitational Waves

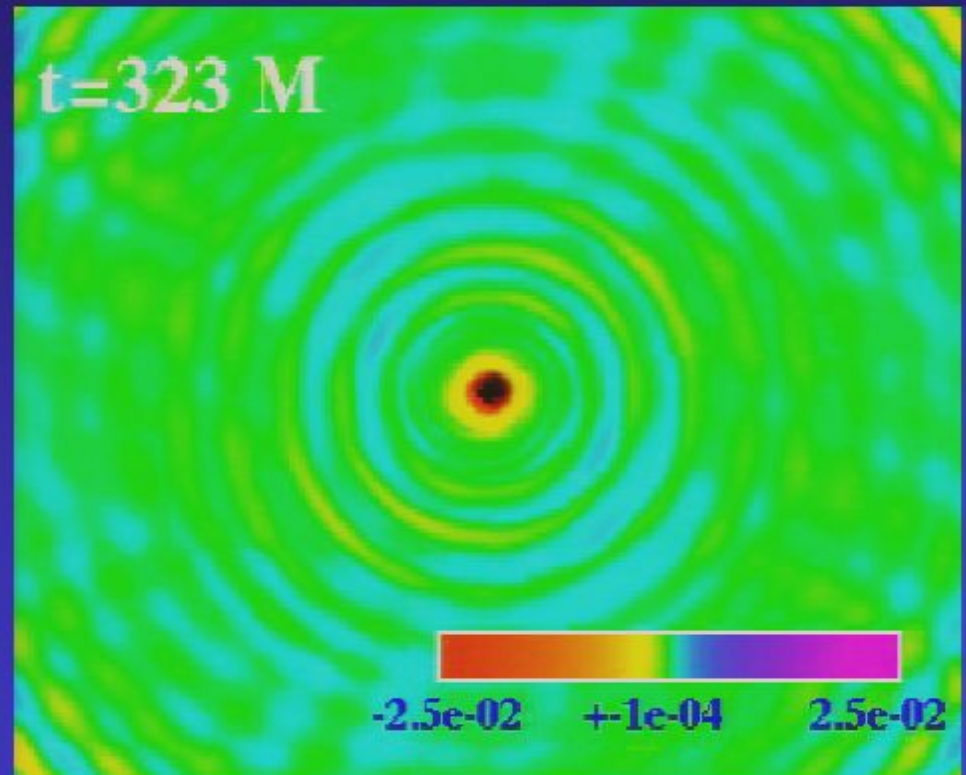
6/8h resolution, $v=0.21909$ merger example

t=348 M



Lapse function α , orbital plane

t=323 M

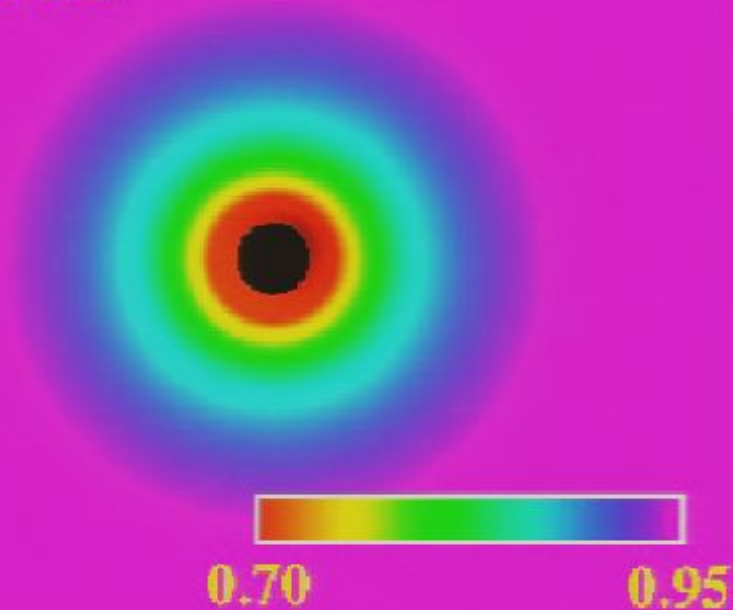


Real component of the Newman-Penrose scalar Ψ_4 (times rM), orbital plane

Lapse and Gravitational Waves

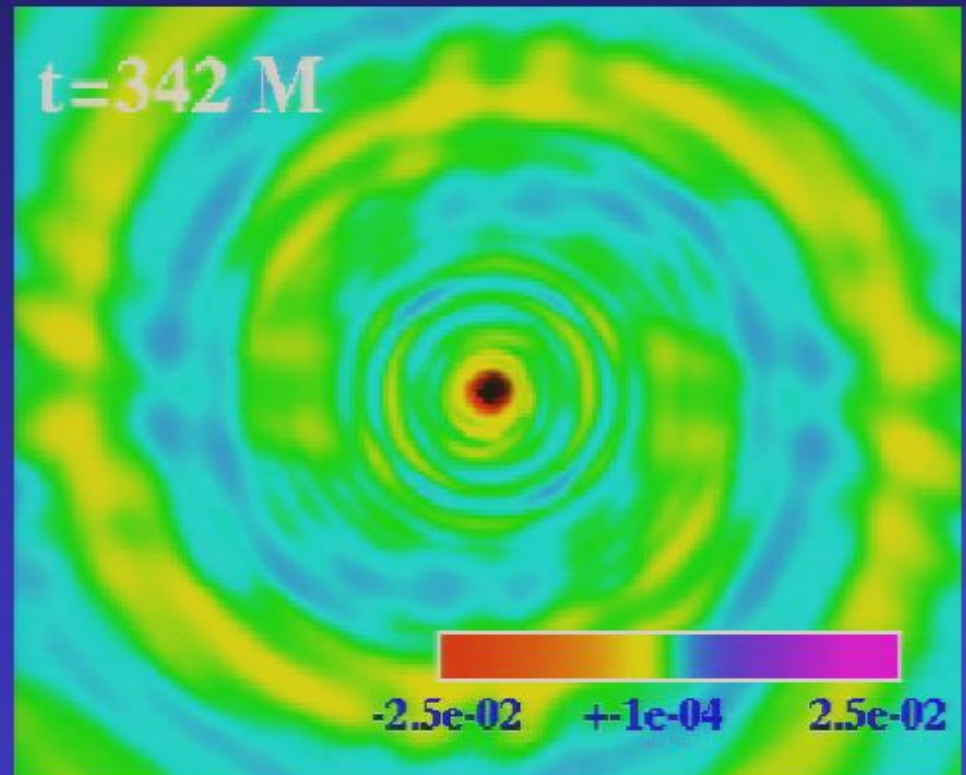
6/8h resolution, $v=0.21909$ merger example

t=348 M



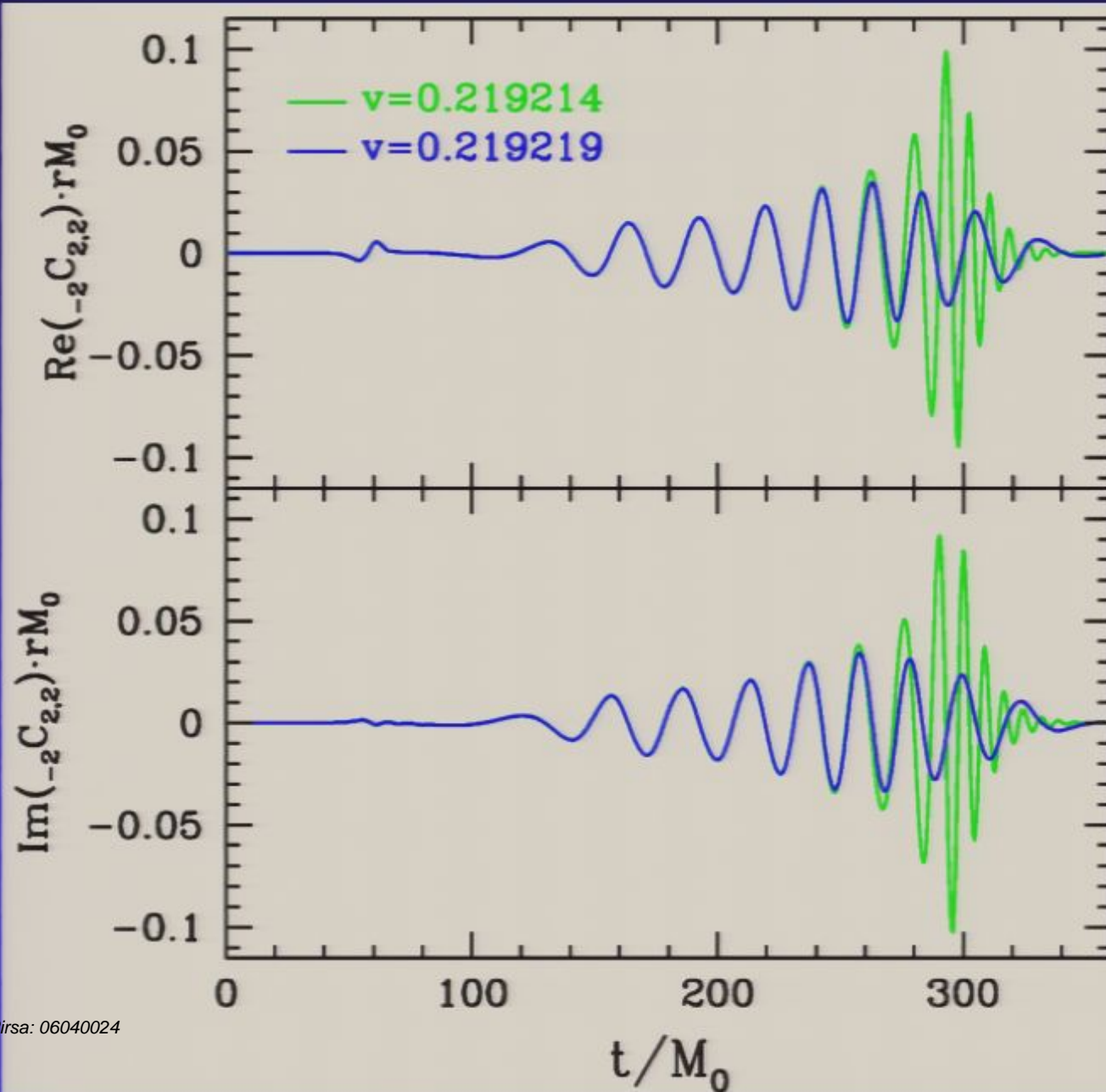
Lapse function α , orbital plane

t=342 M



Real component of the Newman-Penrose scalar Ψ_4 (times rM), orbital plane

Waveforms



The real and imaginary components of the spin weight -2 , $l=2$, $m=2$ spherical harmonic component of Ψ_4 times rM , measured at a coordinate distance of $50M$ from the center of the orbit, from the two $6/8 h$ resolution simulations fine-tuned the most

How far can this go?

- System is losing energy, and quite rapidly, so there must be a limit to the number of orbits we can get
- **Hawking's area theorem:** assume cosmic censorship and "reasonable" forms of matter, then net area of all black holes in the universe can *not* decrease with time
 - the area of a single, isolated black hole is:

$$A = 8\pi M^2 \left(1 + \sqrt{1 - \frac{J^2}{M^4}} \right)$$

- initially, we have two non-rotating ($J=0$) black holes, each with mass $M/2$:

$$\sum A_i = 8\pi M^2$$

- maximum energy that can be extracted from the system is if the final black hole is also non-rotating:

$$A_f = 16\pi M_f^2 \geq 8\pi M^2$$

in otherwords, the maximum energy that can be lost is a factor $1 - 1/\sqrt{2} \sim 29\%$

- If the trend in the simulations continues, and the final $J \sim 0.7M^2$, we still get close to 24% energy that could be radiated

- the simulations further suggest around 1% energy is lost per whirl, so we may get as close to 20-20 orbits at the threshold of this fine-tuning process!

h-resolution runs

v	n	p_m/M_0	d_m/M_0	m_f/M_0	a/m_f	(E/M_0)
0.21000	1.3	-	-	0.89 ± 0.03	0.75 ± 0.05	0.032
0.21125	1.4	-	-	0.88 ± 0.03	0.74 ± 0.05	0.035
0.21234	2.3	-	-	0.83 ± 0.03	0.73 ± 0.05	?
0.21250	2.7	4.0	3.6	-	-	0.020
0.21500	1.5	5.5	4.6	-	-	0.006
0.22000	1.0	7.2	5.8	-	-	0.005

6/8 h-resolution runs

v	n	p_m/M_0	d_m/M_0	m_f/M_0	a/m_f	(E/M_0)
0.20960	0.9	-	-	0.97 ± 0.01	0.65 ± 0.03	0.028
0.21750	1.4	-	-	0.92 ± 0.01	0.72 ± 0.03	0.037
0.21875	2.0	-	-	0.88 ± 0.01	0.70 ± 0.03	0.046
0.21906	2.4	-	-	0.86 ± 0.01	0.70 ± 0.03	0.052
0.219180	2.8	-	-	0.82 ± 0.02	0.70 ± 0.05	0.063
0.219200	3.0	-	-	0.80 ± 0.02	0.75 ± 0.05	0.064
0.219209	3.3	-	-	0.78 ± 0.02	0.71 ± 0.05	0.067
0.219214	3.7	-	-	0.75 ± 0.02	0.71 ± 0.05	0.074
0.219219	4.9	3.2	3.0	-	-	0.058
0.21938	2.5	4.8	4.2	-	-	0.019
0.22000	1.9	5.3	4.4	-	-	0.014

4/8 h-resolution runs

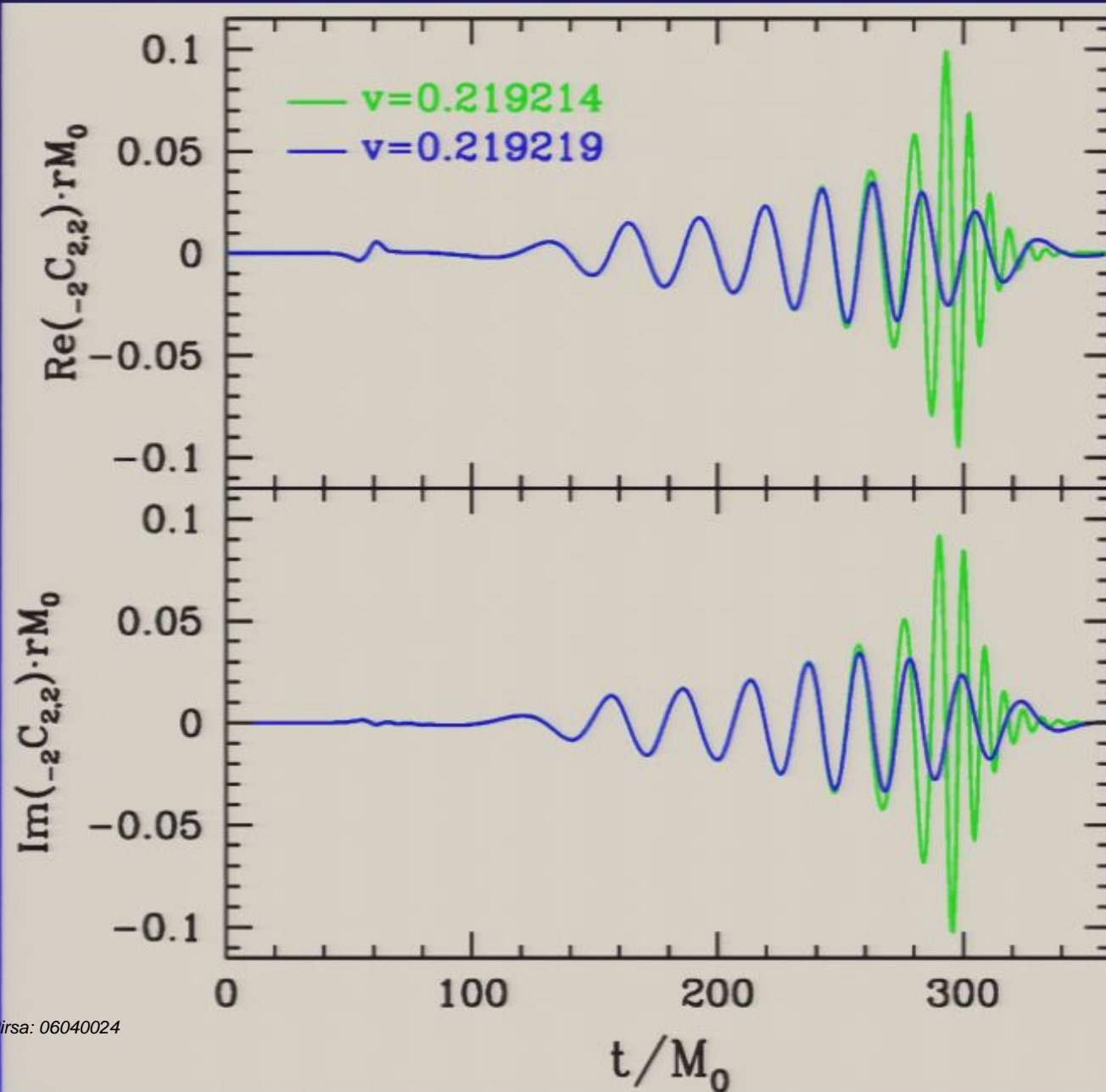
v	n	p_m/M_0	d_m/M_0	m_f/M_0	a/m_f	(E/M_0)
0.21500	1.4	-	-	0.945 ± 0.005	0.71 ± 0.02	0.042
0.22000	2.1	5.7	4.8	-	-	?

Pirsa: 06040024

Early indications of “extreme” sensitivity to initial conditions

- What’s going on??
 - **warning:** large cumulative numerical errors, especially for the lower resolutions (though does not necessarily mean qualitative features are wrong, c.f. critical gravitational collapse)
 - could be the fully non-linear analogue of “zoom-whirl” behavior in test particle orbits

Waveforms



The real and imaginary components of the spin weight -2 , $l=2$, $m=2$ spherical harmonic component of Ψ_4 times rM , measured at a coordinate distance of $50M$ from the center of the orbit, from the two $6/8 h$ resolution simulations fine-tuned the most

How far can this go?

- System is losing energy, and quite rapidly, so there must be a limit to the number of orbits we can get
- **Hawking's area theorem:** assume cosmic censorship and "reasonable" forms of matter, then net area of all black holes in the universe can *not* decrease with time

- the area of a single, isolated black hole is:

$$A = 8\pi M^2 \left(1 + \sqrt{1 - \frac{J^2}{M^4}} \right)$$

- initially, we have two non-rotating ($J=0$) black holes, each with mass $M/2$:

$$\sum A_i = 8\pi M^2$$

- maximum energy that can be extracted from the system is if the final black hole is also non-rotating:

$$A_f = 16\pi M_f^2 \geq 8\pi M^2$$

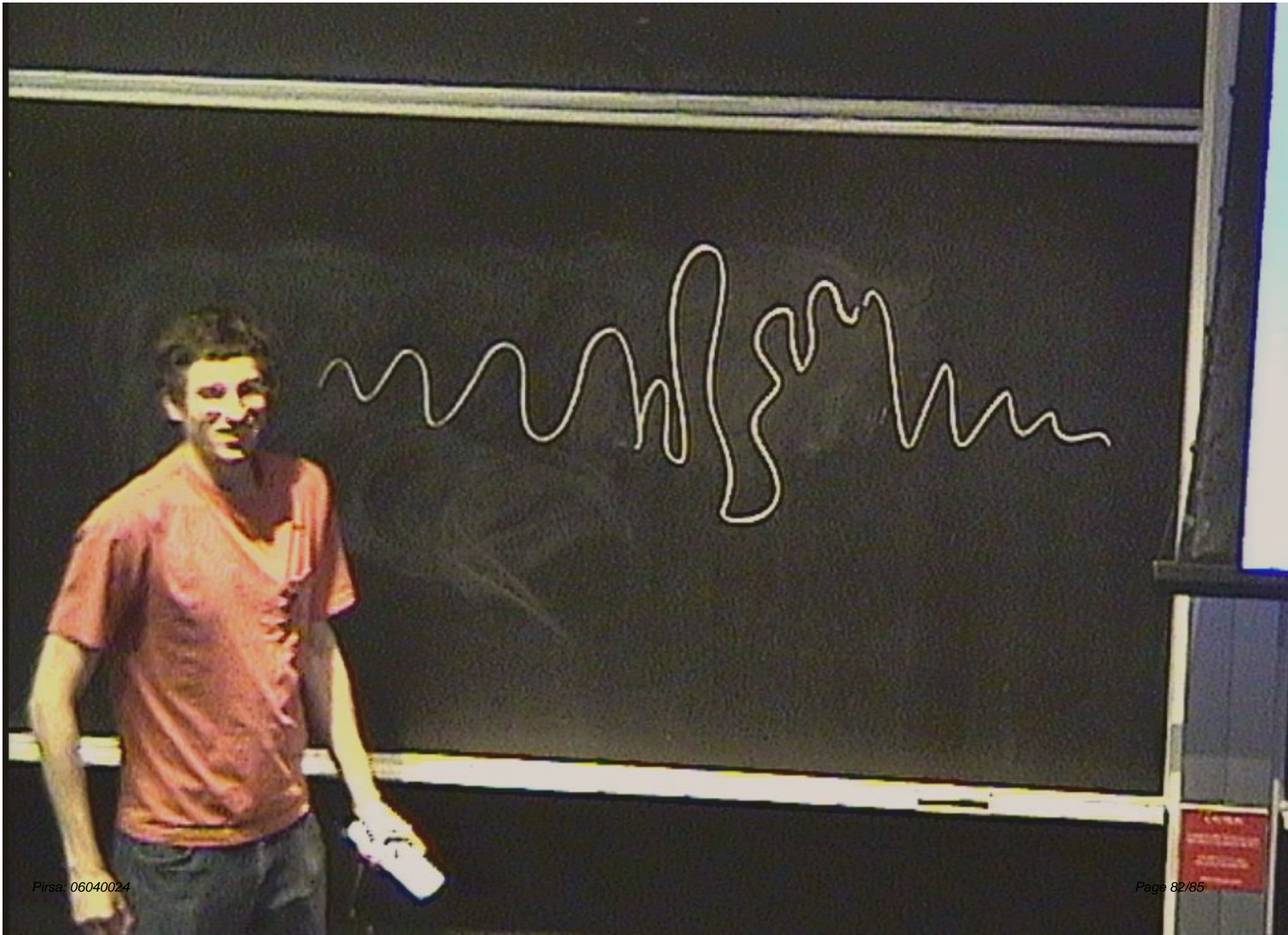
in otherwords, the maximum energy that can be lost is a factor $1 - 1/\sqrt{2} \sim 29\%$

- If the trend in the simulations continues, and the final $J \sim 0.7M^2$, we still get close to 24% energy that could be radiated

- the simulations further suggest around 1% energy is lost per whirl, so we may get as close to 20-20 orbits at the threshold of this fine-tuning process!

Summary and Outlook

- we are hopefully entering a very exciting time in astrophysics if the new gravitational wave detectors allow us to “see” the universe in gravitational waves for the first time
- we are also entering the era where numerical relativity will reveal the fascinating landscape of black hole coalescence
 - current simulations have only scratched the surface of binary configurations, whether of astrophysical or theoretical interest
 - first quasi-circular inspiral results are not “wild”, but then again non-spinning, equal mass, zero-eccentricity orbits are about as plain as one can get
 - F. Herrmann, D. Shoemaker, P. Laguna (*gr-qc/0601026*), and Baker, Centrella, Choi, Koppitz, van Meter and Coleman Miller (*astro-ph/0603204*) studied black hole “kicks” from unequal mass mergers
 - Campanelli, Lousto and Zlochower (*gr-qc/0604012*) noted “orbital” hang-up in black holes with spins aligned with the orbital angular momentum of the binary
 - the tentative indications that zoom-whirl like behavior is present in the fully non-linear case hints that all of the interesting orbital behavior in test-particle orbits will also be present in the full problem



Summary and Outlook

- we are hopefully entering a very exciting time in astrophysics if the new gravitational wave detectors allow us to “see” the universe in gravitational waves for the first time
- we are also entering the era where numerical relativity will reveal the fascinating landscape of black hole coalescence
 - current simulations have only scratched the surface of binary configurations, whether of astrophysical or theoretical interest
 - first quasi-circular inspiral results are not “wild”, but then again non-spinning, equal mass, zero-eccentricity orbits are about as plain as one can get
 - F. Herrmann, D. Shoemaker, P. Laguna (*gr-qc/0601026*), and Baker, Centrella, Choi, Koppitz, van Meter and Coleman Miller (*astro-ph/0603204*) studied black hole “kicks” from unequal mass mergers
 - Campanelli, Lousto and Zlochower (*gr-qc/0604012*) noted “orbital” hang-up in black holes with spins aligned with the orbital angular momentum of the binary
 - the tentative indications that zoom-whirl like behavior is present in the fully non-linear case hints that all of the interesting orbital behavior in test-particle orbits will also be present in the full problem

